TARGETED, SYSTEMIC NON-VIRAL DELIVERY OF SMALL INTERFERING RNA *IN VIVO*

Thesis by

Jeremy David Heidel

In Partial Fulfillment of the Requirements for the

degree of

Doctor of Philosophy

CALIFORNIA INSTITUTE OF TECHNOLOGY

Pasadena, California

2005

(Defended May 17, 2005)

ACKNOWLEDGMENTS

I would like to acknowledge the many collaborators and co-workers who have been extremely helpful to me throughout the course of my graduate studies; I performed virtually none of the work described here entirely by myself. I am endebted to the efforts of many who have helped to start and maintain the transgenic mice, including Janet Baer, Claire Lindsell, Bruce Kennedy, Shirley Pease, Juan Silva, Lorena Sandoval, Cirila Arteaga, and Gustavo Munoz. I appreciate the assistance and support I also received from Cynthia Tognazzini, Ana Colon, Lehong Chow, Diane Solis, and especially Gwen Williams for the *in vivo* work. I would also like to thank Dr. Timothy Triche, Xang Liu, Jean Lee, and Hu Wong from Children's Hospital—Los Angeles, as well as Dr. John Rossi, Dongho Kim, Mohammed Amarzguioui, Bret Heale, and Daniela Castanotto from the City of Hope Cancer Center for helpful discussions and materials.

I received a lot of assistance from previous members of the Davis group when I first began working here, especially from Suzie Pun, Nathalie Bellocq, and Theresa Reineke. I also appreciate the assistance I have received from Chris Dartt and especially Greg Jensen at Insert Therapeutics. My labmate Swaroop Mishra has always been especially gracious in helping me with anything I have asked him for, especially microscopy, and has made the lab and office enjoyable places to be.

I would like to express special appreciation to Siwen Hu, a post-doctoral fellow in the laboratory of Dr. Triche, for all of her contributions to our collaborative projects over the years. Her efforts were critical to the success of all of the animal work contained in the document. More than her techniques and work ethic, though, her pleasant disposition has made her a pleasure to work with.

I would also like to thank my labmate Derek Bartlett with whom I have worked most closely since he started in the lab. He contributed immensely to the animal work described here and performed the EPCR measurements of CDP/siRNA polyplexes shown in Chapter 3. This project could not continue in more capable hands.

Finally, I would like to express my deep and heartfelt appreciation to my family, especially my sister, Jennifer, and my parents, Allen and Mary Ann. After graduating from high school, I have done nothing but move farther away from home, and I appreciate their constant support throughout the years here and in Boston. Every day I strive to employ the sense of humility and the strong work ethic that they have instilled in me.

ABSTRACT

Armed with the complete sequence of the human genome and an ever-increasing array of biological techniques, researchers continue to learn more about the genetic basis of diseases. For two decades, scientists and physicians have been developing therapeutic strategies for treating many diseases at the genetic level, creating the field of "gene therapy." For those diseases caused by loss-of-function mutations in a specific gene, delivery of a wild-type copy of that gene to affected cells can reduce or eliminate the disease phenotype. Viruses, having evolved to be extremely effective at delivering nucleic acids (i.e., their own genes for viral production) to cells, have been modified to include therapeutic genes of interest. While such viral gene therapy vectors are the most efficient vectors developed, concerns about their safety and immunogenicity have prompted many to investigate non-viral vector alternatives. Cationic polymers and lipids have emerged as leading non-viral vector materials. Our laboratory has developed a class of cyclodextrin-containing polycations (CDPs) that condense DNA into complexes that can be endocytosed by cells, achieve expression of their genetic payload in those cells, and may be modified to target particular cell types within an animal.

In the past five years, scientists have discovered a new mechanism for the reduction of gene expression in mammalian cells via sequence-specific cleavage of a particular messenger RNA (mRNA); this phenomenon is known as RNA interference (RNAi). Since RNAi is triggered by nucleic acids (small interfering RNA (siRNA) duplexes), I hypothesized that CDPs may be suitable vectors for the delivery of siRNA. In my thesis work, the safety of synthetic siRNA duplexes is examined both in cultured cells and *in vivo*. Using a number of different siRNA sequences, two different strains of mice, and three different methods of

administration, I fail to observe any cytokine (IL-12 or IFN-α) responses, morphological changes, or alterations in complete blood counts (CBCs) or liver enzyme levels.

The ability of CDP to serve as a delivery vehicle for siRNA is also explored. I demonstrate that CDP/siRNA complexes can be formed that are small enough to be endocytosed, can be modified to ensure stability in physiological fluid, and protect the siRNA payload from serum nuclease degradation. Finally, down-regulation of specific target genes, including genes implicated in disease, is shown *in vitro* and in mice. An endogenous reporter gene (luciferase) in the livers of transgenic mice is down-regulated by galactosylated CDP/siRNA formulations that target hepatocytes. The level of a chimeric oncogene, EWS-Fli1, is reduced by polyplex formulations in cultured Ewing's sarcoma cells and by transferrin-targeted formulations in tumor-bearing mice; this *in vivo* down-regulation corresponds to an inhibition of tumor growth. These results suggest that CDP-containing siRNA formulations have the potential for development into therapeutics.

TABLE OF CONTENTS

Acknowledgments iii
Abstract v
Table of Contents vii
List of Figures x
Chapter 1: An Introduction to RNA Interference 1
1.1 Abstract 1
1.2 Antisense oligonucleotides 2
1.3 RNA interference 4
1.3.1 Discovery of RNA interference 4
1.3.2 MicroRNAs (miRNAs) 8
1.3.3 Chemical modification of synthetic siRNAs 10
1.3.4 Synthesis of siRNAs: *in vitro* transcription vs. chemical synthesis 11
1.3.5 Evolutionary role of RNAi 12
1.4 Preliminary therapeutic applications of RNAi 14
1.5 References 15
Chapter 2: Investigation of siRNA Immunogenicity 20
2.1 Abstract 20
2.2 Introduction 21
2.3 Methods 23
2.3.1 Nucleic acids 23
2.3.2 RAW-264.7 studies 23
2.3.3 Mouse studies 24
2.4 Results 26
2.4.1 Naked synthetic siRNA fails to induce a cytokine response in cultured cells 26
2.4.2 Naked synthetic siRNA fails to induce a cytokine response in mice 28
2.4.3 Synthetic siRNA achieves sequence-specific gene knockdown in cultured cells 32
2.4.4 Synthetic siRNA achieves sequence-specific gene knockdown in mice 34
2.5 Discussion 39
2.6 References 42
Chapter 3: Creation and Characterization of CDP/siRNA Complexes 45
3.1 Abstract 45
3.2 Introduction 46
3.3 Methods 52
3.3.1 Polymers 52
3.3.2 Nucleic acids 52
3.3.3 Gel retardation studies 52
3.3.4 Dynamic light scattering (DLS) studies of polyplex size and zeta potential 53

3.3.5 Flow cytometry and confocal microscopy to assess polyplex uptake.....55
3.3.6 Serum nuclease stability 55
3.3.7 Measurement of unbound polymer.....56
3.3.8 Isothermal titration calorimetry (ITC).....56
3.3.9 Turbidity analysis.....57
3.4 Results……. 58
3.4.1 CDP condenses siRNA into polyplexes.....58
3.4.2 PEGylation of CDP/siRNA polyplexes confers salt stability and reduces dependence of size on concentration.....60
3.4.3 CDP/siRNA polyplexes are readily endocytosed by cultured cells 62
3.4.4 siRNA within polyplexes is protected from serum nuclease degradation64
3.4.5 Measurement of unbound CDP and "effective polyplex charge ratio"....66
3.4.6 Stoichiometry and strength of AD-PEG/CDP binding: isothermal titration calorimetry 68
3.5 Discussion.....73
3.6 References.....75
Chapter 4: *In Vitro* and *In Vivo* Efficacy of CDP/siRNA Polyplexes.....77
4.1 Abstract…..77
4.2 Introduction.....78
4.3 Methods…. 80
4.3.1 Polymers.....80
4.3.2 Nucleic acids 80
4.3.3 HeLa and BHK transfections, luciferase assays 81
4.3.4 TC71 transfection, Western blot.....82
4.3.5 Preparation of formulations and injections of transgenic mice 82
4.3.6 Determination of transferrin receptor (TFR) level of TC71 cells 83
4.3.7 Generation of luciferase-expressing TC71 (TC71-LUC) cells.....83
4.3.8 Injection of NOD/scid mice with TC71-LUC cells 84
4.3.9 Bioluminescence imaging of mice 84
4.3.10 Magnetic resonance imaging 85
4.3.11 Preparation of formulations and injections of NOD/scid mice 86
4.3.12 Toxicity, immune response, and pathology studies 87
4.4 Results…..88
4.4.1 siRNA-containing polyplexes down-regulate co-delivered luciferase in cultured cells 88
4.4.2 siRNA-containing polyplexes reduce expression of the EWS-Fli1 oncogene in cultured Ewing's sarcoma cells 90
4.4.3 Galactosylated polyplexes down-regulate hepatic luciferase in transgenic mice 92
4.4.4 Transferrin-targeted polyplexes inhibit Ewing's sarcoma tumor formation in mice 94
4.5 Discussion…..104
4.6 References…. 107
Chapter 5: Recommendations 111
5.1 Abstract…..111

5.2 Recommended Future Directions 112
5.2.1 Quantification of siRNA payload.....112
5.2.2 Quantification of ligand density 114
5.2.3 Alternative ligands for improving targeting.....117
5.2.4 Alternative dsRNA duplexes for improved potency.....119
5.3 References.....120
Appendix……. 122

LIST OF FIGURES AND TABLE

Figure 1.1. Mechanism of RISC formation 6
Figure 1.2. Mechanisms of immunogenicity of dsRNA.....7
Figure 1.3. A comparison of microRNA and small interfering RNA (siRNA) processing ..9

Figure 2.1. RNase degradation of poly(I:C) 26
Figure 2.2. Poly(I:C), but not synthetic siRNA, induces IL-12 secretion by RAW-264.7 cells.....28
Figure 2.3. Poly(I:C), but not synthetic siRNA, induces IL-12 secretion by mice.....29
Figure 2.4. IFN-α induction in mice 30
Figure 2.5. Synthetic siRNA does not alter mouse CBC or liver enzyme levels 31
Figure 2.6. Lack of IL-12 and IFN-α induction by siRNA in C57BL/6 mice 32
Figure 2.7. Degradation kinetics of synthetic siRNA in mouse serum.....33
Figure 2.8. Sequence-specific target down-regulation by siRNA in RAW-264.7 cells.....34
Figure 2.9. Efficacy of synthetic siRNA in mice.....35
Figure 2.10. Synthetic siRNA accomplishes sequence-specific RNAi of an exogenous target in mice.....36
Figure 2.11. Synthetic siRNA accomplishes sequence-specific RNAi of an endogenous target in mice.....37

Figure 3.1. Structures of amine- and imidazole-terminated β-cyclodextrin-containing polycations…. 46
Figure 3.2. Imidazole-modification of CDP increases intracellular unpackaging of polyplexes……. 47
Figure 3.3. Modification of CDP/DNA polyplexes with AD-PEG confers salt stability....49
Figure 3.4. Gel retardation assay for CDP/siRNA and CDP/pDNA polyplexes.....58
Figure 3.5. Determination of CDP/siRNA and CDP/pDNA polyplex size by dynamic light scattering.....59
Figure 3.6. AD-PEG confers salt stability to CDP/siRNA polyplexes.....60
Figure 3.7. Pre-PEGylation generates CDP/siRNA polyplexs of uniform, small size and reduces their zeta potential.....61
Figure 3.8. CDP/siRNA polyplexes are readily taken up by adherent cultured cells.....63
Figure 3.9. CDP protects siRNA duplexes from serum nuclease degradation 65
Figure 3.10. The amount of bound CDP within formulations is independent of overall formulation charge ratio.....67
Figure 3.11. Isothermal titration calorimetry (ITC) analysis of AD-PEG binding to β-CD, CDP, and CDP-containing polyplexes 69
Figure 3.12. Addition of “excess” AD-PEG leads to enhanced protection of CDP/pDNA polyplexes from salt-induced aggregation 71

Figure 4.1. CDP/siRNA down-regulates co-delivered luciferase in HeLa and BHK cells.89

Figure 4.2. CDP/siRNA down-regulates oncogenic EWS/Fli-1 in cultured Ewing's sarcoma cells 91
Figure 4.3. GalactosylatedCDP/siRNA down-regulates luciferase in livers of transgenic mice 93
Figure 4.4. TC71 Ewing's sarcoma cells display high levels of transferrin receptor (TfR)95
Figure 4.5. Establishment of a disseminated Ewing's sarcoma model in mice.....96
Figure 4.6. Targeted polyplexes containing siRNA against EWS-Fli1 reduced tumor bioluminescence in mice.....97
Figure 4.7. Targeted polyplexes containing siEFBP2 reduced EWS-Fli1 mRNA levels in tumors 98
Figure 4.8. Targeted polyplexes containing siEFBP2 reduced tumor growth levels in mice 100
Figure 4.9. Formulated siRNA failed to exhibit toxicity or elicit an immune response in mice 102

Figure 5.1. Calculation of average polyplex stoichiometry 113
Figure 5.2. Centrifugal filtration to separate unbound material from polyplex formulations 116

Table 4.1. Treatment groups for long-term tumor inhibition study…….99

CHAPTER 1: An Introduction to RNA Interference

1.1 ABSTRACT

There are numerous medical indications that could be treated by reducing the expression of one or more target genes, such as viral infection (genes required for viral replication) and cancer (oncogenes). Scientists have developed some nucleic acid-based molecular therapeutics, such as antisense oligonucleotides and ribozymes, that can accomplish this down-regulation. However, issues with potency, specificity, and delivery have hampered development of these molecules for more therapeutic applications. In the past few years, a novel mechanism for down-regulation of genes in mammalian cells has been discovered. Triggered by double-stranded RNA and acting by sequence-specific cleavage of the messenger RNA (mRNA) gene product, this phenomenon is known as "RNA interference," or RNAi. Already having become the tool of choice for researchers to identify gene targets and elucidate function, RNAi has an exciting potential for therapeutic applications that is just starting to be realized. This chapter contains a discussion of the current state of knowledge of RNAi, including comparisons to antisense technology, the mechanism of action, and highlights of therapeutic results.

1.2 ANTISENSE OLIGONUCLEOTIDES

Prior to the discovery of RNAi and its still-emerging application as a therapeutic, the tool of choice for the down-regulation of a specific target gene was the antisense oligonucleotide. The effector molecule, typically single-stranded DNA (ssDNA, which is more stable to nucleases than ssRNA), is designed to be complementary to the messenger RNA (mRNA) of the desired target gene such that it will anneal to the mRNA and prevent translation. The specificity of this approach is based on Watson-Crick base pairing interactions, and the most effective knockdown using this technique is often observed with a an RNase-H dependent cleavage mechanism of mRNA targets.

Despite their promise, the specificity of the biological effects observed by antisense molecules has fallen under question in recent years. In order to minimize the non-specificity and toxicity associated with antisense molecules that have been observed *in vitro* and *in vivo*, they have been chemically modified to improve their target binding affinity and to prevent nuclease degradation. As one example, incorporation of an entirely phosphorothioate (P=S) backbone and incorporation of 2'-methyoxyethyl modifications on the terminal (5' and 3' ends) bases gives nuclease resistance and increased mRNA binding while permitting RNase-mediated degradation[1-2]. Much longer studied than RNA inteference, there is already one antisense oligonucleotide product approved for local therapy of cytomegalovirus retinitis (Vitravene) and nearly twenty others in late-stage clinical trials and development targeting, among others, *bcl-2*, *PKC*-α, and DNA methyltransferase.

Antisense oligonucleotides have not developed into ubiquitous molecular therapeutics as was initially hoped. Despite the successes mentioned above, folding of target RNAs and/or

their association with specific proteins in the cell often prevent the antisense molecules from binding to their targets. This requires employment of relatively high doses in order to achieve a therapeutic effect; these high doses, as well as the consequently high toxicity that is sometimes observed, have made antisense molecules less than ideal for therapeutic product development. As discussed below, the discovery of RNA interference, requiring double-stranded RNA, demonstrates greatly enhanced potency and thus is attracting a great deal of interest as a possible improvement upon/successor to antisense.

1.3 RNA INTERFERENCE

1.3.1 Discovery of RNA interference

The phenomenon of double-stranded RNA-(dsRNA-)induced gene silencing that we now call RNA interference (RNAi) emerged from studies dating back to the 1980s. It was initially observed in plants that introduction of exogenous "transgenes" could alter the levels of expression of endogenous genes that possessed some amount of sequence homology; this was termed "homology-dependent gene silencing" (HDGS)[3]. Further work suggested that HDGS was found in a wide variety of organisms[4-5] and that it could be correlated to covalent modifications of genomic DNA, particularly methylation of cytosine residues[6], which can lead to conversion to thymidine[7]. Interestingly, the effect of methylation was different depending on the region of the gene being methylated—methylation of promoter sequences led to transcription silencing[8-9] ("transcriptional gene silencing," TGS), while methylation of the coding sequence corresponds to mRNA destabilization ("post-transcriptional gene silencing," PTGS).

It wasn't until some investigations in worms (*C. elegans*) in the 1990s that RNA was shown to trigger gene silencing in an inheritable manner. Both sense and antisense RNAs, when injected separately, were equally effective at silencing homologous target genes[10]. The seminal discovery following this was made by Fire and Mello, who demonstrated that the combination of sense and antisense RNAs (essentially dsRNA) together gave greater than ten times down-regulation than either RNA alone[11]. It was this finding that led to the realization that RNA was responsible for the HDGS phenomena observed up to a decade earlier and sparked the cascade of research on RNAi in mammalian cells that continues to grow.

Initial *in vitro* investigations of RNAi showed that RNAi-induced silencing was realized via degradation of messenger RNA (mRNA)[12]. An assembly of the dsRNA with a nuclease to form a "RNA-induced silencing complex" (RISC) was observed. After extracts from RNAi-induced cells were shown to possess discrete ~25 nt RNAs homologous to the target gene, it was discovered shortly thereafter that these RNAs cofractionated with the RISC[13-14]. A critical extension was made in cell-free systems by Zamore and co-workers who determined that cell extracts contained the ability to process dsRNA into 22-nt effector RNAs termed "small interfering RNAs" (siRNAs)[15].

Quickly, more became known about the details of RISC, both its protein and nucleic acid components. Having a total size of ~500 kDa, the RISC was shown to contain the Argonaute-2 (Ago-2) protein and a family of RNase III proteins called Dicer[16]. Dicer contains dual RNase III domains and dsRNA-binding motifs; it processes dsRNA into siRNAs and is recruited into the RISC by association between the PAZ domains found on both Dicer and Ago-2[17]. A detailed description of the current understanding of RISC formation is shown in **Figure 1.1**.

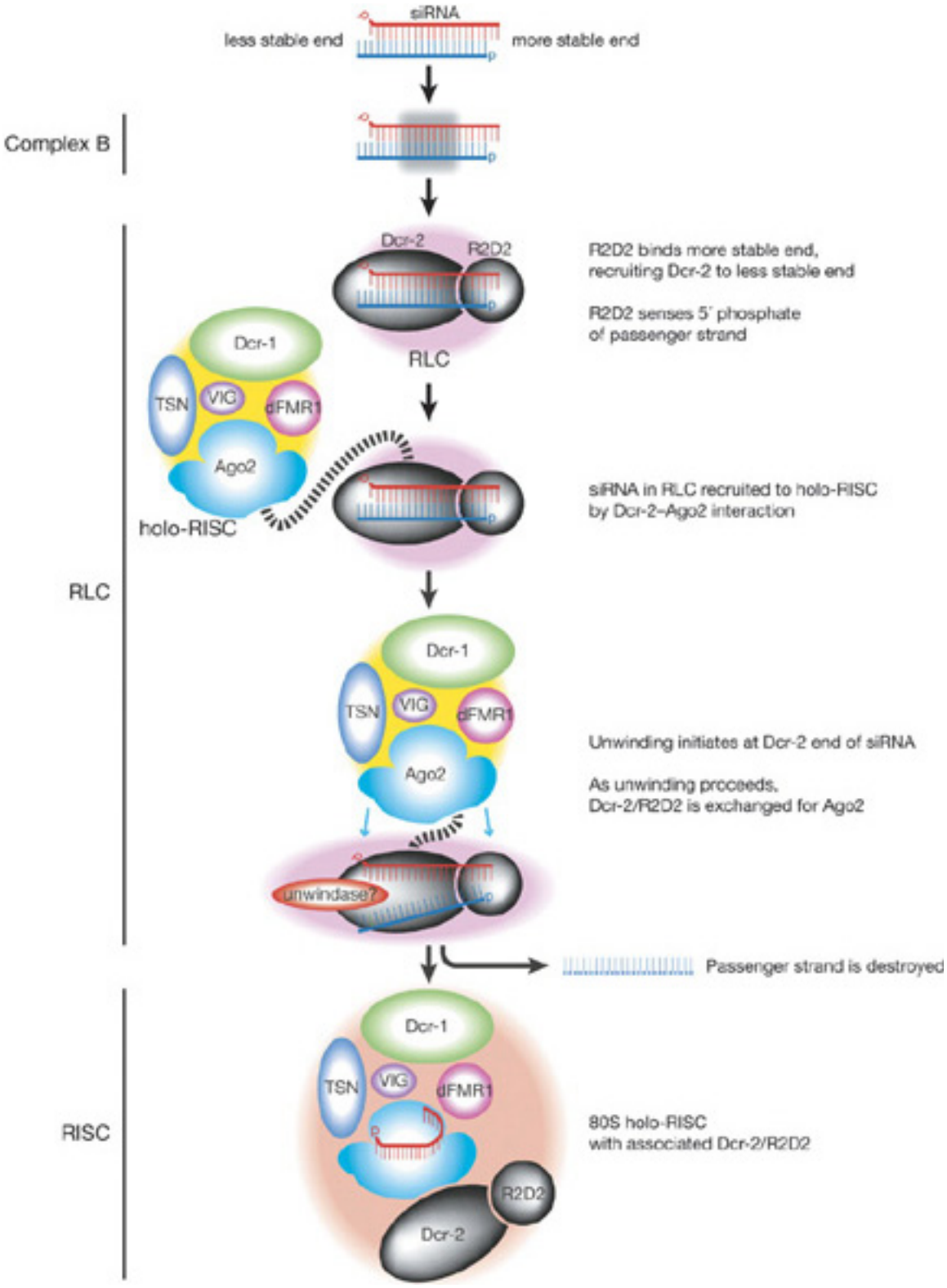

Figure 1.1 Mechanism of RISC formation. [Reproduced from Tomari and Zamore, 2005[18]] RLC: RISC-loading complex; Dcr-1: Dicer 1; Dcr-2: Dicer 2; Ago2: Argonaut 2.

Despite having developed this understanding of the key players and mechanism of RNAi, a significant hurdle remained to the development of RNAi as a research and therapeutic tool. The long dsRNA molecules that were cleaved into siRNA by Dicer are known to also interact with other cellular proteins that cause undesired, interferon-regulated responses (**Fig. 1.2**). One of these proteins, the dsRNA-dependent protein kinase PKR, binds to and is activated by dsRNAs longer than 30 bp in length, leading to phosphorylation of eIF2α and global translational arrest[19-20]. Another, 2',5'-oligoadenylate synthetase, is activated by dsRNA and causes non-specific mRNA degradation via 2',5'-oligoadenylate-activated ribonuclease L[21].

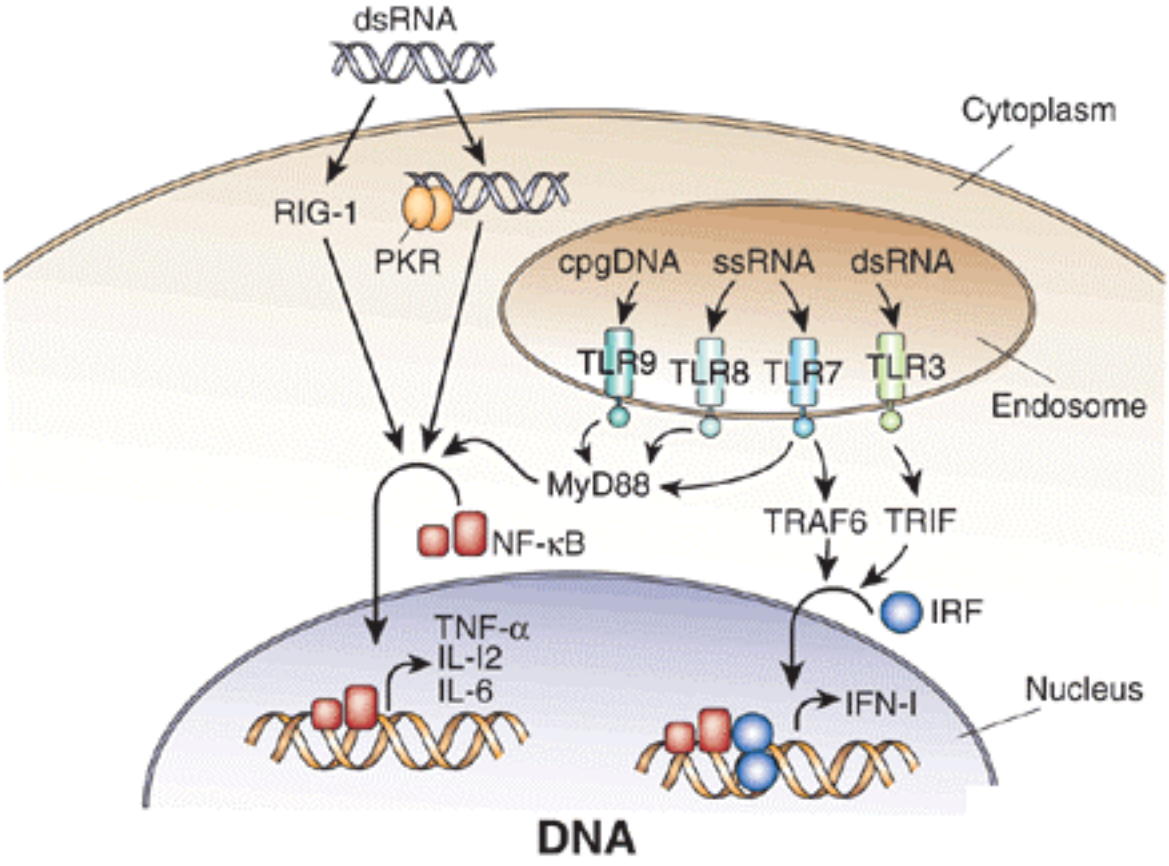

Figure 1.2 Mechanisms of immunogenicity of dsRNA. [Reproduced from Robbins and Rossi, 2005[22]]

A critical breakthrough came when Elbashir and co-workers generated synthetic siRNAs (21-nt duplexes having symmetric 2-nt 3' overhangs) and demonstrated that these could perform RNAi without needing cleavage by Dicer and without generating a PKR/interferon response[23]. This finding opened the floodgates as the number of experimenters working with siRNA, and related small hairpin RNA (shRNA), has proliferated. Today it is one of, if not the most, commonly used techniques to reduce levels of a particular gene to study its function or to elucidate a drug target.

1.3.2 MicroRNAs (miRNAs)

First discovered in *C. elegans* in 1993, small temporal RNAs (stRNAs), now known as microRNAs (miRNAs), are endogenous RNAs that accomplish targeted gene down-regulation in a manner very similar to that of siRNA. Sharing part of the mechanism of RNA interference described above, miRNAs have contributed significantly to the understanding of RNAi and its role in cellular and developmental biology.

The first step of miRNA maturation is the nuclear cleavage of a primary miRNA transcript (pri-miRNA) to liberate a ~60 – 70 nt stem loop intermediate called the pre-miRNA (miRNA precursor)[24]. This cleavage is performed by the nuclear enzyme Drosha, an RNase III endonuclease (just like Dicer), and generates a 5' phosphate and 2-nt 3' overhang on the stem-loop[25]. Exportin-5 and Ran-GTP then transport the pre-miRNA from the nucleus to the cytoplasm. In the cytoplasm, the second end of the mature miRNA is generated by Dicer, the same enzyme implicated in the generation of siRNA. It is worth noting that the specificity of the initial cleavage (mediated by Drosha in the nucleus) determines the correct register of cleavage within the pre-miRNA and thus defines both

mature ends of the miRNA[26]. This stands in contrast to the non-specific, progressive cleavages seen with Dicer. Indeed, it has very recently been shown that small hairpin RNAs (shRNAs), 29-nt stem loop analogues of pri-miRNAs, also demonstrate a unique cleavage product that can be predicted[27]. Having been cleaved by Dicer, the resulting miRNAs are recruited into the RNA-induced silencing complex (RISC) and proceed to silence homologous mRNA either via mRNA cleavage or translational repression. A schematic comparison of miRNA and siRNA processing is shown in **Figure 1.3**.

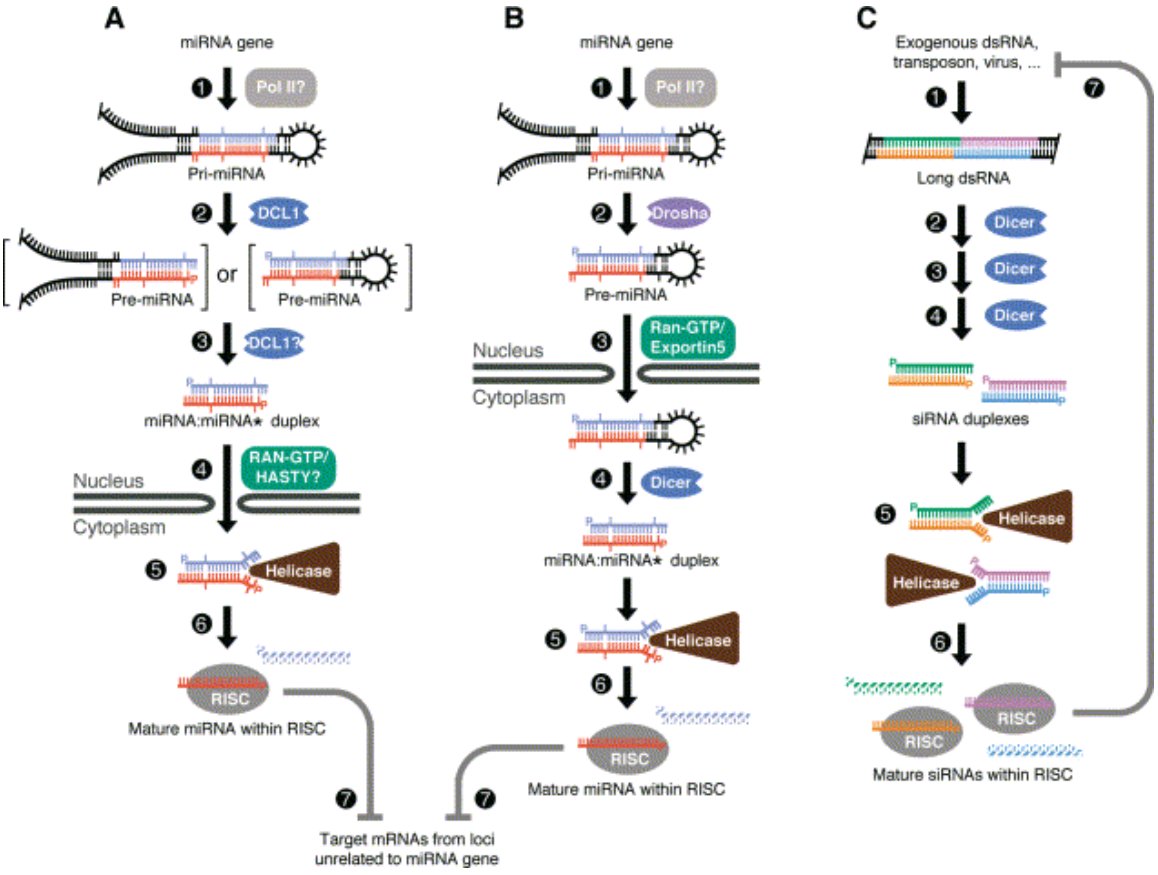

Figure 1.3 A comparison of microRNA (miRNA) and small interfering RNA (siRNA) processing. [Reproduced from Bartel, 2004[29]] **A**. Biogenesis of plant miRNA. **B**. Biogenesis of metazoan miRNA. **C**. Biogenesis of animal siRNAs.

Despite their functional similarity to siRNAs, miRNAs differ from siRNAs in regard to their origin, evolutionary conservation, and the types of genes they silence[28]. Whereas

endogenous siRNAs are often derived from mRNAs, viruses, or transposons, miRNAs derive from loci that are unique for other recognized genes. While endogenous siRNA sequences are rarely conserved, miRNA sequences are nearly always conserved among related organisms. Finally, endogenous siRNAs "auto-silence," i.e., they silence genes at the same locus, or very similar loci, from which they originate. In contrast, miRNAs "hetero-silence" genes that are very different from their own origination.

1.3.3 Chemical modification of synthetic siRNAs

The seminal work with synthetic siRNA duplexes by Elbashir and colleagues demonstrated that 21-nt RNA (phosphodiester) duplexes with symmetric 2-nt, 3' overhangs (either DNA or RNA) were sufficient to perform sequence-specific RNAi in mammalian cells[23]. Since this initial discovery, a large body of work has been performed to investigate the tolerance for chemical modifications at all possible locations with these duplexes, including the termini and the backbones.

A variety of modifications to the termini of siRNA duplexes, and their effect, if any, on their potency, have been examined. It is clear that a 5'phosphate group is required on the antisense strand for mRNA cleavage; this requirement does not extend to the sense strand[30-31]. However, phosphorylation of a 5' hydroxyl group on the antisense strand is performed by an intracellular kinase, so synthetic siRNA duplexes need not possess a 5' phosphate group on the antisense strand. As long as the 5' phosphodiester linkage is maintained on the antisense strand, further modifications (e.g., incorporation of a fluorophore) to the antisense strand are tolerated[30,32]. Many modifications to the 3' end of antisenses strand are permitted without loss of potency (e.g., an inverted deoxy abasic residue[33], puromycin or

biotin[34], or a dideoxycytosine (ddC)[31]), but a couple of alternations have abrogated RNAi activity (2-hydroxyethylphosphate or 2'-*O*,4'-*C*-ethylene thymidine[35]). While the TAT peptide or a TAT-derived oligocarbamate could be conjugated to the 3' end of the antisense strand without compromising silencing activity[36], fluorophore conjugation to this terminus (but not any others within the siRNA duplex) did abolish gene silencing[32].

Many experiments have been performed to understand the effect of interior modifications of siRNA duplexes and, in general, the results and conclusions are variable. Two groups showed that the silencing activity of siRNA duplexes containing phosphorothioate (P=S) linkages (instead of phosphodiester (P=O)) was unaffected by this modification[32,37]. However, another group showed that P=S modification did indeed reduce siRNA activity[38]. Incorporation of a boranophosphonate (P=B) backbone within T7-synthesized duplexes (containing 5' triphosphates) was better tolerated in the sense strand than antisense strand, and modification at the terminal regions of the strands only permitted retained activity of extended duration[39]. Some sugar modifications, including 2'-deoxy-2'-fluoro (2'-F) and locked nucleic acid (LNA), have been shown to improve target binding affinity, and 2'-F siRNA shows enhanced serum stability but gives provides only comparable activity to unmodified duplexes *in vivo*[40].

1.3.4 Synthesis of siRNAs: *in vitro* transcription vs. chemical synthesis

As an alternative to the more costly chemical synthesis of siRNA duplexes, many researchers have generated siRNA through *in vitro* transcription (IVT) methods. This is generally done using bacteriophage promoters with (linearized) DNA templates, and the most common system employed (using the bacteriophage T7 RNA polymerase) produces

very potent siRNAs[41-42]. However, it was demonstrated that T7-synthesized siRNAs are potent inducers of type I interferons (IFN-α and IFN-β) in numerous cell lines; single-stranded oligos made in the same way generated similar responses[43]. In fact, the presence of a 5' triphosphate on these RNAs was implicated in this interferon response, leading to the development of an alternative IVT system that incorporates two 3' adenosines[43]. These adenosines prevent base-pairing with the initiating guanosines, thereby allowing the initiating 5' nucleotides and triphosphates to be removed (by CIP and RNase T1). This discovery should be considered when evaluating both the potency and immunogenicity of IVT siRNAs in previously-published and forthcoming reports.

1.3.5 Evolutionary role of RNAi

As we continue to learn more about the mechanism of RNAi and the similarity in processing between endogenous microRNAs (miRNAs) and exogenous dsRNA, the evolutionary purpose of the phenomenon of RNAi is a subject of much interest. Indeed, at least three distinct roles of RNAi have been identified and are discussed briefly here: antiviral response, protection of the genome, and regulation of development.

While dsRNA is not a participant in the central dogma of cell biology, the genetic material of numerous viruses is either directly packaged as dsRNA or its intracellular processing proceeds through a dsRNA intermediate. It is logical, therefore, that cells have evolved a capacity to recognize dsRNA as foreign material and developed mechanisms for protection. Indeed, interferon responses and apoptosis mediated through dsRNA-mediated binding of cellular proteins, such as Toll-like receptor 3, protein kinase (PKR) or 2',5'-oligoadenylate synthetase (2'-AS), are clear examples of this. Research on plants has also shown that

genes implicated in RNAi are essential for viral protection; for example, *Arabidoposis* mutants in RNAi genes (*sgs2* or *sgs3*) show hypersensitivity to infection by the cucumovirus[44]. Perhaps RNAi evolution extends cellular protection to include shorter viral dsRNA triggers that complement the larger ones recognized by the other proteins mentioned above.

All complex genomes contain unstable elements (transposons), often possessing repetitive sequences, whose motility can contribute to genomic mutagenesis. There is evidence that RNAi-deficient worms (*C. elegans*) show increased rates of transposition[45]. Also, sequencing of ~22-nt siRNAs has uncovered guide sequences corresponding to endogenous transposons that move via both RNA and DNA intermediates in *Drosophila*[46]. These observations raise the possibility that RNAi has evolved to protect organisms from endogenous parasitic nucleic acids, such as transposons.

A third role of RNAi is suggested to be within organism developmental control. Mutations to Dicer or Argonaute-2 analogs in *Arabidopsis* led to stem cell defects causing developmental abnormalities or even embryo lethality[47-48]. Worms that are defective in either of those genes, as well as the miRNA *let-7*, show similar phenotypes, including abnormal oocytes and the inability to fertilize eggs. Thus the link between control of development timing and RNAi is clear and will likely continue to become better understood.

1.4 PRELIMINARY THERAPEUTIC APPLICATIONS OF RNAi

A number of publications have come out that demonstrate the therapeutic potential of RNAi in animals, particularly mice. Perhaps the most commonly examined therapeutic application of RNAi has been cancer, often owing to the specificity of the mutated gene target within cancer cells (and not others) and the relative ease of targeting these cells, which frequently over-express particular cell surface receptors. Non-targeted DOTAP-based liposomes have been used to deliver siRNA targeting the c-*raf* oncogene to human breast xenograft tumors in mice, resulting in 73% suppression of tumor growth[49]. Untargeted polyethylenimine-(PEI-)siRNA complexes reduced the growth of sub-cutaneous SKOV-3 tumor xenografts in athymic mice due to specific HER-2 down-regulation[50]. Finally, the use of PEI-siRNA complexes that were PEGylated and targeted to integrins (at sites of neovasculature) via an RGD peptide reduced levels of EGFR and provided correspondingly reduced tumor angiogenesis and growth[51].

Many non-cancer therapeutic applications of siRNA have been demonstrated as well. Retro-orbital injection of PEI-formulated siRNA against influenza virus inhibits viral production in virus-infected mice[52]. Systemic (intravenous) injection of polymer-bound siRNA against VEGF pathway genes reduces ocular angiogenesis[53]. Electroporation of human livers cells with siRNA targeting the hepatic C genome (ssRNA) sharply reduced virus-specific protein expression and RNA synthesis[54].

These successful experimental results and others like them indicate that the therapeutic potential of RNAi is high and may be realized soon. However, the known immunogenicity and/or toxicity of the non-viral vectors in these reports warrants investigation of alternative siRNA delivery systems that overcome these obstacles.

1.5. REFERENCES

[1] McKay RA, Miraglia LJ, Cummins LL, Owens SR, Sasmor H & Dean NM. Characterization of a potent and specific class of antisense oligonucleotide inhibitor of human protein kinase C-alpha expression. *J. Biol. Chem*. **274**, 1715-1722 (1999).

[2] Monia BP, Lesnik EA, Gonzalez C, Lima WF, McGee D, Guinosso CJ, Kawasaki AM, Cook PD & Freier SM. Evaluation of 2'-modified oligonucleotides containing 2'-deoxy gaps as antisense inhibitors of gene expression. *J. Biol. Chem*. **268**, 14514-14522 (1993).

[3] Jorgensen R. Altered gene expression in plants due to *trans* interactions between homologous genes. *Trends Biotechnol*. **8**, 340-344 (1990).

[4] Romano M & Macino G. Quelling: Transient inactivation of gene expression *Neurospora crassa* by transformation with homologous sequences. *Mol. Microbiol*. **6**, 3343-3353 (1992).

[5] Ruiz F, Vayssie L, Klotz C, Sperling L & Madeddu L. Homology-dependent gene silencing in *Paramecium*. *Mol. Biol. Cell* **9**, 931-943 (1998).

[6] Cambereri EB, Jensen BC, Schabtach E & Selker EU. Repeat-induced G-C to A-T mutations in Neurospora. *Science* **244**, 1571-1575 (1989).

[7] Selker EU. Epigenetic phenomena in filamentous fungi: Useful paradigms or repeat-induced confusion? *Trends Genet*. **13**, 296-301 (1997).

[8] Ingelbrecht I, Van Houdt H, Van Montagu M & Depicker A. Post-transcriptional silencing of reporter transgenes in tobacco correlates with DNA methylation. *Proc. Natl. Acad. Sci. USA* **91**, 10502-10506 (1994).

[9] Dieguez MJ, Vaucheret H, Paszlowski J & Mittelsten Scheid O. Cytosine methylation at CG and CNG sites is not a prerequisite for the initiation of transcriptional gene silencing in plants, but it is required for its maintenance. *Mol. Gen. Genet*. **259**, 207-215 (1998).

[10] Guo S & Kemphues KJ. par-1, a gene required for establishing polarity in *C. elegans* embryos, encodes a putative Ser/Thr kinase that is asymmetrically distributed. *Cell* **81**, 611-620 (1995).

[11] Fire A, Xu S, Montgomery MK, Kostas SA, Driver SE & Mello CC. Potent and specific genetic interference by double-stranded RNA in *Caenorhabditis elegans*. *Nature* **391**, 806-811 (1998).

[12] Tuschl T, Zamore PD, Lehmann R, Bartler DP & Sharp PA. Targeted mRNA degradation by double-stranded RNA in vitro. *Genes & Dev*. **13**, 3191-3197 (1999).

[13] Hammond SM, Bernstein E, Beach D & Hannon GJ. An RNA-directed nuclease mediates posttranscriptional gene silencing in *Drosophila* cells. *Nature* **404**, 293-296 (2000).

[14] Hamilton AJ & Baulcombe DC. A species of small antisense RNA in posttranscriptional gene silencing in plants. *Science* **286**, 950-952 (1999).

[15] Zamore PD, Tuschl T, Sharp PA & Bartel DP. RNAi: Double-stranded RNA directs the ATP-dependent cleavage of mRNA at 21 to 23 nucleotide intervals. *Cell* **101**, 25-33 (2000).

[16] Bernstein E, Caudy AA, Hammond SM & Hannon GJ. Role for a bidentate ribonuclease in the initation step of RNA interference. *Nature* **409**, 363-366 (2001).

[17] Hammond SM, Boettcher S, Caudy AA, Kobayashi R & Hannon GJ. Argonaute2, a link between genetic and biochemical analyses of RNAi. *Science* **293**, 1146-1150 (2001).

[18] Tomari Y & Zamore PD. Perspective: machines for RNAi. *Genes & Dev*. **19**, 517-529 (2005).

[19] Manche L, Green SR, Schmedt C & Mathews MB. Interactions between double-stranded RNA regulators and the protein kinase DAI. *Mol. Cell Biol*. **12**, 5238-5248 (1992).

[20] Williams BR. Role of the double-stranded RNA-activated protein kinase (PKR) in cell regulation. *Biochem. Soc. Trans*. **25**, 509-513 (1997).

[21] Minks MA, West DK, Benvin S & Baglioni C. Structural requirements of double-stranded RNA for the activation of 2',5'-oligo(A) polymerase and protein kinase of interferon-treated HeLa cells. *J. Biol. Chem*. **254**, 10180-10183 (1979).

[22] Robbins MA & Rossi JJ. Sensing the danger in RNA. *Nat. Med*. **11**, 250-251 (2005).

[23] Elbashir SM, Harborth J, Lendeckel W, Yalcin A, Weber K & Tuschl T. Duplexes of 21-nucleotide RNAs mediate RNA interference in cultured mammalian cells. *Nature* 411, 494-498 (2001).

[24] Lee Y, Jeon K, Lee JT, Kim S & Kim VN. MicroRNA maturation: stepwise processing and subcellular localization. *EMBO J*. **21**, 4663-4670 (2002).

[25] Basyuk E, Suavet F, Doglio A, Bordonne R & Bertrand E. Human *let-7* stem-loop precursors harbor features of RNase III cleavage products. *Nucleic Acids Res*. **31**, 6593-6597 (2003).

[26] Lee Y, Ahn C, Han J, Choi H, Kim J, Yim J, Lee J, Provost P, Radmark O, Kim S & Kim VN. The nuclease RNase III Drosha initiates microRNA processing. *Nature* **425**, 415-419 (2003).

[27] Siolas D, Lerner C, Burchard J, Ge W, Linsley PS, Paddison PJ, Hannon GJ & Cleary MA. Synthetic shRNAs as potent RNAi triggers. *Nat. Biotechnol*. **23**, 227-231 (2005).

[28] Bartel B & Bartel DP. MicroRNAs: at the root of plant development? *Plant Physiol.* **132**, 709-717 (2003).

[29] Bartel DP. MicroRNAs: genomics, biogenesis, mechanism, and function. *Cell* **116**, 281-297 (2004).

[30] Nykanen A, Haley B & Zamore PD. ATP requirements and small interfering RNA structure in the RNA interference pathway. *Cell* 107, 309-321 (2001).

[31] Schwarz DS, Hutvagner G, Haley B & Zamore PD. Evidence that siRNAs function as guides, not primers, in the Drosophila and human RNAi pathways. *Mol. Cell*. 10, 537-548 (2002).

[32] Harborth J, Elbashir SM, Vandenburgh K, Manninga H, Scaringe SA, Weber K & Tuschl T. Sequence, chemical, and structural variation of small interfering RNAs and short hairpin RNAs and the effect on mammalian gene silencing. *Antisense Nucleic Acid Drug Dev*. 13, 83-105 (2003).

[33] Czauderna F, Fechtner M, Dames S, Aygun H, Klippel A, Pronk GJ, Giese K & Kauffmann J. Structural variations and stabilizing modifications of synthetic siRNAs in mammalian cells. *Nucleic Acids Res* 31, 2705-2716 (2003).

[34] Chiu YL & Rana TM. RNAi in human cells: basic structural and functional features of small interfering RNA. *Mol. Cell* 10, 549-561 (2002).

[35] Hamada M, Ohtsuka T, Kawaida R, Koizuma M, Morita K, Furukawa H, Imanishi T, Miyagishi M & Taira K. Effects on RNA interference in gene expression (RNAi) in cultured mammalians cell of mismatches and the introduction of chemical modifications at the 3'-ends of siRNAs. *Antisense Nucleic Acid Drug Dev*. 12, 301-309 (2002).

[36] Chiu YL, Ali A, Chu C, Cao H & Rana TM. Visualizing a correlation between siRNA localization, cellular uptake, and RNAi in living cells. *Chem. Biol*. 11, 1165-1175 (2004).

[37] Amarzguioui M, Holen T, Babaie E & Prydz H. Tolerance for mutations and chemical modifications in a siRNA. *Nucleic Acids Res.* 31, 589-595 (2003).

[38] Chiu YL & Rana TM. siRNA function in RNAi: a chemical modification analysis. *RNA* 9, 1034-1048 (2003).

[39] Hall AH, Wan J, Shaughnessy EE, Ramsay Shaw B & Alexander KA. RNA interference using boranophosphate siRNAs: structure-activity relationships. *Nucleic Acids Res*. 15, 5991-6000 (2004).

[40] Layzer JM, McCaffrey AP, Tanner AK, Huang Z, Kay MA & Sullenger BA. *In vivo* activity of nuclease-resistant siRNAs. RNA 10, 766-771 (2004).

[41] Donze O & Picard D. RNA interference in mammalian cells using siRNAs synthesized with T7 RNA polymerase. *Nucleic Acids Res*. 30, e46 (2002).

[42] Sohail M, Doran G, Riedermann J, Macaulay V &Southern EM. A simple and cost-effective method for producing small interfering RNAs with high efficacy. *Nucleic Acids Res*. 31, e28 (2003).

[43] Kim DH, Longo M, Han Y, Lundberg P, CantinE & Rossi JJ. Interferon induction by siRNAs and ssRNAs synthesized by phage polymerase. *Nat. Biotechnol*. 22, 321-325 (2004).

[44] Mourrain P, Beclin C, Elmayan T, Feuerbach F, Godon C, Morel JB, Houette D, Lacombe AM, Nikic S, Picault N, Remoue K, Sanial M, Vo TA & Vaucheret H. *Arabidopsis* SGS2 and SGS3 genes are required for posttranscriptional gene silencing and natural virus resistance. *Cell* 101, 533- 542 (2000).

[45] Grishok A, Tabara H & Mello CC. Genetic requirements for inheritance of RNAi in *C. elegans*. *Science* 287, 2494-2497 (2000).

[46] Elbashir SM, Lendeckel W & Tuschl T. RNA interference is mediated by 21- and 22-nucleotide RNAs. *Genes & Dev*. 15, 188-200 (2001).

[47] Bohmert K, Camus I, Bellini C, Bouchez D, Caboche M & Benning C. AGO1 defines a novel locus of *Arabidopsis* controlling leaf development. *EMBO J*. 17, 170-180 (1998).

[48] Jacobsen SE, Running MP & Meyerowitz EM. Disruption of an RNA helicase/RNase III gene in *Arabidopsis* causes unregulated cell division in floral meristems. *Development* 126, 5231-5243 (1999).

[49] Chien PY, Wang J, Carbonaro D, Lei S, Miller B, Sheikh S, Ali SM, Ahmad MU & Ahmad I. Novel cationic cardiolipin analogue-based liposomes for efficient DNA and small interfering RNA delivery in vitro and in vivo. *Cancer Gene Ther*. **12**, 321-328 (2005).

[50] Urban-Klein B, Werth S, Abuharbeid S, Czubayko F & Aigner A. RNAi-mediated gene-targeting through systemic application of polyethylenimine (PEI)-complexed siRNA *in vivo*. *Gene Ther*. **12**, 461-466 (2005).

[51] Schiffelers RM, Ansari A, Xu J, Zhou Q, Tang Q, Storn G, Molema G, Lu PY, Scaria PV & Woodle MC. Cancer siRNA therapy by tumor selective delivery with ligand-targeted sterically stabilized nanoparticle. *Nucleic Acids Res.* **32**, e149 (2004).

[52] Ge Q, Filip L, Bai A, Nguyen T, Eisen HN & Chen J. Inhibition of influenza virus production in virus-infected mice by RNA interference. *Proc. Natl. Acad. Sci. USA* **101**, 8676-8681 (2004).

[53] Kim B, Tang Q, Biswas PS, Xu J, Schiffelers RM, Xie FY, Ansari AM, Scaria PV, Woodle MC, Lu P & Rouse BT. Inhibition of ocular angiogenesis by siRNA targeting vascular endothelial growth factor pathway genes. *Am. J. Pathol.* **165**, 2177-2185 (2004).

[54] Wilson JA, Jayasena S, Khvorova A, Sabatinos S, Rogrigue-Gervais IG, Arya S, Sarangi F, Harris-Brandts M, Beaulieu S & Richardson CD. *Proc. Natl. Acad. Sci. USA* **100**, 2783-2788 (2003).

CHAPTER 2: Investigation of siRNA Immunogenicity

2.1 ABSTRACT

RNA interference (RNAi) has rapidly become the method of choice for the elucidation of gene function and the identification of drug targets. However, some recent reports suggest that small interfering RNA (siRNA) duplexes that perform RNAi may induce an immune response in cells that take them up, most notably upregulating type I interferons (IFNs). Such immunogenicity would render therapeutic *in vivo* applications of siRNA unsafe for the patient and would preclude investigation of our polymeric system to deliver these duplexes. However, the generality of the conclusions of these reports have been questioned for a variety of reasons, including the means of generation of the duplexes themselves, the lack of *in vivo* results to support these claims (only cell culture results were included), the use of a delivery vehicle for all samples (siRNA alone samples were not included), and the relatively high dose of siRNA employed. Here, we carefully examine whether or not naked synthetic siRNA duplexes themselves induce a cytokine response, both in cultured cells and in mice. Our results suggest that, even when administered *in vivo* by hydrodynamic delivery such that these naked siRNAs enter cells and are efficacious, synthetic siRNA duplexes do not induce a detectable immune response. Our findings have very recently been confirmed by multiple other researchers. From these results, we conclude that synthetic siRNA duplexes may indeed be safe for *in vivo* applications, and the ability of our polymeric system to deliver them merits exploration.

2.2 INTRODUCTION

First discovered in plants two decades ago, the phenomenon of RNA interference (RNAi) has rapidly become the method of choice for the elucidation of gene function and the identification of drug targets in mammalian cells. RNAi is achieved by double-stranded RNA (dsRNA) that triggers recognition and cleavage of the corresponding messenger RNA (mRNA) via the RNA-induced silencing complex (RISC) within the cytoplasm of cells. An intracellular enzyme (Dicer) cuts dsRNA into duplexes (21-23 nucleotoides (nt) in length) that are suitable for interaction with RISC. While dsRNA larger than 21-23 nt in length may be appropriately Diced, it has been demonstrated in mammalian cells that dsRNA longer than 30 nt triggers a non-specific interferon pathway (through interaction with the protein kinase PKR[1] and 2',5'-oligoadenylate synthetase[2]) rather than RNAi. In fact, small interfering RNA (siRNA) duplexes 21-23 nt in length can bypass Dicer and induce RNAi by incorporating within RISC directly, thereby eliminating the PKR/interferon response[3,4]. Thus, although additional work has been done with both plasmids that express siRNAs and short hairpin RNAs (shRNAs) showing their suitability for RNAi, synthetic siRNA duplexes are preferred for most common, transient applications.

While numerous reports have come out demonstrating the efficacy of siRNA duplexes to down-regulate a variety of targets in cultured cell lines, there have also been some reports of adverse effects of siRNA on cells that take them up. Most notably, it has been claimed that siRNAs, while small enough to avoid interaction with PKR, activate an interferon response in a sequence-independent matter[5-7]. If this were generally true, the potential of siRNA as a therapeutic would be sharply reduced, if not completely eliminated.

Careful inspection of these reports, however, suggests that all siRNA may not be immunogenic under all conditions. For example, the siRNA examined was generated from a variety of sources, including chemical synthesis, processing of shRNA, and *in vitro* (T7) transcription. Also, work was done in cultured cell models only (no *in vivo* results) and concentrations much higher than may be necessary for down-regulation (up to 100 nM) were employed. Finally, all exposures to siRNA were performed in the presence of a delivery vector, either liposomal or viral in nature, which complicates interpretation of the results.

Prior to exploration of whether our polymer-based system might be suitable for siRNA delivery, we decided to expand on the previous work investigating the interferon response to siRNA. Since our delivery system has previously been shown to be non-toxic and well-tolerated in mice[8], we first investigated whether or not chemically synthesized siRNAs alone (without a delivery vector) elicit a cytokine response in cultured cells and in mice; for *in vivo* experiments, three different means of administration were compared. Taken together, our results strongly suggest that chemically synthesized siRNAs do not elicit an immune response in mice, even when administered under conditions that permit them to be taken up by cells and perform detectable down-regulation of a target gene.

2.3 METHODS

2.3.1 Nucleic acids

Poly(I:C) was purchased from Amersham Biosciences. siRNA duplexes against luciferase ("siGL3"), *FAS* ("siFAS"), *c-Myc* ("siCMYC"), and a non-targeting control duplex ("siCNTL") were purchased from Dharmacon. All came purified and pre-annealed by the manufacturer ("Option C"). Sequences:

siGL3:
5′-CUUACGCUGAGUACUUCGAdTdT-3′
3′-dTdTGAAUGCGACUCAUGAAGCU-5′

siFAS:
5′-GUGCAAGUGCAAACCAGACdTdT-3′
3′-dTdTCACGUUCACGUUUGGUCUG-5′

siCMYC:
5′-UCCCGCGACGAUGCCCCUCdTdT-3′
3′-dTdTAGGGCGCUGCUACGGGGAG-5′

siCNTL:
5′-GACGUAAACGGCCACAAGUUC-3′
3′-CGCUGCAUUUGCCGGUGUUCA-5′

The luciferase-encoding plasmid (containing the firefly luciferase gene under the control of the human α_1-antitrypsin promoter and the apolipoprotein E locus control region) was a generous gift of A. McCaffrey and M. Kay. Where indicated, nucleic acids were pre-incubated with 50 μg/mL RNase (Roche) at 37 ^{o}C for 30 min prior to use.

2.3.2 RAW-264.7 studies

RAW-264.7 cells were purchased from the American Type Culture Collection and cultured in Dulbecco's Modified Eagle's Medium supplemented with 10% fetal bovine serum (heat-inactivated) and 1^{x} antibiotic-antimycotic (penicillin, streptomycin, and amphoterecin B).

5 x 10^6 cells were plated per well of a 24-well plate in medium containing 1.2% DMSO. After 24 h, mIFN-γ (Sigma) was added for 8 h to stimulate TLR3 expression. Lipopolysaccharide (LPS, Sigma, 1 μg/well), poly(I:C), or siRNA (siGL3) in indicated doses was added directly to appropriate wells for 24 h prior to harvesting the supernatant. IL-12(p40) levels were measured by ELISA (BD Biosciences) according to the manufacturer's instructions.

2.3.3 Mouse studies

Female BALB/c and C57BL/6 mice (Jackson Laboratories) were treated according to the NIH Guidelines for Animal Care and as approved by the Caltech Institutional Animal Care and Use Committee. All mice were 6-8 weeks of age at the time of injection. siRNA was formulated in D5W (5% (50 mg/mL) glucose in water) such that a 10% (vol/wt) injection provided a 2.5 mg/kg dose, unless otherwise indicated. Mouse tails were warmed with a heating pad prior to injection of a 0.2-mL (for "low-pressure") or a 2-mL (for "high-pressure") volume (per 20-g mouse) over ~3–5 sec. For co-injections of siRNA with plasmid DNA, 0.25 mg/kg DNA was delivered with 2.5 mg/kg of the appropriate siRNA. To determine luciferase levels, 0.2 mL of a 15 mg/mL solution of D-luciferin (Xenogen; in PBS) was injected intraperitoneally 10 min prior to imaging. To measure plasma cytokine levels, blood was harvested from mice 2 h post-injection by cardiac puncture, and plasma was isolated using Microtainer tubes (Becton Dickinson). [In preliminary experiments comparing the IL-12 response at 2 h, 6 h, and 24 h, post-injection, the maximum response was consistently observed at 2 h; therefore, data from the 2 h timepoint is used here.] IL-12(p40) and IFN-α levels (PBL Biomedical Laboratories) were measured by ELISA according to the manufacturer's instructions. To measure *FAS* mRNA levels, total RNA

was isolated from ~100 mg of liver tissue using the FastRNA Pro Green Kit (Qbiogene) and FastPrep Instrument (Qbiogene) for 40 sec at a speed setting of 6.0.

1 μg total RNA was first digested with amplification grade DNase I (Invitrogen) and then reverse transcribed into double-stranded cDNA using oligo-dT and Superscript II (Invitrogen) following the manufacturer's instructions. PCR primers were designed with MacVector 7.0 (Accelrys). The primer sequences are:

FAS (sense): 5'-GCAAACCAGACTTCTACTGCGATTC-3'
FAS (antisense): 5'-CCTTTTCCAGCACTTTCTTTTCCG-3'

For each PCR reaction, 1/40 (1 μL) of the cDNA reaction was amplified in a 25 μL reaction volume containing 0.5 μM of each primer and QuantiTect SYBR Green master mix (Qiagen). The real time quantitative PCR was performed and analyzed on SmartCycler (Cepheid). Standard curves were constructed by four serial 10-fold dilutions of cDNA starting from 1/20 (2 μL) of the cDNA reaction. Initial PCR conditions were 95 ^{o}C for 900 s; followed by 40 cycles of 95 ^{o}C for 15 s, 55 ^{o}C for 30 s, and 72 ^{o}C for 30 s; then a final denaturing stage of gradual increasing temperature from 60 ^{o}C to 95 ^{o}C. The denaturing stage is used to generate the melting curve of PCR products, which correlate with the size and GC content of the PCR product. A parallel internal control (β-actin) was amplified at an annealing temperature of 60 ^{o}C. All PCR products were analyzed on a 1% (wt/vol) agarose gel and a single band corresponding to the desired PCR product was observed in all reactions except negative controls. The reproducibility of the quantitative measurement of each sample was evaluated by at least three PCR measurements. The expression level of target gene was normalized to internal β-actin, and the mean and standard deviation of the target/β-actin ratios were calculated for sample-to-sample comparison.

2.4 RESULTS

2.4.1 Naked synthetic siRNA fails to induce a cytokine response in cultured cells

Poly(inosinic acid:cytidylic acid) (poly(I:C)), an analog of RNA, was included in these studies as a positive control for cytokine responses. In order to generate a sample of digested poly(I:C) for comparison with intact material, poly(I:C) was incubated with various concentrations of RNase and electrophoresed on an agarose gel (**Fig. 2.1**).

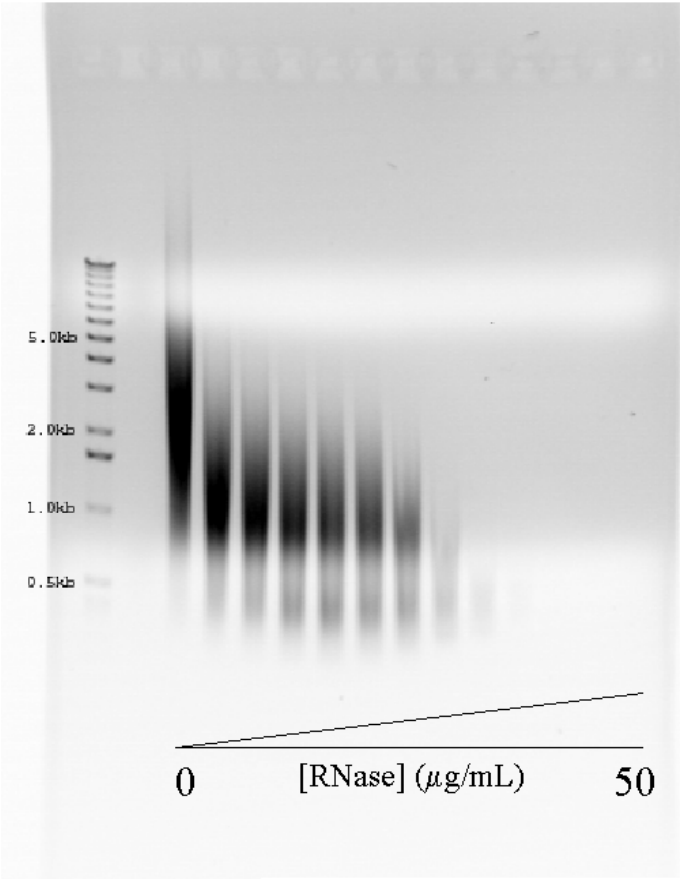

Figure 2.1 RNase degradation of poly(I:C). 1 μg poly(I:C) was incubated with RNase (at concentrations from 0–50 μg/mL) at 37 ^{o}C for 30 min, then electrophoresed on a 1% (wt/vol) agarose gel. A complete absence of nucleic acid signal was seen for all RNase concentrations of 50 μg/mL and higher.

Poly(I:C) is clearly very polydisperse, generating a broad smear even without exposure to RNase. As the concentration of RNase is increased, the poly(I:C) migrates further,

consistent with it being degraded into smaller fragments. For the highest RNase cconcentrations employed, no signal is visible on the gel, suggesting that the poly(I:C) has been completely degraded. This result suggests that the highest RNase concentration used (50 μg/mL) is satisfactory to induce total degradation of poly(I:C) under these conditions, and it will be used for subsequent experimental work.

We compared the effect of naked poly(I:C) and siRNA on cultured RAW-264.7 cells, a mouse monocyte/macrophage line that can be induced to secrete cytokines or express an NFκB-dependent reporter gene upon stimulation with poly(I:C). We exposed RAW-264.7 cells to various doses of intact poly(I:C), RNase-treated poly(I:C), or a synthetic siRNA duplex against luciferase (siGL3) for 24 h and measured levels of secreted IL-12(p40) in cell supernatants by enzyme-linked immunosorbent assay (ELISA) (**Figure 2.2**).

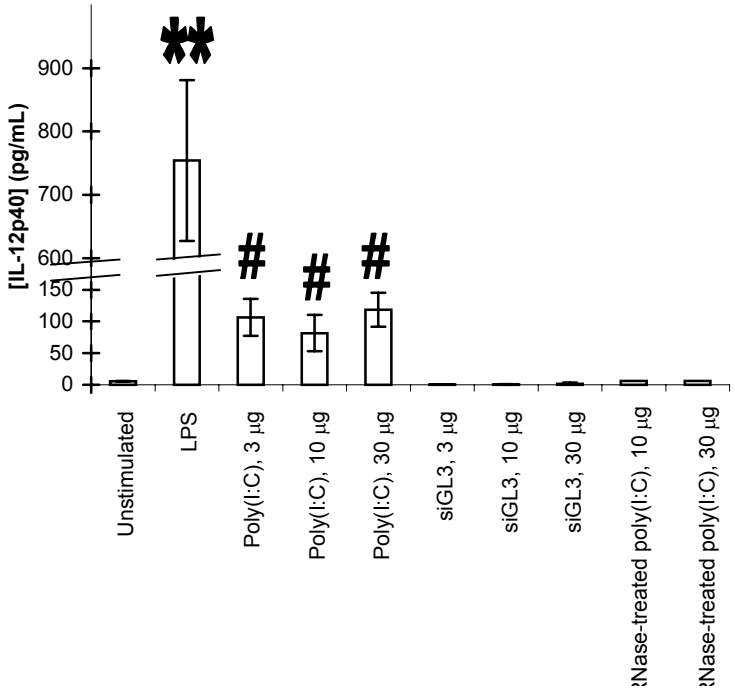

Figure 2.2 Poly(I:C), but not synthetic siRNA, induces IL-12 secretion by RAW-264.7 cells. IL-12(p40) levels in cell culture supernatants were measured upon 24 h exposure to the indicated nucleic acids and doses. The average of three replicate treatments is presented and error bars represent one standard deviation. Lipopolysaccharide (LPS), which is known to induce a strong IL-12 response through interaction with Toll-like receptor 4[9], was used as a positive control for the detection of IL-12 in the assay. [** denotes $P < 0.005$, # denotes $P < 0.30$]

At all three doses examined (3 μg, 10 μg, and 30 μg), poly(I:C) invoked a clear IL-12 response. In contrast, synthetic siRNA failed to induce a measureable IL-12 response at any dose. Pre-treatment of poly(I:C) with RNase completed abrogated the IL-12 response.

2.4.2 Naked synthetic siRNA fails to induce a cytokine response in mice

The effect of siRNA on IL-12 secretion was further examined in female BALB/c mice. Administrations of synthetic siRNA duplexes or poly(I:C) were performed as intraperitoneal (IP) injections or via the tail vein using either 'low-pressure' (LPTV, 1%

vol/wt) or 'high-pressure' (HPTV, 10% vol/wt) methods[10-12]. Blood was collected 2 h after injection, plasma was isolated, and IL-12(p40) levels were examined by ELISA (**Fig. 2.3**).

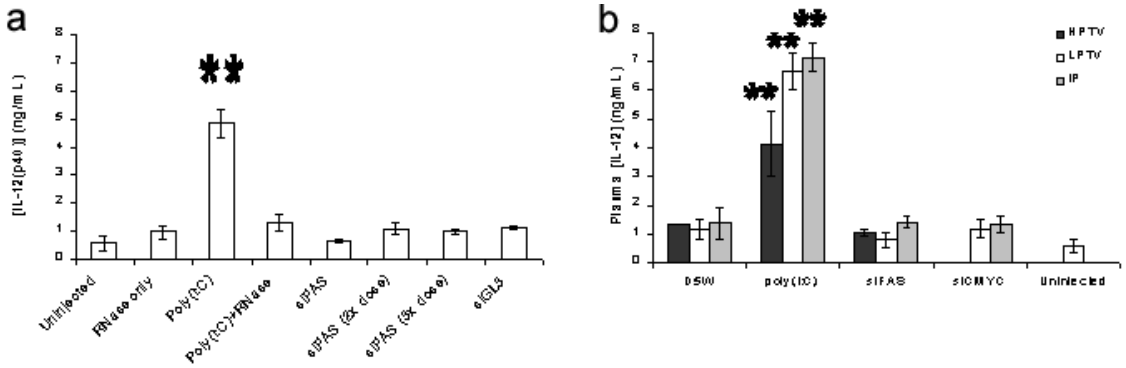

Figure 2.3 Poly(I:C), but not synthetic siRNA, induces IL-12 secretion in mice. (**a**) Plasma IL-12 levels in female BALB/c mice. 2.5 mg/kg (unless otherwise indicated) of nucleic acid was injected by high-pressure (10% vol/wt). and plasma was collected 2 h post-injection. The average of three replicate mice is presented. and error bars represent one standard deviation. (**b**) Effect of various types of administration. Mice received 2.5 mg/kg nucleic acid either intraperitoneally (IP) or through the tail vein via low-pressure (1% vol/wt, LPTV) or high-pressure (10% vol/wt, HPTV). The average of three replicate mice is presented. and error bars represent one standard deviation. [** denotes $P < 0.005$]

ELISA analyses of plasma IL-12 levels show, for each of the three different injection types, a strong induction by poly(I:C) that is absent with either a synthetic siRNA against *FAS*, *c-MYC*, or luciferase (siFAS, siCMYC, siGL3), or RNase-treated poly(I:C), even when the siFAS dose is increased up to threefold.

In addition to determining IL-12 concentrations, these experiments allow us to test for interferon responses. The plasma levels of IFN-α in BALB/c mice exposed to siRNA (siFAS, siGL3, or siCMYC) or poly(I:C) were measured by ELISA (**Fig. 2.4**).

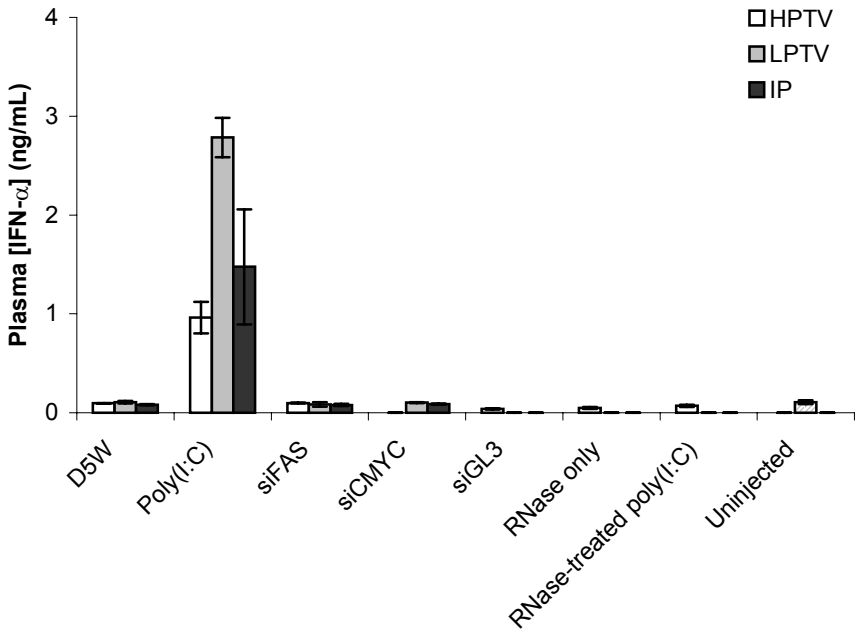

Figure 2.4 IFN-α induction in mice. 2.5 mg/kg of indicated nucleic acids were injected either intraperitoneally (IP) or through the tail vein via low-pressure (1% vol/wt, LPTV) or high-pressure (10% vol/wt, HPTV). Plasma was collected 2 h post-injection, and IFN-α levels were determined by ELISA. The average of three replicate mice is presented, and error bars represent one standard deviation. [* denotes $P < 0.005$, # denotes $P < 0.025$ vs. all other groups of same injection type]

As was observed with IL-12, each siRNA failed to elicit an IFN-α response whereas poly(I:C) induced a strong response that was eliminated by pre-treatment with RNase. Further, injected synthetic siRNAs (siFAS and siCMYC) failed to induce any significant changes in critical blood chemistry or liver enzyme levels except for the cases where the HPTV method of injection is used (**Fig. 2.5**).

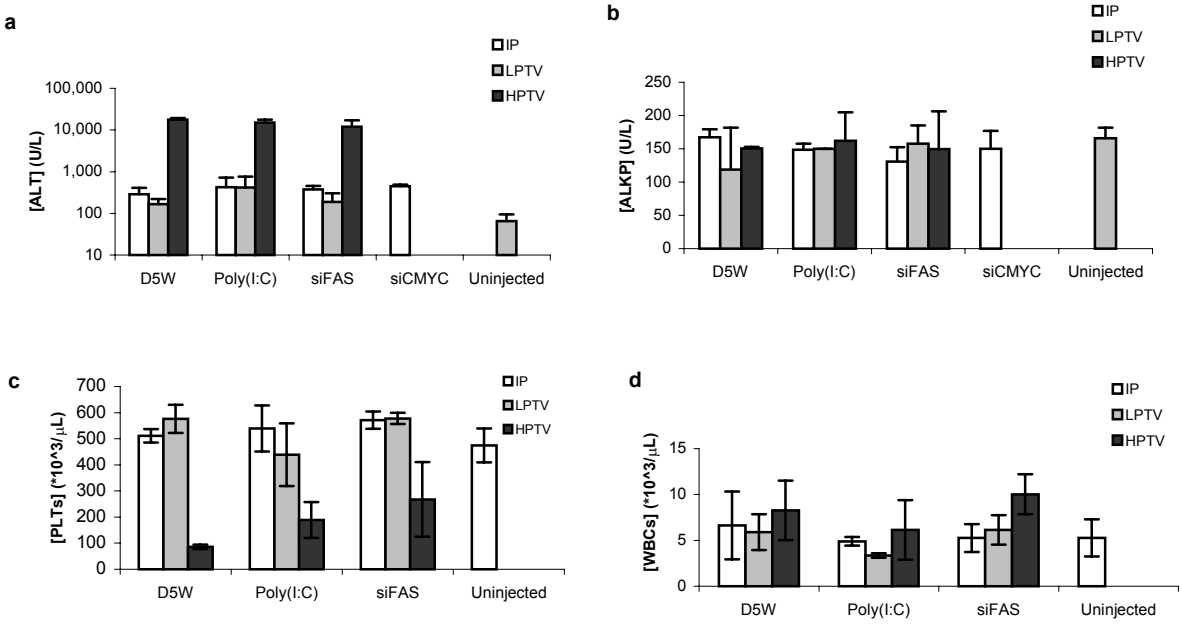

Figure 2.5 Synthetic siRNA does not alter mouse CBC or liver enzyme levels. (**a**) Alanine aminotransferase (ALT). (**b**) Alkaline phosphatase (ALKP). (**c**) Platelets (PLTs). (**d**) White blood cells (WBCs). For all panels, mice were injected with 5% (wt/vol) glucose in water (D5W) or 2.5 mg/kg indicated nucleic acids (in D5W) either intraperitoneally (IP) or through the tail vein via low-pressure (1% vol/wt, LPTV) or high-pressure (10% vol/wt, HPTV). Blood was collected 2 h post-injection. Whole blood was used to determine PLT and WBC levels, while plasma was isolated and used to determine ALT and ALKP levels. The average of three replicate mice is presented, and error bars represent one standard deviation.

Finally, since there is the possibility that the PKR response in BALB/c mice may be compromised relative to other mouse strains[13], some of the cytokine investigation experiments (originally performed with BALB/c mice) were reproduced in C57BL/6 mice, which are fully immunocompetent. The results show that the effects observed are consistent within these two strains (**Fig. 2.6**).

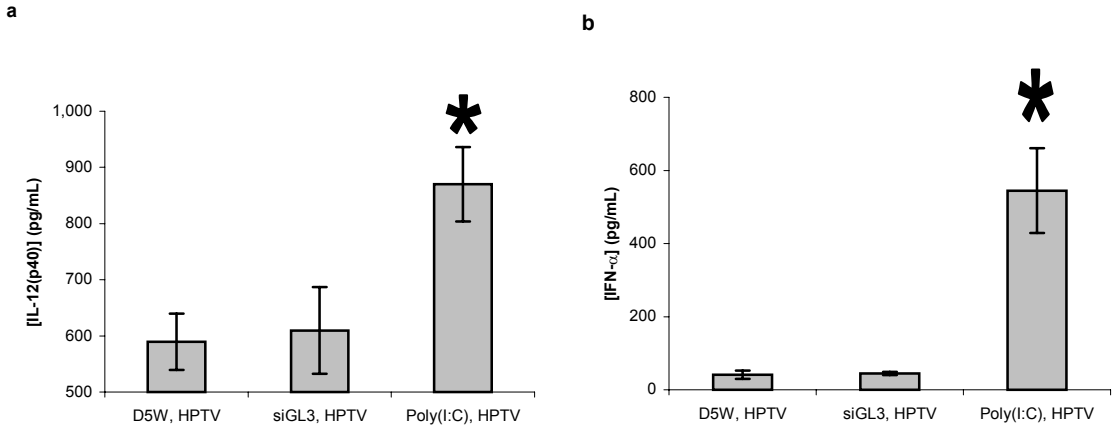

Figure 2.6 Lack of IL-12 and IFN-α induction by siRNA in C57BL/6 mice. (**a**) Plasma IL-12(p40) and (**b**) IFN-α levels in female C57BL/6 mice. 2.5 mg/kg of nucleic acid was injected by high-pressure (10% vol/wt), and plasma was collected 2 h post-injection. The average of three replicate mice is presented, and error bars represent one standard deviation. [* denotes $P < 0.005$ vs. all other treatment groups]

2.4.3. Synthetic siRNA achieves sequence-specific gene knockdown in cultured cells

While these results support the hypothesis that naked, synthetic siRNA duplexes do not induce an immune response in mice, further experimentation to verify nucleic acid stability and intracellular localization in the mice is necessary. A synthetic siRNA duplex (siCNTL) was exposed to active mouse serum for up to 8 h and then examined for degradation via agarose gel electrophoresis (**Fig. 2.7**).

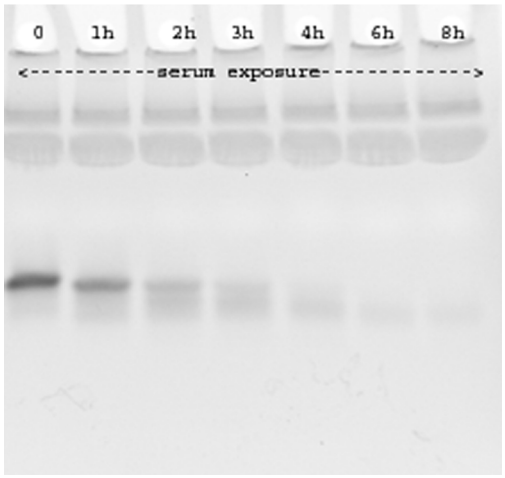

Figure 2.7 Degradation kinetics of synthetic siRNA in mouse serum. 40 pmol siCNTL was incubated in 20 μL mouse serum (active) at 37 ^{o}C for indicated times before being electrophoresed on a 15% (wt/vol) TBE gel.

This result indicates that some of the siRNA is still intact after exposure to serum for 2 h, which is the timeframe at which an IL-12 response was investigated in mice (see Fig. 2.3). Further, siRNA duplexes have been shown to achieve down-regulation of genes for several days in cultured cells[14]. When synthetic siRNA targeting luciferase (siGL3) is co-delivered with a luciferase-encoding plasmid (pGL3CV) to RAW-264.7 cells, sequence-specific down-regulation is observed 2 d post-transfection (**Fig. 2.8**).

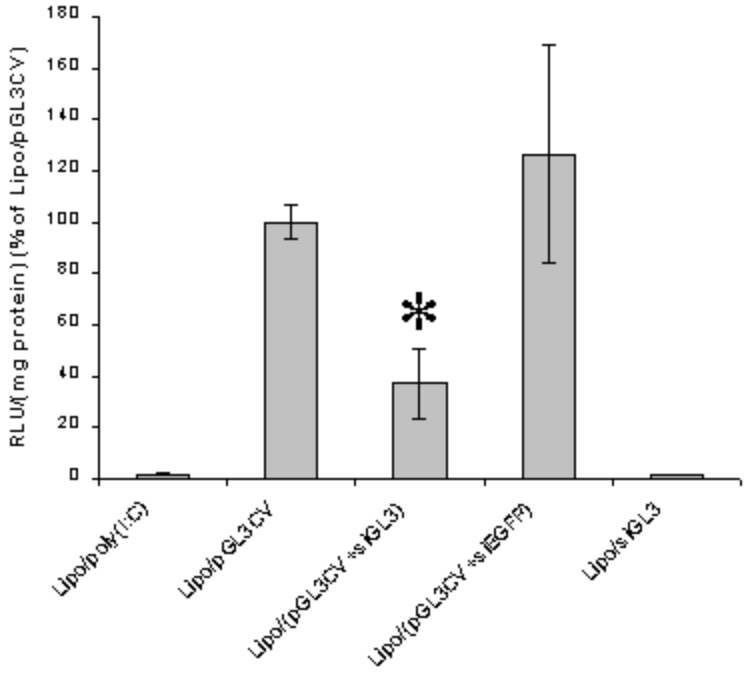

Figure 2.8. Sequence-specific target down-regulation by siRNA in RAW-264.7 cells. Co-lipofection of siRNA with pGL3CV in RAW-264.7 cells achieves sequence-specific luciferase down-regulation. Cultured RAW-264.7 cells were exposed to lipoplexes (containing Lipofectamine, made according to the manufacturer's instructions) containing 1 mg DNA and 20 nM siRNA (where indicated) for 4 h and then lysed at 48 h for measurement of luciferase and total protein levels. The average of three replicate treatments is present as the ratio of luciferase level (RLU; relative light units) to total protein level (mg protein) for each sample. Data are normalized to the average value for Lipofectamine/pGL3CV samples (no siRNA); this value ("100%") is equal to 7.51 x 10^6 RLU/(mg protein). Error bars represent one standard deviation. [* denotes $P < 0.05$ vs. all other treatment groups]

2.4.4 Synthetic siRNA achieves sequence-specific gene knockdown in mice

Additionally, we injected BALB/c mice with a luciferase-containing plasmid (encoding the firefly luciferase gene under the control of the liver-specific hAAT promoter with ApoE HCR enchancer, pApoEHCRLuc) alone or co-injected this plasmid with siRNA that contains the appropriate sequence to perform luciferase down-regulation (siGL3) or an unrelated sequence (siCNTL); all injections were HPTV. The *in vivo* luciferase expression was followed for two weeks after injection by live whole-animal bioluminescence

imaging[14-15]. A representative image containing one mouse from each of the three treatment groups 2 d post-injection is shown in **Figure 2.9**.

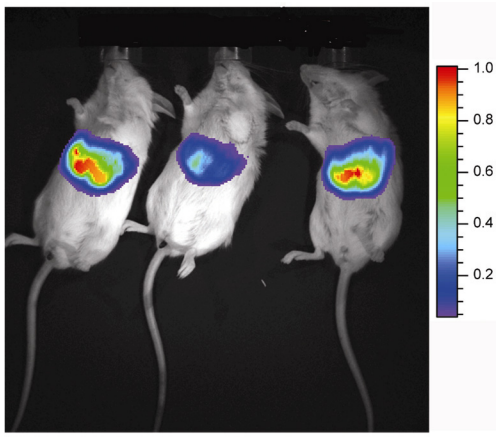

Figure 2.9. Efficacy of synthetic siRNA in mice. *In vivo* whole-body imaging of female BALB/c mice injected by HPTV with luciferase-encoding plasmid alone (left) or with siRNA targeting luciferase (siGL3, center) or non-targeting control siRNA (siCNTL, right). These mice were imaged 2 d post-injection and 10 min after IP administration of D-luciferin (for visualization). Scale bar has units of [photons/s/cm^2/sr]. Sequence-specific reduction in luciferase signal is seen for the siGL3-treated mouse (center).

The cumulative signal from each mouse was quantified at each time point, and the results are plotted in **Figure 2.10**.

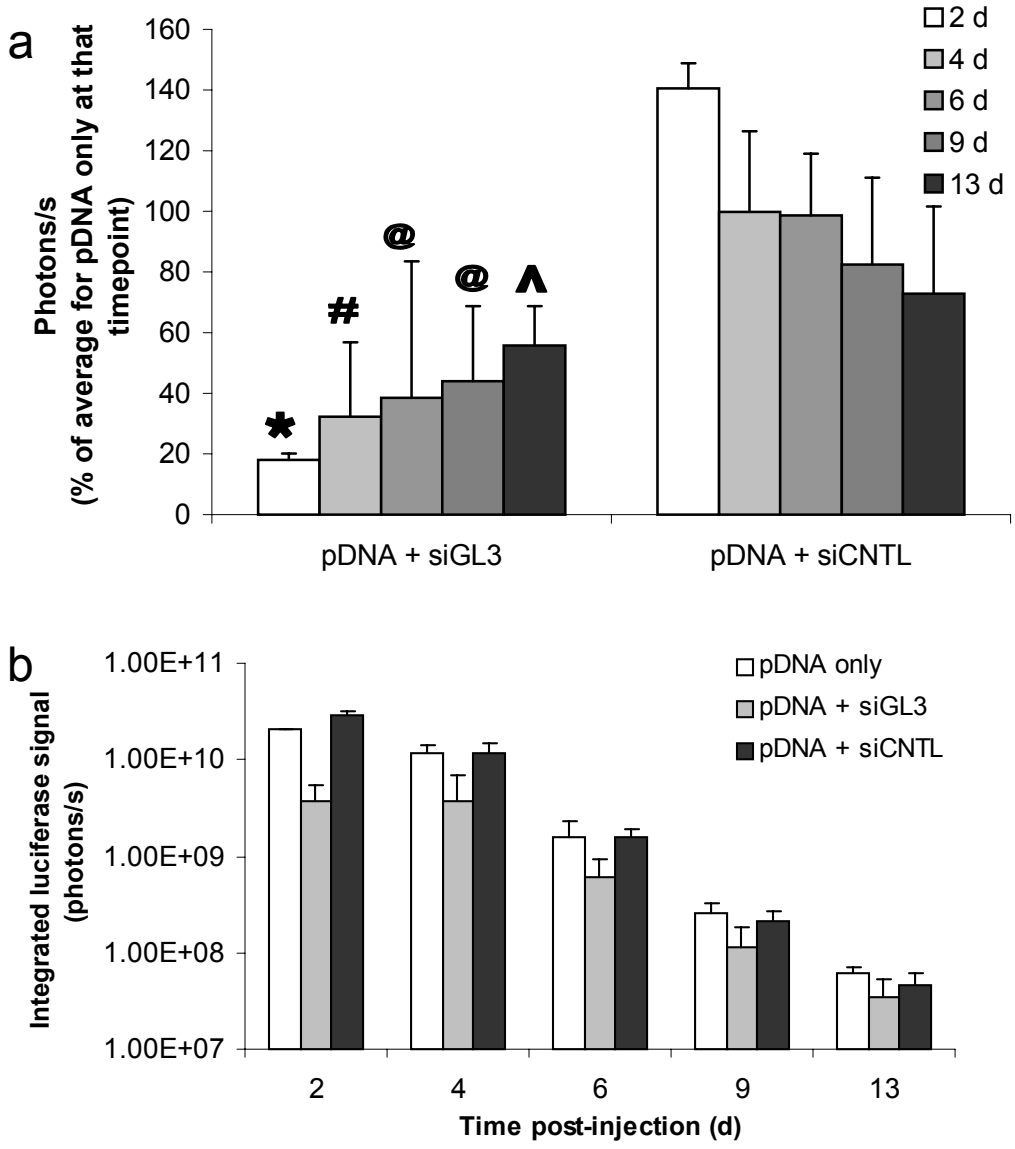

Figure 2.10. Synthetic siRNA accomplishes sequence-specific RNAi of an exogenous target in mice. (**a**) BALB/c mice were imaged over two weeks post-injection and total luciferase signals were integrated, quantified, and normalized to mice that received pDNA only at each time point. The average of three or more replicate mice is presented, and error bars represent one standard deviation. [* denotes $P < 0.005$ at t=2 d, # denotes $P < 0.025$ at t=4 d, @ denotes $P < 0.05$ at t=6,9 d, ^ denotes $P < 0.1$ at t=13 d. The "pDNA + siCNTL" group was not statistically different from mice that received pDNA only at these levels of significance for any of the timepoints examined.] (**b**) Raw (unnormalized) results from mice presented in (a).

Mice co-injected with the luciferase-targeting siRNA display a significant ($P < 0.1$ or better for all time points) down-regulation of luciferase expression that is not observed with the control siRNA. The sequence-specific RNAi demonstrates that intact siRNA do reach intracellular targets and are functional *in vivo* at the conditions of our studies.

A second efficacy experiment in mice showed that HPTV injection of siFAS reduces the level of *FAS* mRNA in mouse liver (**Fig. 2.11**).

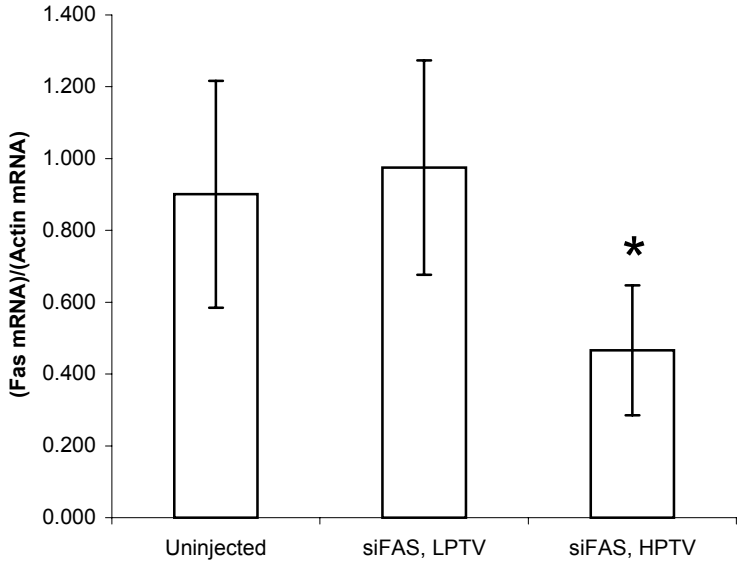

Figure 2.11 Synthetic siRNA accomplishes sequence-specific RNAi of an endogenous target in mice. BALB/c mice were injected with siFAS by HPTV or LPTV and sacrificed 24 h post-injection. *FAS* mRNA levels were quantified and normalized to β-actin by RT-PCR. The average of three replicate mice is presented, and error bars represent one standard deviation. [* denotes $P < 0.1$]

Both of these experiments demonstrate that, at least when delivered under these conditions, synthetic siRNA can be efficacious *in vivo*. Thus the HPTV method of administering siRNA used here for examination of immunogenicity also provides for cellular uptake and gene down-regulation in the livers of mice[14,16-17]. Given the stability and efficacy of multiple siRNAs, the lack of IL-12 and IFN-α expression obtained in mice suggests that

synthetic siRNAs used in this study do not elicit an observable immune response when administered naked by LPTV, HPTV, or IP methods in the amounts used here.

2.5 DISCUSSION

Because small interfering RNA (siRNA) has shown impressive efficacy for down-regulation of a target mRNA in a number of different cell lines and *in vivo* models, it has tremendous potential for development into a therapeutic. However, some published reports have linked siRNA with off-target gene down-regulation and immunogenicity. The objective of the work in this chapter is to determine whether or not synthetic siRNA duplexes are indeed immunostimulatory, both in cultured cells and in mice, prior to investigation of our polymeric system to deliver them.

In cultured cells, there are reports of non-specific gene target effects that include off-target gene suppression and upregulation of type I interferons (IFNs)[5-7,18-19]. Hypotheses for the mechanism belying this IFN response include recognition of the siRNA by Toll-like receptors 3 (TLR3) and 9 (TLR9) and/or induction of protein kinase PKR pathways. When we applied naked synthetic siRNA to cultured cells known to be responsive to the downstream target of TLR3 and TLR9 signaling, the transcription factor NFκB, we failed to observe a cytokine response. PKR is known to recognize dsRNA molecules of at least ~30 bp in length[1]; the synthetic duplexes we examined here should all be too small to trigger an PKR response. The cytokine response induced by poly(inosinic acid:cytidylic acid) (poly(I:C)), a large analog of RNA that is known to elicit an immune response in mice[20-21], could be eliminated by pre-treatment with RNase.

It is known that TLR3 is located both on the cell surface and intracellularly in human fibroblasts but remains intracellular in others, such as monocyte-derived immature dendritic cells[22]. CpG-containing oligonucleotide/TLR9 interactions require internalization of the nucleic acid with TLR9-bearing cells[23]. Thus, proof of nucleic acid stability and

intracellular localization in the mice are necessary. We showed that ~50% of synthetic siRNA remains intact upon exposure to active mouse serum of 2 h. This suggests that the lack of plasma cytokine (IL-12, IFN-α) responses seen in mice 2 h after injection with siRNA is truly the result of intact siRNA failing to trigger any response. Further, in showing down-regulation of both exogenous (luciferase) and endogenous (*FAS*) targets after injection of synthetic siRNA in mice, we demonstrate the efficacy of these duplexes *in vivo* under our experimental conditions. The down-regulation of *FAS* observed upon 'high-pressure' tail vein (HPTV) injection was not seen upon 'low-pressure' injection (LPTV) of the same siRNA at the same dose, consistent with previous observations that high-pressure is required to achieve down-regulation of a target gene by naked siRNA in mice, even if the siRNA is chemically stabilized[14].

There is the possibility that the PKR response in BALB/c mice may be compromised relative to other mouse strains[13]. Researchers have shown IL-12 responses to poly(I:C) *in vitro* with RAW-264.7 cells and in serum after IP injection in C57BL/6 mice like those shown here with the same cell line and BALB/c mice[24]. We reproduced some of our experiments performed with the BALB/c mice in C57BL/6 mice, and the results show that the effects observed are consistent within those two strains.

In conclusion, we examined the response of mice to naked siRNAs. Plasma IL-12 and IFN-α levels that were observed in mice by injection of poly(I:C) (used as a positive control) were not obtained with siRNA. Pre-digestion of poly(I:C) with RNase abrogated these responses. Co-injection of siRNA and a luciferase-expressing plasmid into mice followed by *in vivo* whole-animal imaging confirms the uptake and sequence-specific function of injected synthetic siRNA. HPTV injection of siRNA alone was also shown to

down-regulate an endogenous target gene (*FAS*) in mice. Taken together, the results contained within this chapter suggest that synthetic siRNAs are well tolerated in mice and that it is indeed possible for siRNAs to down-regulate targets *in vivo* without stimulating an interferon response.

Finally, very recently, the lack of immunogenicity seen here with naked synthetic siRNAs has been confirmed by multiple other researchers[25-26], further strengthening the claim made here that synthetic siRNAs may be safe and efficacious for applications in animals. There have been additional reports that particular motifs within siRNA duplexes endow them with sequence-specific immunogenicity[25-28]. This issue, in the context of our polymeric delivery system, will be discussed in more detail in Chapter 4.

2.6 REFERENCES

[1] Manche L, Green SR, Schmedt C & Mathews MB. Interactions between double-stranded RNA regulators and the protein kinase DAI. *Mol. Cell Biol.* **12**, 5238-5248 (1992).

[2] Minks MA, West DK, Benvin S & Baglioni C. Structural requirements of double-stranded RNA for the activation of 2',5'-oligo(A) polymerase and protein kinase of interferon-treated HeLa cells. *J. Biol. Chem*. **254**, 10180-10183 (1979).

[3] Elbashir SM, Harborth J, Lendeckel W, Yalcin A, Weber K & Tuschl T. Duplexes of 21-nucleotide RNAs mediate RNA interference in cultured mammalian cells. *Nature* **411**, 494-498 (2001).

[4] Harborth J, Elbashir SM, Bechert K, Tuschl T, & Weber K. Identification of essential genes in cultured mammalian cells using small interfering RNAs. *J. Cell Sci.* **114**, 4557-4565 (2001).

[5] Sledz CA, Holko M, de Veer MJ, Silverman RH & Williams BRG. Activation of the interferon system by short-interfering RNAs. *Nat. Cell Biol.* **5**, 834-839 (2003).

[6] Bridge AJ, Pebernard S, Ducraux A, Nicoulaz A-L & Iggo R. Induction of an interferon response by RNAi vectors in mammalian cells. *Nat. Genet*. **34**, 263-264 (2003).

[7] Moss EG & Taylor JM. Small interfering RNAs in the radar of the interferon system. *Nat. Cell Biol.* **5**, 771-772 (2003).

[8] Hwang SJ, Bellocq NC & Davis ME. Effects of structure of beta-cyclodextrin-containing polymers on gene delivery. *Bioconjug. Chem*. **12**, 280-290 (2001).

[9] Chow JC, Young DW, Golenbock DT, Christ WJ & Gusovsky F. Toll-like receptor-4 mediates lipopolysaccharide-induced signal transduction. *J. Biol. Chem*. **274**, 10689-10692 (1999).

[10] Lecocq M, Andrianaivo F, Warnier M-T, Wattiaux-De Coninck S, Wattiaux R & Jadot M. Uptake by mouse liver and intracellular fate of plasmid DNA after a rapid tail vein injection of a small or a large volume. *J. Gene Med*. **5**, 142-156 (2003).

[11] Andrianaivo F, Lecocq M, Wattiaux-De Coninck S, Wattiaux R & Jadot M. Hydrodynamics-based transfection of the liver: entrance into hepatocytes of DNA that causes expression takes place very early after injection. *J. Gene Med*. **6**, 877-883 (2004).

[12] Crespo A, Peydro A, Dasi F, Benet M, Calvete JJ, Revert F & Alino SF. Hydrodynamic liver gene transfer mechanism involves transient sinusoidal blood stasis and massive hepatocyte endocytic vesicles. *Gene Ther*. **Advanced Online Publication**, 1-9 (Feb 24, 2005).

[13] Durbin RK, Mertz SE, Koromilas AE & Durbin JE. PKR protection against intranasal vesicular stomatitis virus infection is mouse strain dependent. *Viral Immunol*. **15**, 41-51 (2002).

[14] Layzer JM, McCaffrey AP, Tanner AK, Huang Z, Kay MA & Sullenger BA. In vivo activity of nuclease-resistant siRNAs. *RNA* **10**, 766-771 (2004).

[15] Wu JC, Sundaresan G, Iyer M & Gambhir SS. Non-invasive optical imaging of firefly luciferase reporter gene expression in skeletal muscles of living mice. *Molecular Therapy* **4**, 297-306 (2001).

[16] Zender L, Hutker S, Liedtke C, Tillmann HL, Zender S, Mundt B, Waltermathe M, Gosling T, Flemming P, Malek NP, Trautwein C, Manns MP, Kuhnel F & Kubicka S. Caspase 8 small interfering RNA prevents acute liver failure in mice. *Proc. Natl. Acad. Sci USA* **100**, 7797-7802 (2003).

[17] Song E, Lee SK, Wang J, Ince N, Ouyang N, Min J, Chen J, Shankar P & Lieberman J. RNA interference targeting Fas protects mice from fulminant hepatitis. *Nat. Med*. **9**, 347-351 (2003).

[18] Kim D-H, Longo M, Han Y, Lundberg P, Cantin E & Rossi JJ. Interferon induction by siRNAs and ssRNAs synthesized by phage polymerase. *Nat. Biotechnol.* **22**, 321-325 (2004).

[19] Jackson AL, Bartz SR, Schelter J, Kobayashi SV, Burchard J, Mao M, Li B, Cavet G & Linsley PS. Expression profiling reveals off-target gene regulation by RNAi. *Nat. Biotechnol.* **21**, 635-637 (2003).

[20] Alexopoulou L, Czopik Holt A, Medzhitov R & Flavell RA. Recognition of double-stranded RNA and activation of NF-kappaB by Toll-like receptor 3. *Nature* **413**, 732-738 (2001).

[21] Matsumoto M, Kikkawa S, Kohase M, Miyake K & Seya T. Establishment of a monoclonal antibody against human Toll-like receptor 3 that blocks double-stranded RNA-mediated signaling. *Biochem. Biophys. Res. Commun*. **293**, 1364-1369 (2002).

[22] Matsumoto M, Funaki K, Tanabe M, Oshiumi H, Shingai M, Seto Y, Yamamato A & Seya T. Subcellular localization of Toll-like receptor 3 in human dendritic cells. *J. Immunol*. **171**, 3154-3162 (2003).

[23] Ahmad-Nejad P, Hacker H, Rutz M, Bauer S, Vabulas RM & Wagner H. Bacterial CpG-DNA and lipopolysacchardies activate Toll-like receptors at distinct cellular compartments. *Eur. J. Immunol*. **32**, 1958-1968 (2002).

[24] Whitmore MM, De Veer MK, Edling A, Oates RK, Simons B, Lindner D & Williams BR. Synergistic activation of innate immunity by double-stranded RNA and CpG DNA promotes enhanced antitumor activity. *Cancer Res.* **64**, 5850-5860 (2004).

[25] Ma Z, Li J, He F, Wilson A, Pitt B & Li S. Cationic lipids enhance siRNA-mediated interferon response in mice. *Biochem. Biophys. Res. Commun*. **330**, 755-759 (2005).

[26] Judge AD, Sood V, Shaw JR, Fang D, McClintock K & MacLachlan I. Sequence-dependent stimulation of the mammalian innate immune response by synthetic siRNA. *Nat. Biotechnol*. **23**, 457-462 (2005).

[27] Hornung V, Guenthner-Biller M, Bourquin C, Ablasser A, Schlee M, Uematsu S, Noronha A, Manoharan M, Akira S, de Fougerolles A, Endres S & Hartmann G. Sequence-specific potent induction of IFN-alpha by short interfering RNA in plasmacytoid dendritic cells through TLR7. *Nat. Med.* **11**, 263-270 (2005).

[28] Sioud M. Induction of inflammatory cytokines and interferon responses by double-stranded and single-stranded siRNAs is sequence-dependent and requires endosomal localization. *J. Mol. Biol*. **348**, 1079-1090 (2005).

CHAPTER 3: Creation and Characterization of CDP/siRNA Complexes

3.1 ABSTRACT

In Chapter 2 the safety (non-immunogenicity) of synthetic small interfering RNA (siRNA) duplexes, both in cultured cells and in mice, was demonstrated. Here the interaction of siRNA with a cyclodextrin-containing polycation (CDP) into complexes suitable for delivery to cells is investigated. When added to nucleic acids, either siRNA or plasmid DNA (pDNA), CDP condenses them into small polymer-siRNA or polymer-pDNA complexes ("polyplexes") that have ~50-100 nm in diameter. Complexation with CDP endows siRNA with protection from nucleases and permits high levels of uptake by recipient cells. These polyplexes can be stabilized by incorporation of a neutral polymer, poly(ethylene glycol) (PEG), to which a ligand, such as lactose or transferrin, can be tethered for targeting of particular cell type(s). These CDP/siRNA polyplexes are excellent candidates to achieve RNA interference (RNAi) of a desired target gene.

3.2 INTRODUCTION

The synthesis and characterization of cyclodextrin-containing polycations (CDPs), the first polycations designed specifically for the delivery of DNA, have been described[1]. Systematic investigations of modifications in the presence and type of sugar and the type of and spacing between charge centers have led to a thorough understanding of the effects of these parameters on the gene delivery efficiency and toxicity of polymer-DNA complexes ("polyplexes")[2-4]. From these and other studies[5], an amine-terminated, β-cyclodextrin- (β-CD-)containing polymer possessing cationic amidine groups separated by six methylene groups emerged as a leading candidate for further development (**Fig. 3.1a**).

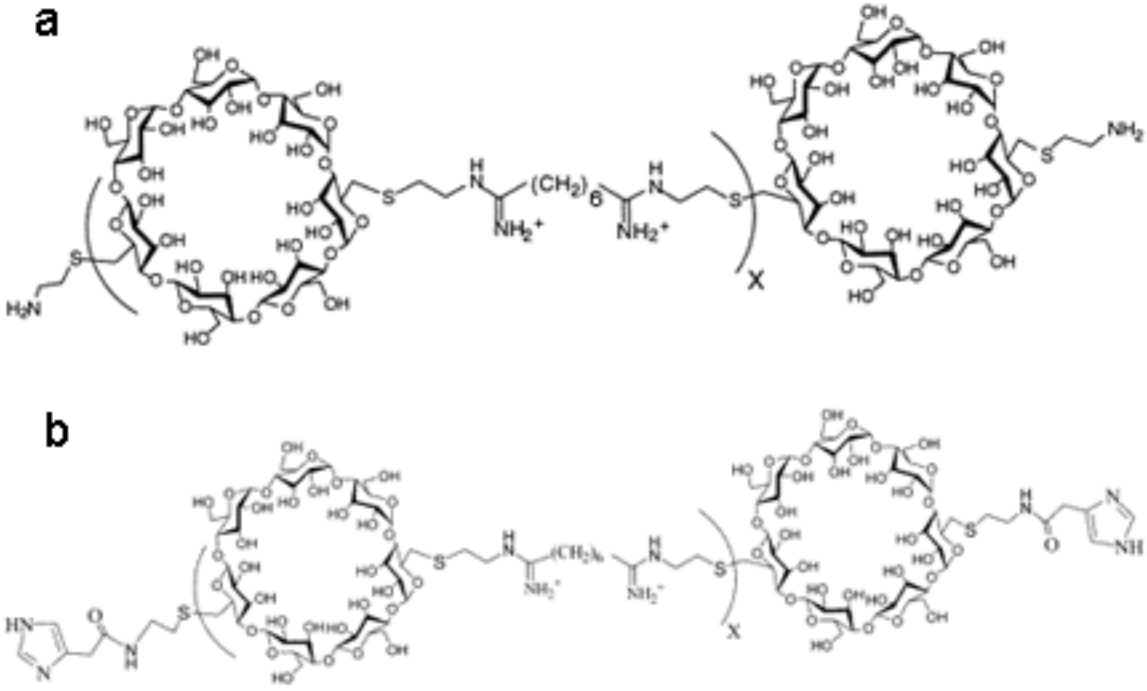

Figure 3.1. Structures of amine- and imidazole-terminated β-cyclodextrin-containing polycations. (**a**) Amine-terminated polycation. (**b**) Imidazole-terminated polycation.

While transfection with polyplexes made with this amine-terminated polymer generated levels of gene expression in cultured cells comparable to that seen with the best

commercially-available polycation and lipid reagents[1,6], microscopic analysis of transfected cells suggested that the majority of intracellular polyplexes were sequestered within endosomal vesicles[6-7]. These vesicles are known to acidify within the cell and ultimately fuse with lysosomes, leading to degradation of intravesicular contents. Modification of polymer termini to contain imidazole (Im) moieties (**Fig. 3.1b**), which are known to act as a buffer within the pH range of vesicular acidification, leads to increased gene expression and the observation of unpackaging polyplexes within transfected cells (**Fig. 3.2**).

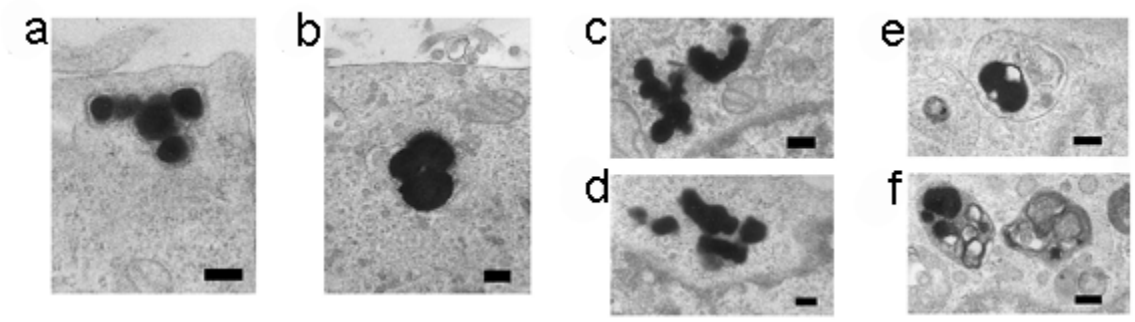

Figure 3.2. Imidazole-modification of CDP increases intracellular unpackaging of polyplexes. Cultured BHK (baby hamster kidney) cells were exposed to DNA-containing polyplexes made with either amine-terminated (**a**, **c**, **d**) or imidazole-terminated (**b**, **e**, **f**) CDP and examined by transmission electron microscopy (TEM). In (**a**) and (**b**), shortly after uptake, polyplex-containing vesicles are at relatively neutral pH and are located close to the plasma membrane. In (**c**)-(**f**), after additional intracellular trafficking, vesicles have acidified and have translocated to the perinuclear region. Unpacking of polyplexes made with an imidazole-terminated CDP (**e**, **f**) is observed but not for those with amine-terminated CDP (**c**, **d**). [These images adopted from Mishra *et al*., 2004[7]]

While they are potent gene delivery systems in cultured cells, these CDP-containing polyplexes readily aggregate at physiological conditions, owing to their positively-charged colloidal nature[8]. This problem of polyplex aggregation is most commonly overcome by covalent modification of polyplexes with a neutral polymer, such as poly(ethylene glycol) (PEG). While it is possible to perform this covalent PEGylation and not disrupt polyplexes[9], others have reported that this modification alters polyplex morphologies[10] or

even prevents DNA condensation[11]; similar difficulties were observed with covalently PEGylated CDP[8].

However, the unique structure of β-CD allows for a novel approach to the PEGylation of CDP-containing polyplexes. PEG is tethered to a small molecule, adamantane (AD), that is known to form strong, non-covalent inclusion complexes with β-CD[12] (**Fig 3.3a**). Addition of AD-PEG conjugates to CDP and the resulting inclusion complex formation permits the introduction of PEG at sites allosteric to those involved in nucleic acid binding (**Fig. 3.3b**). Indeed, unlike their unPEGylated counterparts, CDP-containing polyplexes modified with AD-PEG retain their as-formulated size when exposed to salt[8] (**Fig. 3.3c**).

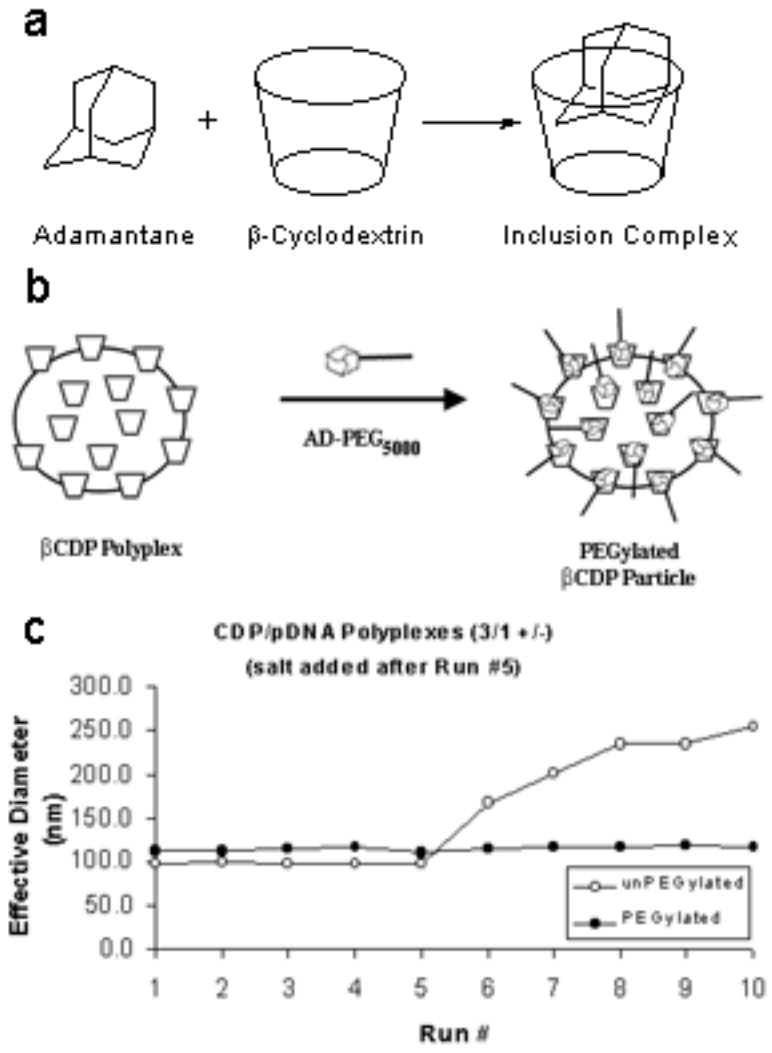

Figure 3.3. Modification of CDP/DNA polyplexes with AD-PEG confers salt stability. (**a**) Adamantane (AD) interacts strongly and non-covalently with β-cyclodextrin (β-CD) through inclusion complex formation. (**b**) Polyplexes prepared with a β-CD-containing polycation (CDP) are modified with poly(ethylene glycol) (PEG) by addition of an AD-PEG conjugate. (**c**) The sizes of CDP/DNA polyplexes, PEGylated vs. unPEGylated, are measured in salt-free and salt-containing media by dynamic light scattering (DLS). Measurements were made in water for 30-sec periods over 2 min, then 0.11 volumes of phosphate-buffer saline (PBS) were added to bring the solution to a 1^x (150 mM) final concentration. Measurements were continued for an additional 2.5 min. While a steady increase in size was seen for unPEGylated polyplexes after the addition of salt, the size of PEGylated polyplexes remained stable.

CDP-containing polyplexes can be further modified to incorporate a targeting ligand to direct their selective uptake by particular cell types. For example, transferrin (Tf) can be

introduced through synthesis of an AD-PEG-Tf conjugate; this conjugate had been shown to enhance polyplex uptake by cells that express high levels of the cell-surface transferrin receptor (TfR)[13-14].

While much work has already been done to better understand this CDP system, there still remain a number of unanswered questions regarding the exact composition and nature of CDP-containing polyplexes. The amount and effect of unbound (i.e., not within polyplexes) material within polyplex formulations remain heretofore undetermined. Quantification of AD-PEG binding to polyplexes and its effect on cellular uptake warrant investigation. Further, all of the developmental work discussed above was done in the context of DNA, almost exclusively with relatively large (~3-10 kbp) plasmids. It remains to be determined if polyplexes can be prepared with small interfering RNA (siRNA) duplexes and, if so, how the polyplex properties might be affected. All of these issues are addressed in Chapter 3.

A gel retardation assay is employed to demonstrate that an equivalent amount of imidazole-terminated polymer is required to bind the same mass of pDNA or siRNA. Despite the ~100-fold difference in molecular weight between a single siRNA duplex and pDNA molecule, polyplexes prepared with both nucleic acid types have comparable size and display similar dependences of size on concentration. PEGylation of both siRNA-containing and pDNA-containing polyplexes (via AD-PEG) confers salt stability, sharply reduces variation in size with formulation concentration, and lowers measured surface charge (zeta potential). Flow cytometry and fluorescence microscopy are used to demonstrate that siRNA-containing polyplexes are readily endocytosed by cultured cells, and an *in vitro* serum stability assay indicates that siRNA within these polyplexes is

protected from serum nuclease degradation. A method is developed to quantify the amount of polymer bound (vs. unbound) within siRNA- and pDNA-containing polyplexes; for both nucleic acid types and at all overall charge ratios examined, this amount is just enough to provide sufficient positive charges to balance the negative charges within the nucleic acids. Taken together, these results suggest that CDP/siRNA polyplexes will be suitable for RNAi applications in cultured cells and *in vivo*.

3.3 METHODS

3.3.1 Polymers

Unless otherwise noted, an imidazole-terminated, cyclodextrin-containing polycation (CDP) was used for all studies and synthesized as described previously[1,13]. Adamantane-poly(ethylene glycol) (AD-PEG) conjugates, made with PEG_{5000}, were synthesized as described previously[8]. Ligand-containing modifiers, including lactose (AD-PEG-Lac) and transferrin (AD-PEG-Tf), were synthesized as described previously[13,15].

3.3.2 Nucleic acids

For all DNA-containing samples, the pGL3-Control Vector (Promega) was used. For all samples containing unlabeled siRNA, the "Luciferase GL3 duplex" ("siGL3," Dharmacon), was used. Fluorescein-labeled siRNA (single, covalent fluorescein modification at the 5' end of the sense strand; "FL-siRNA") used was the "FL-siGL2" duplex (Dharmacon). Sequences:

siGL3:
```
5′-CUUACGCUGAGUACUUCGAdTdT-3′
3′-dTdTGAAUGCGACUCAUGAAGCU-5′
```

FL-siGL2:
```
5′-[Fluorescein]CGUACGCGGAAUACUUCGAdTdT-3′
          3′-dTdTGCAUGCGCCUUAUGAAGCU-5′
```

3.3.3 Gel retardation studies

Solutions of either pDNA or siRNA were prepared by diluting 0.5 μg nucleic acid to a concentration of 0.1 μg/μL in distilled water. An equal volume (5 μL) of CDP (at various concentrations) was added to each pDNA or siRNA solution; the resulting 10-μL solutions were incubated at room temperature for 30 min to allow polyplex formation. Two

microliters of loading buffer (0.03% bromophenol blue, 0.03% xylene cyanol FF, 10 mM Tris-HCl, 50 mM EDTA) were added to each polyplex solution, and 10 μL (of a total of 12 μL) of the resulting solutions were loaded per well of a 1% (for pDNA-containing samples) or 4% (for siRNA-containing samples) agarose gel in 1^x TAE buffer (40 mM Tris-Acetate, 1 mM EDTA, pH 8.3) with 0.1 μg/mL ethidium bromide. Gels were electrophoresed at 100 V for 60 min before visualization.

Charge ratio calculations were made based on each CDP repeat unit having two positive charges and a molecular weight of 1460 Da and each pDNA/siRNA repeat unit (base pair) having two negative charges and a molecular weight of 660 Da. The desired charge ratios (0, 0.5, 1, …, 5 +/-) correspond to the following concentrations:

Charge Ratio (+/-)	**CDP-Im (5 μL)**	**siGL3 or pDNA (5 μL)**
0	0 mg/mL	0.1 mg/mL
0.5	0.1106 mg/mL	0.1 mg/mL
1	0.2212 mg/mL	0.1 mg/mL
1.5	0.3318 mg/mL	0.1 mg/mL
2	0.4424 mg/mL	0.1 mg/mL
2.5	0.553 mg/mL	0.1 mg/mL
3	0.6636 mg/mL	0.1 mg/mL
3.5	0.7742 mg/mL	0.1 mg/mL
4	0.8848 mg/mL	0.1 mg/mL
4.5	0.9954 mg/mL	0.1 mg/mL
5	1.106 mg/mL	0.1 mg/mL

3.3.4 Dynamic light scattering (DLS) studies of polyplex size and zeta potential.

A CDP solution (in distilled water) was added to an equal volume containing 2 μg of pDNA or siRNA at a charge ratio of 3/1 +/-. While the charge ratio was fixed, four different concentration combinations of CDP and nucleic acid were examined:

Sol'n	CDP	pGL3CV or siGL3	H_2O
A	20 μL @ 0.6636 mg/mL	20 μL @ 0.1 mg/mL	1160 μL
B	50 μL @ 0.2654 mg/mL	50 μL @ 0.04 mg/mL	1100 μL
C	100 μL @ 0.1327 mg/mL	100 μL @ 0.02 mg/mL	1000 μL
D	600 μL @ 0.02212 mg/mL	600 μL @ 0.00333 mg/mL	(0 μL)

The resulting solutions were incubated at room temperature for 30 min to allow polyplex formation. An appropriate volume of distilled water (indicated in the above table) was then added to give a total sample volume of 1200 μL.

For formulations PEGylated after polyplex formation ("post-PEGylated"), an appropriate amount of an AD-PEG solution (4.95 μL of a 20 mg/mL AD-PEG solution, corresponding to a 1:1 molar ratio of AD:β-CD) was added prior to "voluming up" to a total sample volume of 1200 μL with water.

For formulations PEGylated before polyplex formation ("pre-PEGylated"), an appropriate amount of an AD-PEG solution (4.95 μL of a 20 mg/mL AD-PEG solution, corresponding to a 1:1 molar ratio of AD:β-CD) was added to CDP. The resulting CDP/AD-PEG solution was added to the nucleic acid solution and subsequently "volumed up" to a total sample volume of 1200 μL with water.

Polyplex solutions were loaded into polystyrene cuvettes and polyplex size (effective hydrodynamic diameter) was determined by dynamic light scattering (DLS) using a ZetaPALS (Brookhaven Instruments) instrument. Ten successive measurements of 30 sec each were performed. For appropriate samples, 600 μL phosphate-buffer saline (PBS) solution was added after the fifth measurement. After measuring polyplex size, the surface charge (zeta potential) of polyplex solutions was subsequently measured using the same instrument (Smoluchowski method, 10 runs, target residual = 0.05, pH = 6.0, SR-101 (solvent-resistant) device).

3.3.5 Flow cytometry and confocal microscopy to assess polyplex uptake

HeLa (human cervical carcinoma) cells were cultured in Dulbecco's Modified Eagle's Medium (CellGro) supplemented with 10% fetal bovine serum (Invitrogen) and 1^x antibiotic-antimycotic solution (Invitrogen). 5 x 10^4 cells were plated in 1 mL growth medium per well of a 24-well tissue culture plate 24 h prior to transfection. UnPEGylated CDP/FL-siRNA polyplexes containing 1 μg siRNA at a charge ratio of 3/1 (+/-) were prepared as described above. For flow cytometry, cells were detached with trypsin and rinsed twice with PBS (containing 0.1% BSA), prior to analysis using a FACScalibur (Becton Dickinson). For laser scanning confocal microsopy, cells were rinsed with PBS and fixed with 4% formaldehyde in 100 mM HEPES for 15 min. Following two more PBS washes, cells were left in PBS, and microscopy was conducted using a Zeiss 410 laser scanning confocal microscope.

3.3.6 Serum nuclease stability

For each sample, 5 μL of active mouse serum (Sigma) was added to an equal volume of water containing 40 pmol siGL3, either naked or within CDP-containig polyplexes (3/1 (+/-) charge ratio); serum was added either before or after a 4 h incubation at 37 ^oC, as indicated. Following this incubation, 2 μL of loading buffer (0.03% bromophenol blue, 0.03% xylene cyanol FF, 10 mM Tris-HCl, 50 mM EDTA) were added to each solution, and 10 μL (of a total of 12 μL) of the resulting solutions were loaded per well of a 15% polyacrylamide gel in 1^x TBE buffer (89 mM Tris, 89 mM boric acid, 2 mM EDTA). The gel was electrophoresed at 100 V for 75 min, then incubated in 50 mL 1^x TBE buffer

containing 0.1 μg/mL ethidium bromide with gentle shaking for 30 min to allow visualization.

3.3.7. Measurement of unbound polymer

pDNA-containing or siRNA-containing polyplexes were prepared using 1 μg nucleic acid and an amine-terminated CDP at various charge ratios. To each 100-μL polyplex solution, 575 μL water and 75 μL 10^{x} PBS was added, giving a final 750-μL solution of polyplexes in 1^{X} PBS. These solutions were centrifuged at 20,800*g for 99 min to pellet aggregated polyplexes. 500 μL of each supernatant was then used for determination of unbound CDP via end-group analysis (amine quantification) using a TNBS assay as described previously[21]. Using a CDP standard curve, the amount of free CDP for the entire sample was calculated and subtracted from the total CDP to determine the amount of CDP bound. This mass of CDP was converted to an equivalent charge ratio, an "effective polyplex charge ratio" (EPCR), as described above.

3.3.8 Isothermal titration calorimetry (ITC)

All calorimetric measurements were performed using a MCS ITC calorimeter (Microcal) running MCS Observer and Origin software. The titrant syringe (250-μL volume) was loaded with a 12.68 mg/mL solution of AD-PEG in water (corresponding to [AD] = 2.226 mM). The sample cell (1.5-mL volume) was loaded with a solution of β-CD alone, CDP alone, or CDP/pDNA polyplexes of various charge ratios; for all of these solutions, the concentration of β-CD moieties was kept constant ([β-CD] = 0.225 mM). After a 2-μL pre-injection (as recommended by the manufacturer), twenty-five successive AD-PEG injections of 10 μL each were made. The heat added or removed in order to keep the cell at constant temperature (20 ^{o}C) was measured as a function of time. Using Origin software

provided by the manufacturer, this data was regressed to give best-fit values for stoichiometry (n; number of ligand binding sites), binding strength (K; M^{-1}), and enthalpy of binding (ΔH; kcal/mol of injectant).

3.3.9 Turbidity analysis

Polyplexes were made with 1 μg pDNA and amine-terminated CDP at a charge ratio of 3/1 (+/-) as described above. To each 200-μL polyplex solution, 20 μL of water or an AD-PEG solution (to give 1:1 AD:β-CD ("100%") or 3:1 AD:β-CD ("300%") was added. Then 1000 μL PBS was added, and resulting solutions were incubated at 37 ^{o}C for 1 h. Solution absorbance at 405 nm (A405) was then measured.

3.4 RESULTS

3.4.1 CDP condenses siRNA into polyplexes

Given the electrostatic basis of interaction between our cyclodextrin-containing polycation (CDP), we hypothesized that the amounts of CDP required to bind siRNA would be similar to that observed previously with pDNA[1]. For each of these two nucleic acid types, samples were prepared in which increasing concentrations of CDP were added to a given concentration of nucleic acid. The resulting solutions were electrophoresed on a polyacrylamide (for siRNA-containing samples) or an agarose (for pDNA-containing samples) gel (**Fig. 3.4**).

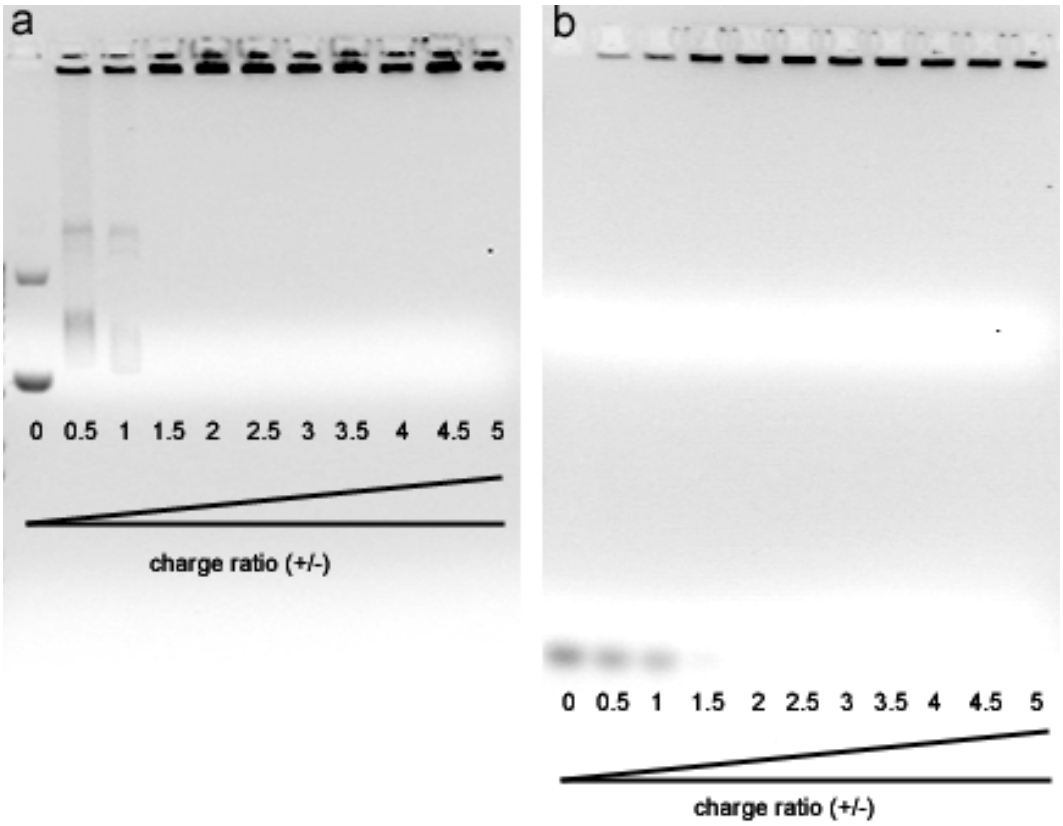

Figure 3.4. Gel retardation assay for CDP/siRNA and CDP/pDNA polyplexes. Increasing amounts of CDP were added to 0.5 μg of (**a**) pDNA or (**b**) siRNA, and resulting solutions were analyzed by gel electrophoresis. For both nucleic acids, complete retardation was observed for all charge ratios greater than 1 +/-.

Unbound nucleic acids can migrate freely through the gel, whereas CDP-bound nucleic acids are trapped within the wells into which they are loaded. For both pDNA and siRNA, as soon as the amount of CDP added created a positive (i.e., greater than 1/1 +/-) charge ratio, all nucleic acids remained within the wells. This observation suggests that, analogous to what has been seen here and previously with pDNA, formulation of siRNA with CDP at a positive charge ratio is sufficient to condense all siRNA within polyplexes.

Because the molecular weight of the siRNA examined here (~1 x 10^4 Da) is only a fraction of that of the pDNA (~1 x 10^6 Da), we wondered how the sizes of CDP/siRNA and CDP/pDNA polyplexes would compare. The sizes (hydrodynamic diameters) of a number of polyplex samples were determined by dynamic light scattering (DLS); the results are shown in **Figure 3.5**.

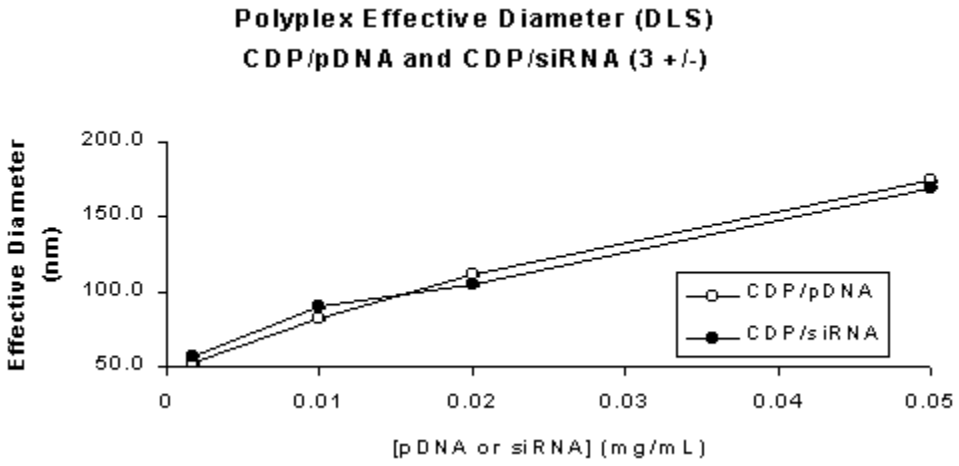

Figure 3.5. Determination of CDP/siRNA and CDP/pDNA polyplex size by dynamic light scattering. CDP/siRNA and CDP/pDNA polyplexes were prepared at the same charge ratio (3 +/-) but at a variety of concentrations. siRNA- and pDNA-containing polyplexes exhibit a very similar dependence of size on formulation concentration: the more dilute the components are at formulation, the smaller the resulting polyplexes are.

The size of pDNA-containing polyplexes, all of which were prepared at the same charge ratio (3 +/-), shows a strong dependence on concentration. The more concentrated the components are at the time of formulation, the larger the diameters of the resulting polyplexes. These results suggest that, as formulation concentrations increase, the number densities and/or mass densities of the polyplexes decrease.

3.4.2 PEGylation of CDP/siRNA polyplexes confers salt stability and reduces dependence of size on concentration

Previous work with CDP/pDNA polyplexes has shown that addition of an adamantane-poly(ethylene glycol) (AD-PEG) conjugate confers stability when polyplexes are exposed to salt[8]. After adding CDP to siRNA to form polyplexes, DLS was used to monitor polyplex size both in water and after addition of salt (phosphate-buffered saline, PBS); these results are compared to those for CDP/pDNA polyplexes and to those to which AD-PEG was added (**Fig. 3.6**).

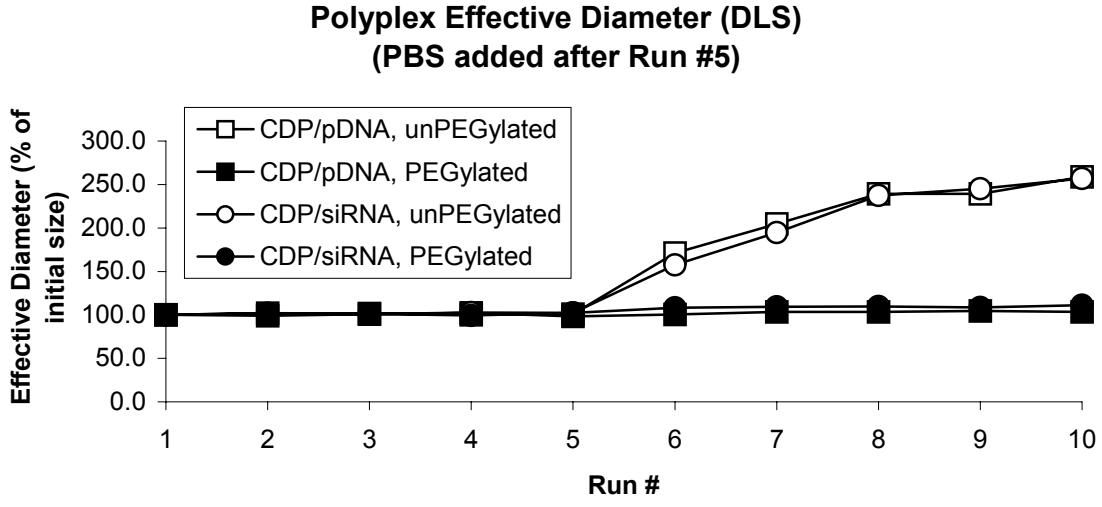

Figure 3.6. AD-PEG confers salt stability to CDP/siRNA polyplexes. The sizes of CDP/siRNA and CDP/pDNA polyplexes (3 +/-) were analyzed by DLS for ten consecutive runs; PBS was added after the fifth run. Polyplex effective diameters are presented as a percentage of the initial size (first run) for each sample. For both types of nucleic acids, the addition of AD-PEG sharply reduces salt-induced polyplex aggregation.

As is seen for polyplexes containing pDNA, AD-PEG confers salt stability to CDP/siRNA polyplexes.

We have previously observed for DNA-containing polyplexes that addition of AD-PEG to CDP prior to polyplex formation ("pre-PEGylation") eliminates the concentration dependence on size that is seen for unPEGylated polyplexes (see Fig. 3.5) and for those to which AD-PEG is added after polyplex formation (data not shown). The sizes of pre-PEGylated CDP/siRNA and CDP/pDNA polyplexes were measured at numerous formulation concentrations (**Fig. 3.7**).

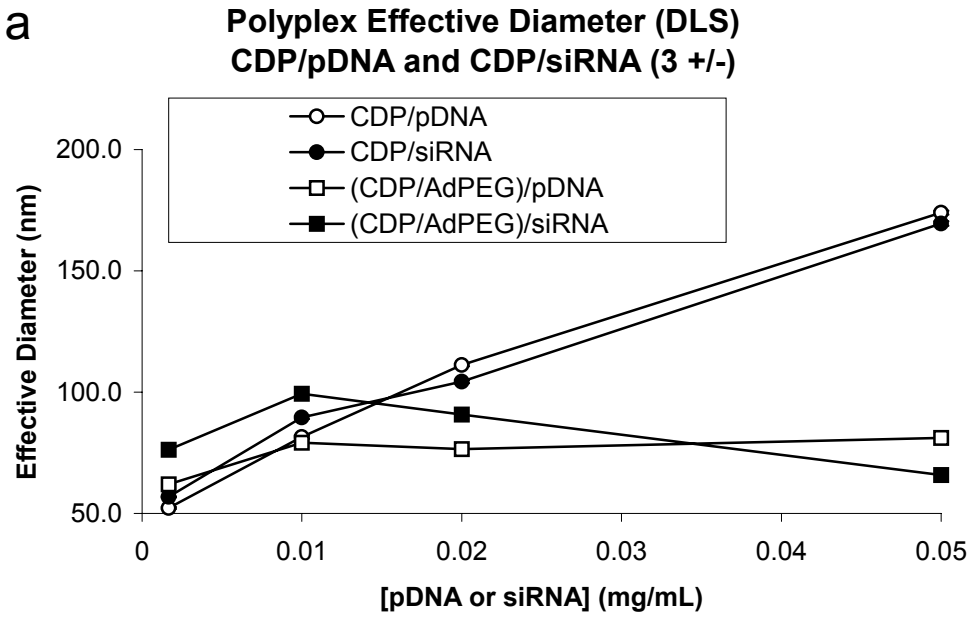

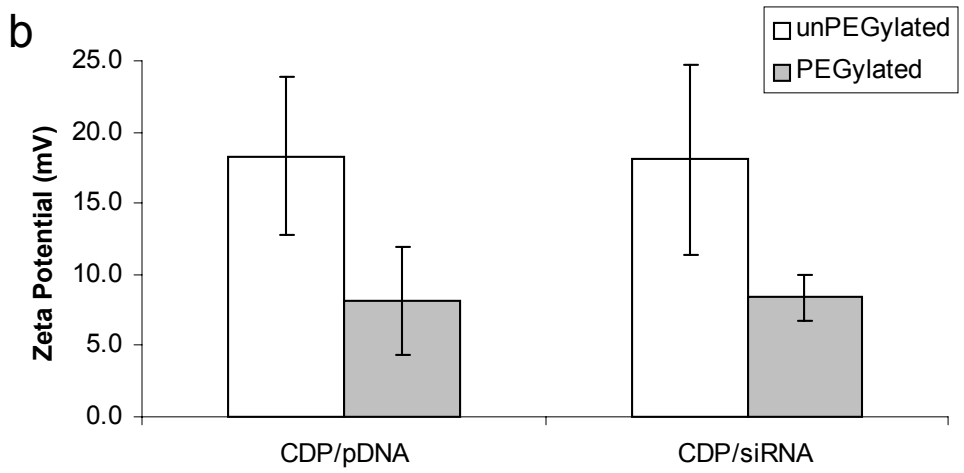

Figure 3.7. Pre-PEGylation generates CDP/siRNA polyplexes of uniform, small size and reduces their zeta potential. (**a**) The sizes of pre-PEGylated CDP/siRNA and CDP/pDNA polyplexes (3 +/-) prepared at various concentrations were analyzed by DLS. Results for unPEGylated polyplexes made under the same conditions (see Fig 3.5) are included here for comparison. For both types of nucleic acids, the addition of AD-PEG to CDP prior to polyplex formation ("pre-PEGylation") sharply reduces variation in polyplex size with formulation concentration. (**b**) The zeta potentials of all sixteen samples (four formulations at four different concentrations each) were measured; bars represent averages and error bars represent standard deviation. PEGylation of CDP/pDNA and CDP/siRNA polyplexes significantly reduces their zeta potential.

3.4.3 CDP/siRNA polyplexes are readily endocytosed by cultured cells

Our previous work with CDP/pDNA polyplexes has shown high levels of cellular uptake when they are exposed to adherent cells in culture[7]. Here, polyplexes were prepared with CDP and siRNA duplexes that were covalently modified to contain fluorescein at their 5' ends (FL-siRNA). Uptake of these polyplexes was assessed through examination of cellular fluorescence by flow cytometry and confocal microscopy (**Fig. 3.8**).

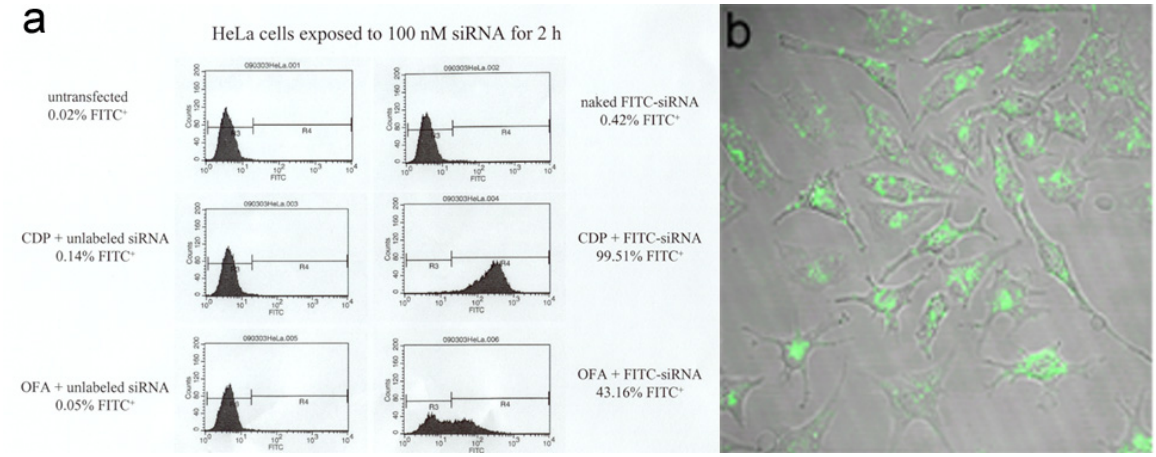

Figure 3.8. CDP/siRNA polyplexes are readily taken up by adherent cultured cells. HeLa cells were exposed to CDP/FL-siRNA polyplexes for 2 h prior to assessment of cellular fluorescence by (**a**) flow cytometry and (**b**) confocal microscopy. Virtually all (>99%) cells exhibit strong fluorescence suggestive of polyplex uptake; neither FL-siRNA alone nor polyplexes containing unlabeled siRNA generated any significant cellular fluorescence.

Negative control samples, uncomplexed FL-siRNA and polyplexes containing unlabeled siRNA, induced negligible (<1%) increases in cellular fluorescence relative to the untreated cells. However, CDP/FL-siRNA polyplexes caused significant fluorescent signal in virtually all (>99%) cells that were exposed. By comparison, a commonly used and commercially available lipid reagent for the delivery of siRNA (Oligofectamine) generated just 43% positive cells under the same conditions. The strong cellular fluorescence measured for the CDP/FL-siRNA sample was confirmed by confocal microscopic analysis. These results indicate there is substantial uptake of CDP/siRNA polyplexes by cultured HeLa cells, strengthening the hypothesis that achieving down-regulation of a target gene in these cells is a possibility.

3.4.4 siRNA within polyplexes is protected from serum nuclease degradation

While CDP/siRNA polyplexes are taken up to a great extent by cultured cells (see Section 3.4.3), polyplexes that are administered *in vivo* will encounter additional barriers to targeted gene down-regulation. The first of these obstacles encountered after injection will be the nuclease-rich environment of the blood. It has been shown by several researchers that, under "normal" delivery conditions (i.e., low-pressure injections) unmodified siRNA duplexes will not be efficiently endocytosed by cells and therefore will not achieve desired gene down-regulation *in vivo*[16-18]. This is due to the rapid degradation of the siRNA duplexes by nuclease proteins within the blood. To avoid this degradation, researchers have employed numerous chemical modifications to the siRNA, most notably changing the interbase linkages from phosphodiesters to phosphorothioates[19-20]. We expect that siRNA within our polyplexes may be protected from nuclease degradation, thereby eliminating the need to use more costly, chemically-modified duplexes.

In order to examine what protection, if any, CDP affords siRNA within polyplexes, siRNA alone and within CDP/siRNA polyplexes were exposed to active mouse serum and then analyzed by gel electrophoresis (**Figure 3.9**).

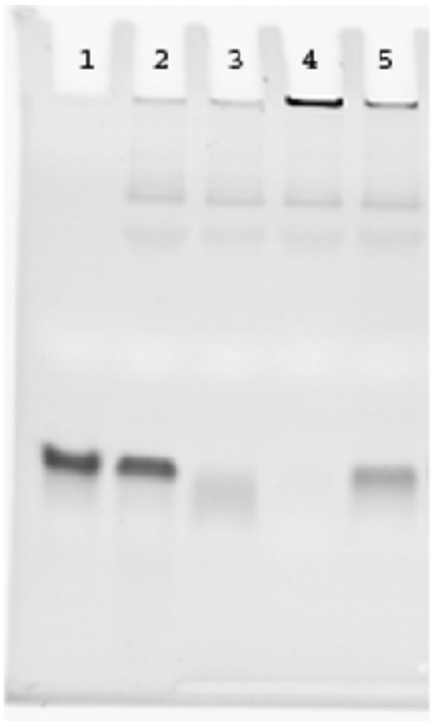

Lane 1: siRNA/H2O

Lane 2: siRNA/serum (t=0)

Lane 3: siRNA/serum (t=4h)

Lane 4: (CDP/siRNA)/serum (t=4h)

Lane 5: (CDP/siRNA)/serum (t=4h), then heparan sulfate (to displace)

Figure 3.9. CDP protects siRNA duplexes from serum nuclease degradation. CDP/siRNA polyplexes were exposed to active mouse serum at 37 ^{o}C for 4 h prior to polyacrylamide gel electrophoresis. Uncomplexed siRNA, either in water (no serum; lane 1) or with only a momentary exposure to serum (lane 2) are included as negative controls for degradation. Heparan sulfate, which displaces CDP/siRNA polyplexes[21], was added immediately prior to gel loading in lane 5. After a 4 h exposure to active mouse serum, siRNA that is displaced from CDP/siRNA polyplexes appears to be intact.

When incubated in water (no serum) prior to gel electrophoresis, the siRNA gives a strong, single band (see lane 1). Addition of mouse serum immediately prior to gel loading (a "t=0 exposure; see lane 2) has no significant effect on the siRNA migration or intensity, suggesting that more time is needed to induce degradation. A 4 h exposure to serum, however, leads to complete degradation of uncomplexed siRNA (see lane 3). When CDP/siRNA polyplexes are subjected to the same conditions and then directly electrophoresed, all of the siRNA remains CDP-bound within the well of the gel (see lane 4). This observation is expected based on previous gel retardation analysis (see Fig. 3.4) for the 3 +/- charge ratio employed here. When heparan sulfate is added to serum-treated

polyplexes to displace the siRNA from CDP, the single siRNA band returns. This suggests that siRNA duplexes within CDP/siRNA polyplexes are protected from nuclease degradation when exposed to active mouse serum.

3.4.5 Measurement of unbound CDP and "effective polyplex charge ratio"

The results shown previously in this chapter demonstrate that CDP can condense siRNA duplexes into polyplexes that are suitable for cellular uptake and protect the siRNA from degradation. It is clear that complete condensation of siRNA can be achieved for all positive charge ratios (greater than 1/1 +/-; see Figure 3.4). But it is unclear from a simple gel retardation study whether all of the "excess" CDP participates in siRNA binding or if some of it remains uncomplexed, as "bystander" CDP molecules. To investigate this unbound polymer, an assay was developed to quantify the amount of uncomplexed CDP within unPEGylated polyplex formulations.

Figure 3.6 demonstrates that unPEGyated polyplexes (containing either pDNA or siRNA) rapidly aggregate when exposed to salt. Solutions of aggregated polyplexes are then centrifuged at high speed to pellet aggregates, leaving any unbound components within supernatants. Indeed, UV/Vis spectrophotometric analysis has confirmed the absence of nucleic acid within these supernatants (data not shown), suggesting that all polyplexes are within aggregates that have been pelleted by centrifugation. Unbound CDP in supernatants is then quantified by end-group analysis[21] and subtracted from the total amount of CDP within the formulation (bound plus unbound) to calculate the amount of CDP within the (aggregated) polyplexes—this amount of bound CDP is used to calculate an "effective polyplex charge ratio" (EPCR) that is reflective of the actual composition of the polyplexes within a given formulation.

EPCR results for CDP/pDNA and CDP/siRNA polyplexes are shown in **Figure 3.10.**

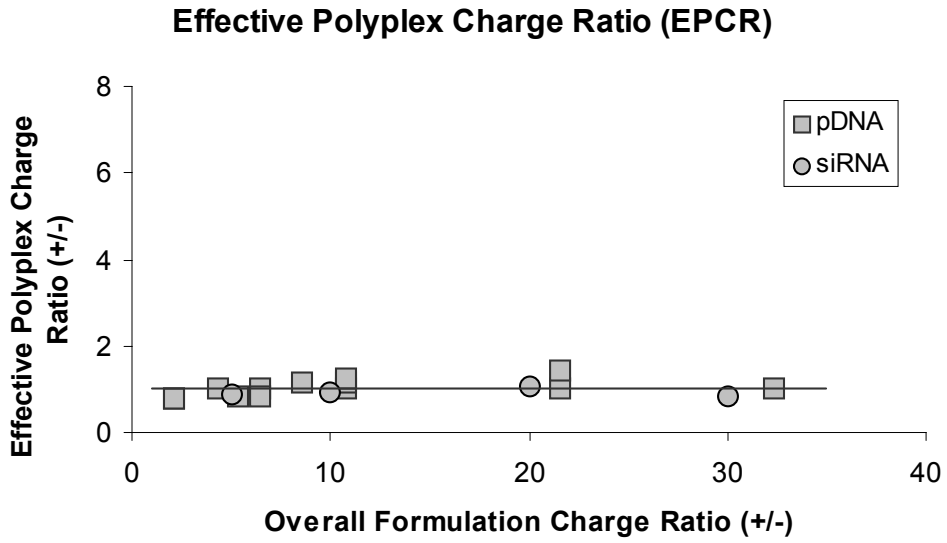

Figure 3.10. The amount of bound CDP within formulations is independent of overall formulation charge ratio. CDP/pDNA and CDP/siRNA polyplexes were formulated at a variety of overall charge ratios (from 2 to 30 +/-). PBS was added to induce polyplex aggregation, and aggregated polyplexes were pelleted by centrifugation. The amount of unbound CDP in the resulting supernatants was quantified by TNBS assay and subtracted from the total amount of CDP within the formulation to determine the amount of bound CDP within polyplexes; this amount of bound CDP was used to calculate the "effective polyplex charge ratio" (EPCR) on the polyplexes. All data points fall along the y = 1 line, corresponding to an EPCR of about 1/1 (+/-).

For all of the charge ratios examined, the amount of unbound CDP recovered in the supernatants scaled with the total amount of CDP within the formulation. As a consequence, the amount of bound CDP across these formulations was about the same; this amount corresponded to an effective charge ratio on the polyplex of about 1/1 +/-. From these observations, it appears that the amount of CDP within polyplexes is just enough to provide an equivalent amount of positive charges to balance the negative charges contributed by the phosphodiester backbones of the nucleic acids. Further, it can be concluded that any differences seen in formulations at high charge ratios (such as toxicity

seen in some cell lines at very high charge ratios[1] may be attributed to the unbound CDP within these formulations.

3.4.6 Stoichiometry and strength of AD-PEG/CDP binding: isothermal titration calorimetry (ITC)

Because of their aggregation in salt, unmodified CDP/siRNA polyplexes are unsuitable for *in vivo* administration. Addition of an adamantine-poly(ethylene glycol) (AD-PEG) conjugate to these polyplexes stabilizes them to salt (see Figure 3.6); the adamantane moiety of AD-PEG forms an inclusion complex with the β-CD moieties within CDP. While the effect of AD-PEG addition was clear, little was known about the stoichiometry and binding strength of this PEGylation. These parameters were examined by isothermal titration calorimetry (ITC).

Sequential additions of an AD-PEG solution were made to an isothermal cell containing either a β-CD solution, a CDP solution, or CDP/pDNA solutions of varying charge ratio (all having same concentration of β-CD moieties). Non-linear least squares analysis of the resulting heat curves determined a stoichiometry of binding (moles AD per mole β-CD) and enthalpy of binding (ΔH) (**Fig. 3.11**).

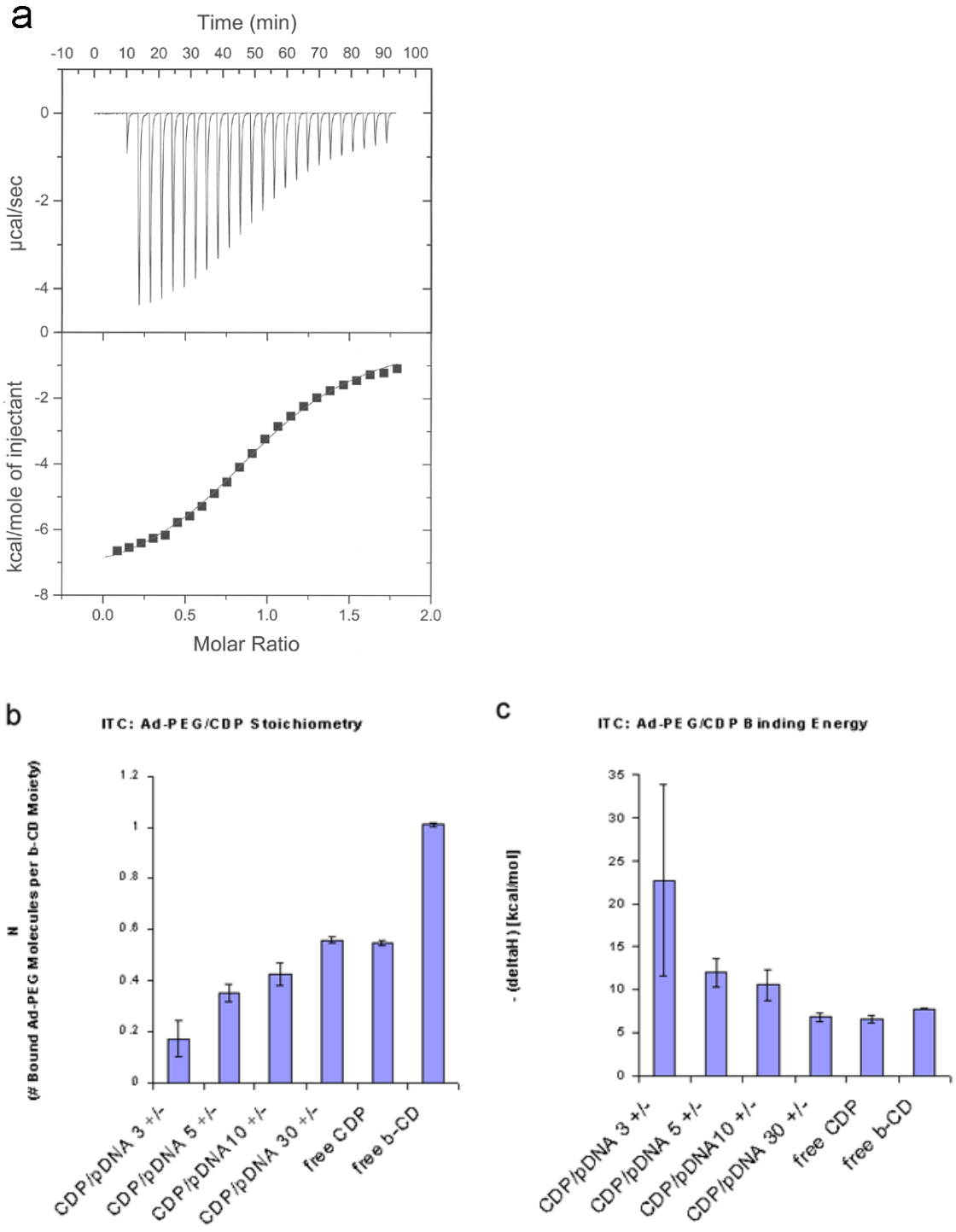

Figure 3.11. Isothermal titration calorimetry (ITC) analysis of AD-PEG binding to β-CD, CDP, and CDP-containing polyplexes. A syringe is loaded with an AD-PEG solution, from which aliquots are injected into an isothermal cell containing a solution of β-CD, CDP alone, or CDP/pDNA polyplexes. The heat required to maintain the cell at constant temperature is measured, and a non-linear least squares regression is performed to determine stoichiometry and strength of binding. (**a**) Representative plot of an AD-PEG/β-

CD ITC run. (**b**) Fitted n values (moles AD bound per mole β-CD). (**c**) Fitted ΔH values (-1 * (calories per mol AD injected)). Stoichiometry results suggest that the majority of β-CD moieties within bound CDP molecules are unoccupied by AD-PEG. The increased binding energy on polyplexes suggests additional cooperative interactions among AD-PEG molecules on the polyplex surface.

ITC analysis of AD-PEG/β-CD interactions generated an equilibrium stoichiometry of n = 0.991, in excellent agreement with the expected value of 1 (AD and β-CD are known to exhibit 1:1 mol:mol binding[12]). The observed binding constant, $K = 3.75 \times 10^4\ M^{-1}$ (data not shown), is in excellent agreement with literature values for AD/β-CD inclusion complexes[12]. When AD-PEG was added to a solution of CDP (containing the same concentration of β-CD moieties), the observed stoichiometry dropped to n = 0.55. This result suggests that, for a pre-PEGylated formulation prepared with equimolar AD-PEG and CDP (with respect to AD and b-CD moieties), just over half of the β-CD cavities are occupied. CDP/pDNA polyplexes at a 30/1 (+/-) charge ratio give a stoichiometry almost identical to that of free CDP (n = 0.57). Given the previous finding that the effective polyplex charge ratio is 1/1 (+/-), one would expect 29/30 (96.7%) of CDP molecules within a 30/1 (+/-) formulation to be unbound, and, therefore, the ITC results to be almost identical to those of CDP alone. As the polyplex charge ratio is reduced from 30/1 (+/-) to 3/1 (+/-), the fraction of unbound CDP molecules drops, and the stoichiometry determined by ITC decreases from n = 0.57 to n = 0.17. This observation strongly suggests that, when AD-PEG is added to polyplexes after they have already been formed ("post-PEGylated"), the overwhelming majority (83%) of β-CD moieties remain unoccupied. The binding energy seen for polyplexes formed at 3/1 (+/-), -23 kcal/mol, is significantly higher than that seen for 30/1 (+/-) polyplexes or CDP alone (-6.9 kcal/mol and –6.7 kcal/mol, respectively). This result implies that there are cooperative interactions occurring between

AD-PEG molecules on the polyplex surface, perhaps through formation of a PEG "brush" layer[22].

These ITC results also imply that, due to the low occupancy of β-CD moieties within CDP-containing polyplexes, adding an excess amount of AD-PEG (moles AD > moles β-CD) may confer additional stability. This was confirmed through a turbidity assay developed as an alternative method (to DLS) to assess polyplex aggregation. Polyplexes were pre-PEGylated or post-PEGylated with AD-PEG at either a 1:1 (AD:β-CD mol:mol, "100%") or 3:1 ("300%") ratio prior to incubation with PBS; aggregation (turbidity) was assessed by measurement of solution absorbance at 405 nm (**Fig. 3.12**).

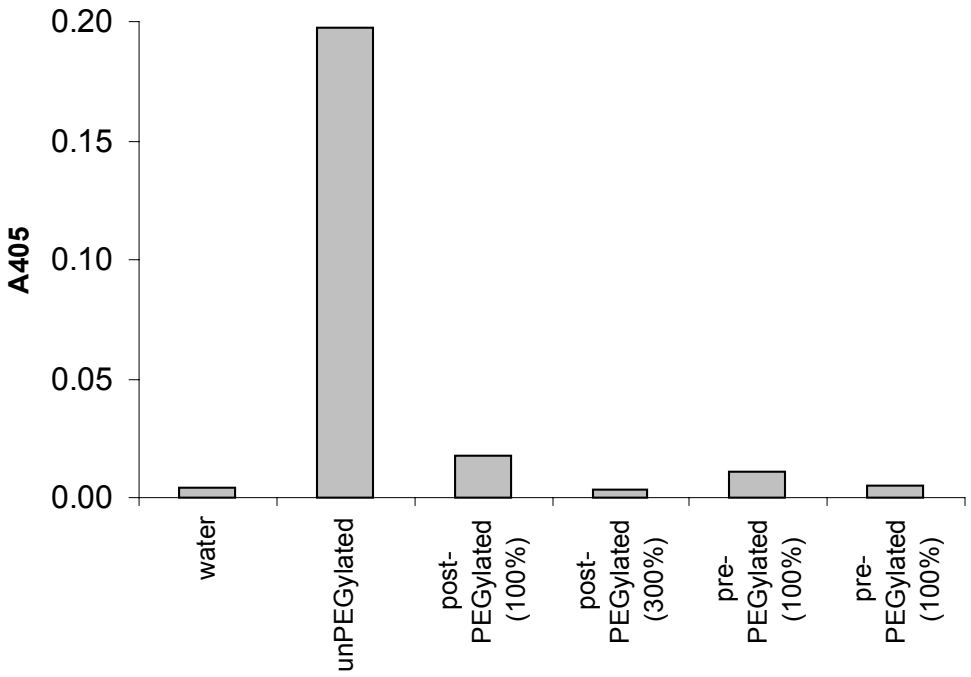

Figure 3.12. Addition of "excess" AD-PEG leads to enhanced protection of CDP/pDNA polyplexes from salt-induced aggregation. Water and PEGylated or unPEGylated CDP/pDNA polyplexes were incubated with phosphate-buffered saline (PBS) for 1 h at 37 ^{o}C followed by measurement of solution absorbance at 405 nm (A405). While equimolar addition of AD-PEG ("100%"), either before or after polyplex formation, sharply reduces the increase in A405 seen for unPEGylated polyplexes, addition of even more AD-PEG ("300%") completely abrogates any increase in A405 value.

Equimolar AD-PEG addition reduced turbidity by >90%, but a three-fold excess of AD-PEG completely abrogated PBS-induced turbidity. This result provides functional confirmation for the hypothesis from previous ITC analysis (see Fig. 3.11) that polyplexes PEGylated with equimolar AD-PEG retain the capacity for additional PEGylation.

3.5 DISCUSSION

The experimental results presented in this chapter suggest that the natures of CDP-containing polyplexes made with either pDNA or siRNA are very similar. An equal mass of either nucleic acid appears to require the same amount of CDP for condensation, and the resulting polyplexes have similar sizes and exhibit the same concentration-dependence. Modification of both types of polyplexes with AD-PEG reduces salt-induced aggregation and lowers surface charge (zeta potential).

Because the fundamental nature of pDNA and siRNA is much the same (linear arrangements of nucleotides connected by phosphodiester linkages), it is not surprising that polyplexes can be formed with either by addition of CDP under the same conditions. However, the difference in size between a single pDNA molecule (the plasmid here had 5256 bp, corresponding to a molecular weight of ~3.5 x 10^6 Da) and an siRNA molecule (the siRNA duplex used here has a molecular weight of 1.33 x 10^4 Da) is about two orders of magnitude. It stands to reason from the experimental results shown above that the amount of CDP within polyplexes, on a per-polyplex basis, is similar for pDNA- and siRNA-containing complexes. It follows, then, that the number of siRNA molecules per polyplex (the "siRNA payload") is much greater than is observed for pDNA. (As is discussed in Chapter 5, multi-angle light scattering (MALS) analyses of CDP/pDNA polyplexes suggest that the number of pDNA molecules per polyplex is very small (~1-2)[23].)

As was mentioned above (see Section 3.2), microscopic analyses of cultured cells exposed to polyplexes made with fluorescently-labeled DNA indicate that the majority of intracellular complexes are sequestered within endocytic vesicles. Even with an imidazole-

terminated CDP that enhances polyplex-mediated gene expression and appears to aid in vesicular release and/or polyplex unpackaging, detection of nucleic acid outside of these vesicles, either CDP-bound or free, is extremely difficult[7]. This implies that an escape of polyplexes from endocytic vesicles is a rare event. Therefore, given the rarity of polyplex escape from intracellular vesicles, the presumably heightened payload per polyplex when siRNA is used (compared to pDNA), and the fact that RNAi occurs in the cytoplasm (while transcription of delivered genes takes place in the nucleus), it seems entirely possible that siRNA-containing polyplexes will be more potent RNAi effectors than pDNA-containing polyplexes are gene delivery agents. The investigation of CDP/siRNA polyplexes to accomplish RNAi is the subject of the next chapter.

3.6 REFERENCES

[1] Gonzalez H, Hwang SJ & Davis ME. New class of polymers for the delivery of macromolecular therapeutics. *Bioconjug. Chem*. **10**, 1068-1074 (1999).

[2] Reineke TM & Davis ME. Structural effects of carbohydrate-containing polycations on gene delivery. 1. Carbohydrate size and its distance from charge centers. *Bioconjug. Chem*. **14**, 247-254 (2003).

[3] Reineke TM & Davis ME. Structural effects of carbohydrate-containing polycations on gene delivery. 2. Charge center type. *Bioconjug Chem*. **14**, 255-261 (2003).

[4] Popielarski SR, Mishra S & Davis ME. Structural effects of carbohydrate-containing polycations on gene delivery. 3. Cyclodextrin type and functionalization. *Bioconjug. Chem*. **14**, 672-678 (2003).

[5] Davis ME, Pun SH, Bellocq NC, Reineke TM, Popielarski SR, Mishra S & Heidel J. Self-assembling nucleic acid delivery vehicles *via* linear, water-soluble, cyclodextrin-containing polymers. *Curr. Med. Chem*. **11**, 1241-1253 (2004).

[6] Hwang SJ. Rational design of a new class of cyclodextrin-containing polymers for gene delivery. *Ph.D. Thesis*, California Institute of Technology (2001).

[7] Mishra S, Webster P & Davis ME. PEGylation significantly affects cellular uptake and intracellular trafficking of non-viral gene delivery particles. *Eur. J. Cell Biol*. **83**, 97-111 (2004).

[8] Pun SH & Davis ME. Development of a nonviral gene delivery vehicle for systemic application. *Bioconjug. Chem*. **13**, 630-639 (2002).

[9] Kwoh DY, Coffin CC, Lollo CP, Jovenal J, Banaszczyk MG, Mullen P, Phillips A, Amini A, Fabrycki J, Bartholomew RM, Brostoff SW & Carlo DJ. Stabilization of poly-L-lysine/DNA polyplexes for in vivo gene delivery to the liver. *Biochem. Biophys. Acta* **1444**, 171-190 (1999).

[10] Nguyen HK, Lemieux P, Vinogradov SV, Gebhart CL, Guerin N, Paradis G, Bronich TK, Alakhov VY & Kabanov AV. Evaluation of polyethyer-polyethyleneimine graft copolymers as gene transfer agents. *Gene Ther*. **7**, 129-138 (2000).

[11] Garrett SW, Davies OR, Milroy DA, Wood PJ, Pouton CW & Threadgill MD. Synthesis and characterization of polyamine-poly(ethylene glycol) constructs for DNA binding and gene delivery. *Bioorg. Med. Chem*. **8**, 1779-1797 (2000).

[12] Cromwell W, Bystrom K & Eftink M. Cyclodextrin adamantanecarboxylate inclusion complexes—studies of the variation in cavity size. *J. Phys. Chem.-US* **89**, 326-332 (1985).

[13] Bellocq NB, Pun SH, Jensen GS & Davis ME. Transferrin-containing, cyclodextrin polymer-based particles for tumor-targeted gene delivery. *Bioconjug. Chem*. **14**, 1122-1132 (2003).

[14] Pun SH, Tack F, Bellocq NC, Cheng J, Grubbs BH, Jensen GS, Davis ME, Brewster M, Janicot M, Janssens B, Floren W & Bakker A. *Cancer Biol. & Ther*. **3**, 641-650 (2004).

[15] Pun SH, Gonzalez N, Davis ME, Bellocq N & Cheng J. Compositions containing inclusion complexes. **Patent# WO02/49676**. Issued 27 June 2002.

[16] McCaffrey AP, Meuse L, Pham TT, Conklin DS, Hannon GJ & Kay MA. RNA interference in adult mice. *Nature* **418**, 38-39 (2002).

[17] Lewis DL, Hagstron JE, Loomis AG, Wolff JA & Herweijer H. Efficient delivery of siRNA for inhibition of gene expression in postnatal mice. *Nat. Genet*. **32**, 107-108 (2002).

[18] Isacson R, Kull B, Salmi P & Wahlestedt C. Lack of efficacy of siRNA in rat brain. *Acta Physiol. Scand.* **179**, 173-177 (2003).

[19] Soutschek J, Akinc A, Bramlage B, Charisse K, Constien R, Donoghue M, Elbashir S, Geick A, Hadwiger P, Harborth J, John M, Kesavan V, Lavine G, Pandey RK, Racie T, Rajeev KG, Rohl I, Toudjarska I, Wang G, Wuschko S, Bumcrot D, Koteliansky V, Limmer S, Manoharan M & Vornlocher HP. Therapeutic silencing of an endogenous gene by systemic administration of modified siRNAs. *Nature* **432**, 173-178 (2004).

[20] Judge AD, Sood V, Shaw JR, Fang D, McClintock K & MacLachlan I. Sequence-dependent stimulation of the mammalian innate immune response by synthetic siRNA. *Nat. Biotechnol*. **23**, 457-462 (2005).

[21] Hwang SJ, Bellocq NC & Davis ME. Effects of structure of beta-cyclodextrin-containing polymers on gene delivery. *Bioconjug. Chem*. **12**, 280-290 (2001).

[22] Meng F, Engbers GHM & Feijen J. Polyethylene glycol-grafted polystyrene particles. *J. Biomed. Mater. Res*. **70A**, 49-58 (2004).

[23] Heidel JD & Davis ME. The first example of a completely self-assembled non-viral gene delivery system for *in vivo* application. *2003 Annual Meeting* American Institute of Chemical Engineers.

CHAPTER 4: *In Vitro* and *In Vivo* Efficacy of CDP/siRNA Polyplexes

4.1 ABSTRACT

Synthetic siRNA duplexes have been shown to be non-immunogenic in cultured cells and in mice and, when administered by high-pressure ("hydrodynamic") tail vein injection, can be effective agents of targeted gene down-regulation in mouse liver. The method of delivery is infeasible for human therapeutic applications, however, prompting the investigation of non-viral systems, including our cyclodextrin-containing polycation (CDP) system, as appropriate delivery agents. This CDP system has been demonstrated to condense siRNA duplexes into small (<100 nm), well-defined complexes that are suitable for cellular uptake and protect the siRNA from nuclease degradation. Here, the efficacy of CDP/siRNA complexes to down-regulate both endogenous and exogenous target genes is examined *in vitro* and *in vivo*. These complexes are capable of eliciting an RNA interference (RNAi) effect in cultured cells, as shown through examples with an exogenous reporter gene (luciferase) and an endogenous oncogene (EWS-Fli1). When these polyplexes are modified to contain an appropriate targeting ligand, down-regulation of a transgene in mouse liver (via a galactose ligand) and therapeutic inhibition of tumor formation in mice (using a transferrin ligand) can be achieved. These results demonstrate the tremendous promise of a CDP-based system for targeted delivery of siRNA for therapeutic *in vivo* applications.

4.2 INTRODUCTION

A tremendous amount of research is being performed to better understand the mechanism of RNA interference (RNAi) in mammalian cells, making *in vivo* therapeutic applications of RNAi increasingly likely to emerge soon. However, systemic applications of virally delivered small interfering RNA (siRNA) duplexes and related RNAi products are unlikely to be viable in the near future, due to host immune responses upon repeated delivery and ineffective tumor targeting. The systemic, non-viral delivery of RNAi molecules has been reported in mice and initially involved high-pressure, high-volume tail-vein injections of naked nucleic acids[1-3]; this method is untenable and unacceptable in humans in routine clinical settings. Subsequently, naked siRNA[4-6], lipid-formulated siRNA[7], plasmids expressing short hairpin RNA[8-9], and polycation-formulated siRNA[10-12] have been administered systemically in mice. Naked or formulated siRNAs have also been directly injected into xenograft tumors in mice[13-16]. Naked siRNAs require chemical stabilization for in *vivo* use[6,17], have non-specific biodistributions that are the same as single-stranded antisense agents[18], and require large and repeated dosages for efficacy[6]. Further, while synthetic siRNAs themselves have been shown to be non-immunogenic in mice[19], some *in vivo* administrations of lipid formulations have been associated with immunogenicity[20-22]. Thus the need for the development of a safe, effective non-viral delivery system for siRNA remains.

The synthesis and characterization of cyclodextrin-containing polycations that can bind and condense DNA into polymer-DNA complexes ("polyplexes") suitable for cellular uptake have been described[23-24]. These can be stabilized by incorporation of a neutral polymer (poly(ethylene glycol); PEG) tethered to a hydrophobic small molecule (adamantane; AD)

that interacts strongly with the interior of β-cyclodextrin moieties within the polymer via inclusion complex formation[25]. Further, these AD-PEG conjugates can be modified by addition of a targeting ligand, such as transferrin (Tf), to endow polyplexes with selectivity for cells that express high levels of a cognate cell surface receptor[26-27]. As was discussed in Chapter 3, this delivery system is suitable for formulation with siRNA duplexes as well. CDP/siRNA polyplexes can be readily taken up by cells, and the siRNA within them is protected from serum nuclease degradation.

In this chapter, the ability of siRNA-containing polyplexes to achieve target gene down-regulation is examined, both in cultured cells and in mice. Sequence-specific knockdown of a co-delivered reporter gene (luciferase) by CDP/siRNA polyplexes is shown in two different cell lines. Evidence of down-regulation of a chimeric oncogene (EWS-Fli1) in cultured Ewing's sarcoma cells is also provided. The efficacy of targeted polyplexes in two different *in vivo* systems is also shown. Galactose-bearing polyplexes elicit down-regulation of luciferase within the livers of transgenic mice. Transferrin-targeted complexes reduce EWS-Fli1 levels in Ewing's tumors, and long-term delivery of these complexes inhibits tumor growth. Finally, and perhaps most importantly, the safety (as measured by histology, critical blood counts (CBC), and liver function) and non-immunogenicity of these polyplexes, even when containing an siRNA duplex possessing a putative immunostimulatory motif, are demonstrated.

4.3 METHODS

4.3.1 Polymers

Unless otherwise noted, an imidazole-terminated, cyclodextrin-containing polycation (CDP) was used for all studies and synthesized as described previously[23,26]. An adamantane-poly(ethylene glycol) (AD-PEG) conjugate, made with PEG_{5000}, was synthesized as described previously[26]. A transferrin-containing modifier, (AD-PEG-Tf), was synthesized as described previously[26]. Another ligand-containing modifier, adamantane-poly(ethylene glycol)-lactose (AD-PEG-Lac), was prepared as described (using PEG_{5000} instead of PEG_{3400})[28].

4.3.2 Nucleic acids

A plasmid encoding the firefly luciferase gene ("pGL3-Control Vector," pGL3CV) was purchased from Promega. siRNA duplexes were used that target luciferase ("Luciferase GL3 duplex," siGL3); enhanced green fluorescent protein (siEGFP); the EWS-Fli1 fusion gene (siEFBP2)[29], a mutated, non-targeting version of siEFBP2 (siEFBP2mut); and a non-targeting control sequence ("siCONTROL Non-Targeting Duplex #1," siCON1). All were chemically synthesized by Dharmacon and used as received. Sequences:

siGL3:
```
   5′-CUUACGCUGAGUACUUCGAdTdT-3′
3′-dTdTGAAUGCGACUCAUGAAGCU-5′
```

siEGFP:
```
   5′-CUUACGCUGAGUACUUCGAdTdT-3′
3′-dTdTGAAUGCGACUCAUGAAGCU-5′
```

siEFBP2:
```
   5′-GCAGAACCCUUCUUAUGACUU
    UUCGUCUUGGGAAGAAUACUG-5′
```

siEFBP2mut:
```
   5′-GCAGAACCAGUCUUAUGACUU
    UUCGUCUUGGUCAGAAUACUG-5′
```

siCON1:

5′-UAGCGACUAAACACAUCAAUU
UUAUCGCUGAUUUGUGUAGUU-5′

[The mutated nucleotides within siEFBP2mut are indicated in **bold**; the putative immunostimulatory motif within siCON1 is underlined.]

4.3.3 HeLa and BHK transfections, luciferase assays

HeLa and BHK cells (American Type Culture Collection) were cultured in Dulbecco's Modified Eagle's Medium supplemented with 10% fetal bovine serum and 1^x antibiotic-antimycotic (penicillin, streptomycin, and amphoterecin B). Cells were seeded in 24-well plates at 50,000 cells per well 24 h prior to transfection. Polyplexes were prepared with pGL3CV alone or in combination with siGL3 or siEGFP at a charge ratio of 3/1 (+/-). Lipoplexes were prepared with the same nucleic acid combinations using Lipofectin (Invitrogen) according to the manufacturer's instructions. For all polyplex and lipoplex samples, each well received 1 μg pDNA and 100 nM of the indicated siRNA. Complexes were incubated with cells in serum-free medium (OptiMEM, Invitrogen) for 4 h, after which solutions were aspirated and replaced with complete growth medium. At a total of 48 h post-transfection, growth medium was aspirated and replaced with 100 μL 1^x Cell Culture Lysis Reagent (Promega). Plates were incubated at room temperature with gentle shaking for ~1 h to allow complete cell lysis. The luminescence of cell lysates was then determined using a Monolight 3010 luminometer (BD Pharmingen) and the Luciferase Assay System (Promega). One hundred microliters substrate solution was added to 10 μL cell lysate, and the resulting luminescent signal was integrated over 10 sec.

4.3.4 TC71 transfection, Western blot

TC71 cells (provided by Dr. Timothy Triche, Children's Hospital—Los Angeles) were cultured in RPMI 1640 medium with 10% fetal bovine serum (no antibiotics). They were plated in 6-well plates and grown until they reached 30% confluency. siRNA was complexed with Oligofectamine (OFA, Invitrogen) according to the manufacturer's recommendations or with CDP at a 3/1 (+/-) charge ratio. The resulting formulations were applied to each well in serum-free medium (OptiMEM) at a final siRNA concentration of 100 nM for 4 h. All transfected cells were harvested at 48 h, and EWS-Fli1 and β-actin protein levels were assessed by Western blot using primary monoclonal antibodies against the C-terminal region of Fli1 (BD Biosciences) and polyclonal antibodies against β-Actin (Santa Cruz Biotechnology).

4.3.5 Preparation of formulations and injections of transgenic mice

Transgenic C57BL/6 mice were prepared by pronuclear injection of a linearized pApoEHCRLuc plasmid (a generous gift of A. McCaffrey and M. Kay), which contains the firefly luciferase gene under the control of the human α_1-antitrypsin promoter and the apolipoprotein E heterologous control region. This plasmid restricts transgene expression to hepatocytes[30]. All mice contained the luciferase gene (as confirmed by PCR analysis of tail cuts obtained when pups were 4 weeks old) and were 6 – 8 weeks of age at the time of the experiment. Mice were treated according to the NIH Guidelines for Animal Care and as approved by the Caltech Institutional Animal Care and Use Committee. All experimental manipulations with the mice were performed under sterile conditions in a laminar flow hood.

Polyplex formulations were prepared containing siGL3 or siCON1 and CDP (at a charge ratio of 3/1 +/-), 20% AD-PEG-Lac/80% Ad-PEG (w:w), and an overall 1:1 β-CD:AD (mol:mol). One volume containing CDP, AD-PEG, and AD-PEG-Lac (in H_2O) was added to an equal volume of siRNA (in H_2O) to form polyplexes. An equal volume of 10% (w:v) glucose (100 mg/mL glucose in H_2O) was added to the polyplex solution to give a final polyplex solution in 5% glucose (D5W). Formulations were administered by low-pressure tail vein (LPTV) injection; injection volumes were adjusted by mouse weight such that each 20-g mouse received 50 μg siRNA (2.5 mg/kg) in a volume of 200 μL (1% v:w).

4.3.6 Determination of transferrin receptor (TfR) level of TC71 cells

TC71, A2780 (American Type Culture Collection), and HeLa cells were analyzed for relative levels of transferrin receptor (TfR) expression. Cells were plated at 300,000/well in 6-well plates 24 h before exposure to 1 mL of antibiotic-free culture medium containing 1% BSA and various concentrations of fluorescein-labeled transferrin (Tf-FITC) (50, 100, or 250 nM) for 1 h at 37 ^{o}C as described previously[27]. The cells were washed twice with phosphate-buffered saline (PBS), collected by trypsin treatment, washed twice in FACS buffer (25 mL of Hank's Buffered Salt Solution supplemented with 2 mM $MgCl_2$ and 10 μL DNase) and resuspended in Hank's Buffered Salt Solution for analysis by flow cytometry using a FACSCalibur (Becton Dickinson).

4.3.7 Generation of luciferase-expressing TC71 (TC71-LUC) cells

SMPU-R-MNCU3-LUC is a lentiviral vector based upon HIV-1 that transduces the firefly luciferase gene. The backbone vector SMPU-R has deletions of the enhancers and promoters of the HIV-1 LTR (**S**IN), has **m**inimal HIV-1 *gag* sequences, contains the c**P**PT/CTS sequence from HIV-1, has 3 copies of the **U**ES polyadenylation enhancement

element from SV40, and a minimal HIV-1 **R**RE (gift of Paula Cannon, Children's Hospital-Los Angeles). The vector has the **U3** region from the **M**ND retroviral vector as an internal promoter driving expression of the firefly **luc**iferase gene from SP-LUC+ (Promega). TC71 cells were transduced with viral supernatant containing SMPU-R-MNCU3-LUC vector[31]. A second cycle of transduction was performed 8 h later by removing old medium and adding new viral supernatant and medium. Twenty-four hours after the initial transduction, cells were thoroughly washed three times with PBS before *in vitro* analysis.

4.3.8 Injection of NOD/scid mice with TC71-LUC cells

TC71-LUC cells were cultured in RPMI 1640 medium with 10% fetal bovine serum (no antibiotics). To prepare for injection, cells were trypsinized from tissue culture flasks and washed twice with PBS. Cells were counted on a hemacytometer slide and resuspended in serum-free RPMI 1640 medium immediately prior to injection. The viability of the cells was tested by trypan blue exclusion; only cells more than 90% viable were used. Female NOD/scid mice were treated according to the NIH Guidelines for Animal Care and as approved by the Caltech Institutional Animal Care and Use Committee. All mice were 6-8 weeks of age at the time of injection. Each mouse was injected with 5×10^6 TC71-LUC cells suspended in 0.2 mL RPMI 1640 (without FBS or antibiotics) through the tail vein using a 27-gauge needle. All experimental manipulations with the mice were performed under sterile conditions in a laminar flow hood.

4.3.9 Bioluminescence imaging of mice

Mice were imaged at indicated time points using an *in vivo* IVIS 100 bioluminescence/optical imaging system (Xenogen). D-luciferin (Xenogen) dissolved in

PBS was injected intraperitoneally at a dose of 150 mg/kg (0.2 mL of a 15 mg/mL solution per 20-g mouse) 10 min before measurement of luminescence. General anesthesia was induced with 5% isoflurane and continued during the procedure with 2.5% isoflurane introduced via a nose cone.

After acquiring photographic images of each mouse, luminescent images were acquired with various (1 – 180 s) exposure times. The resulting grayscale photographic and pseudo-color luminescent images were automatically superimposed by the IVIS Living Image software (Xenogen) to facilitate the matching of the observed luciferase signal with its location within the mouse. Regions of Interest (ROI) were manually drawn around the bodies (NOD/scid) or abdominal regions (transgenic) of the mice to assess signal intensity emitted. Luminescent signal was integrated over these ROIs and is expressed as photons per second emitted. Tumor bioluminescence in mice has been shown to be linearly correlated with the tumor volume[32-33], and we have verified these findings (data not shown). For transgenic mice, fur in the abdominal region was removed by shaving once, prior to the start of the experiment, to permit detection of liver bioluminescence.

4.3.10 Magnetic resonance imaging

Before imaging, each mouse received 100 μL paramagnetic contrast agent MAGNEVIST (1 mL MAGNEVIST contains 469.01 mg gadopentate dimeglumine, 0.99 mg meglumine and 0.4 mg diethylentriamine pentaacetic acid) intraperitoneally to enhance delineation. Mice were sedated with 5% isoflurane and wrapped in cellophane to prevent hypothermia and minimize contamination of the MRI system. Isoflurane gas (0.8% in air) was used for

supplementary sedation as needed. All images were obtained using a BRUKER BIOSPIN MRI with a horizontal magnet of 7.0 Tesla (Bruker Instruments, Inc.).

4.3.11 Preparation of formulations and injections of NOD/scid mice

Polyplex formulations were prepared containing siGL3 or siCON1 and CDP at a charge ratio of 3/1 +/-. Prior to addition to siRNA, CDP was mixed with an adamantane-(polyethylene glycol)$_{5000}$ (AD-PEG) conjugate at a 1:1 AD:β-CD (mol:mol) ratio. Targeted polyplexes also contained transferrin-modified AD-PEG (AD-PEG-Tf) at a 1:1000 AD-PEG-Tf:AD-PEG (w:w) ratio. This mixture was then added to an equal volume of siRNA (in H_2O) to form polyplexes. An equal volume of 10% (w:v) glucose (100 mg/mL glucose in H_2O) was added to the polyplex solution to give a final polyplex solution in 5% glucose (D5W) suitable for injection. Formulations were administered by low-pressure tail vein (LPTV) injection using a 1-mL syringe and a 27-gauge needle; injection volumes were adjusted by mouse weight such that each 20-g mouse received 50 μg siRNA (2.5 mg/kg) in a volume of 0.2 mL (1% v:w).

Fifty female NOD/scid mice were injected with 5 x 10^6 TC71-LUC cells as described above. Immediately after cell injection, each mouse received an additional injection of 0.2 mL of one of the following formulations (2.5 mg/kg siRNA, 10 mice per group): D5W only (group A); naked siEFBP2 only (group B); targeted, formulated siCON1 (group C); targeted, formulated siEFBP2 (group D); or non-targeted, formulated siEFBP2 (group E). Formulations were administered twice-weekly for four weeks. Images were taken immediately after the first injections for quality control of the injections and twice-weekly immediately before the injection of the formulations. We continued to monitor the tumor signal in the mice receiving targeted (group D) and non-targeted (group E) siEFBP2

formulations for an additional three weeks or until the tumor burden was too great for the mice.

4.3.12 Toxicity, immune response, and pathology studies

Female C57BL/6 mice (Jackson Laboratories) were 6 – 8 weeks of age at the time they received a single injection of each of the five formulations listed above (six mice per group). To measure plasma cytokine levels, blood was harvested from mice 2 h and 24 h post-injection (three mice per treatment for each timepoint) by cardiac puncture, and plasma was isolated using Microtainer tubes (Becton Dickinson). Whole blood was used for complete blood count (CBC) analyses, and plasma was used for all liver enzyme and cytokine analyses. IL-12 (p40) (BD Biosciences) and IFN-α levels (PBL Biomedical Laboratories) were measured by ELISA according to the manufacturer's instructions. Major organs of the NOD/scid mice after long-term treatment studies were collected, formalin-fixed, and processed for routine hematoxylin and eosin staining using standard methods. Images were collected using a Nikon epifluorescent microscope with a DP11 digital camera.

4.4 RESULTS

4.4.1 siRNA-containing polyplexes down-regulate co-delivered luciferase in cultured cells

An initial investgation of the ability of CDP/siRNA polyplexes to down-regulate a target gene was performed in HeLa (human cervical carinoma) and BHK (baby hamster kidney) cells, which have been previously shown to express genes delivered from CDP/pDNA polyplexes at high levels[23]. Polyplexes were prepared that contained both a plasmid encoding the gene for luciferase (pGL3CV) alone, or with either an siRNA duplex targeting that luciferase gene (siGL3) or an siRNA duplex targeting an irrelevant gene (siEGFP). Lipoplexes made with Lipofectin and the same combinations of nucleic acids were used as a positive control for down-regulation in HeLa cells. Cells were exposed to polyplexes for 4 h and were lysed at 48 h post-transfection; the luciferase levels in lysates were measured by luminometer (**Fig. 4.1**).

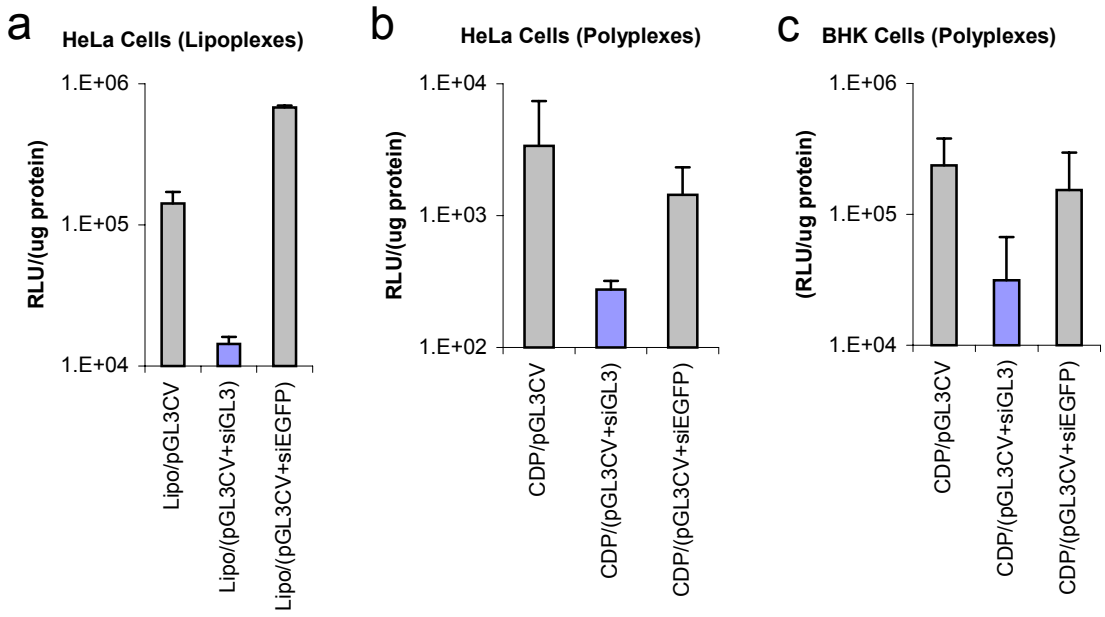

Figure 4.1. CDP/siRNA down-regulates co-delivered luciferase in HeLa and BHK cells. (**a**) Lipoplexes or (**b**, **c**) polyplexes were prepared with CDP and pGL3CV alone or with either siGL3 or siEGFP. Cells were exposed to polyplexes for 4 h and lysed 48 h post-transfection. The luciferase levels in lysates are measured in relative light units (RLUs) and are normalized by the amount of protein in each sample. Bars indicate averages of triplicate wells for each treatment, and error bars represent one standard deviation. Sequence-specific down-regulation from siRNA-containing polyplexes is observed in both cell lines.

Polyplexes containing a control siRNA sequence (siEGFP) show some, but non-zero, suppression of luciferase expression (42% and 35% reduction in HeLa and BHK cells, respectively, compared to CDP/pDNA only). This non-specific down-regulation seen with siEGFP may be a consequence of the relative high dose (100 nM) of siRNA used here and has been reported elsewhere under similar conditions[34-35]. By contrast, the amount of luciferase protein is reduced by 87% and 92% in HeLa and BHK cells, respectively, for siGL3-containing polyplexes. These results are indicative of strong, sequence-specific luciferase suppression.

4.4.2 siRNA-containing polyplexes reduce expression of the EWS-Fli1 oncogene in cultured Ewing's sarcoma cells

Having demonstrated sequence-specific down-regulation of a co-delivered exogenous gene by CDP/siRNA complexes in cultured cells, the ability of these polyplexes to reduce levels of an endogenous gene was examined in cultured Ewing's sarcoma (TC71) cells. siRNA duplexes were obtained that either target the junction of the EWS-Fli1 fusion gene (siEFBP2) or a mutated, non-functional variant (siEFBP2mut). Lipoplexes were made with Oligofectamine, a commercially available lipid reagent, as a positive control for down-regulation. EWS-Fli1 protein levels were measured in the lysates of cells 48 h after transfection by Western blotting (**Fig. 4.2**).

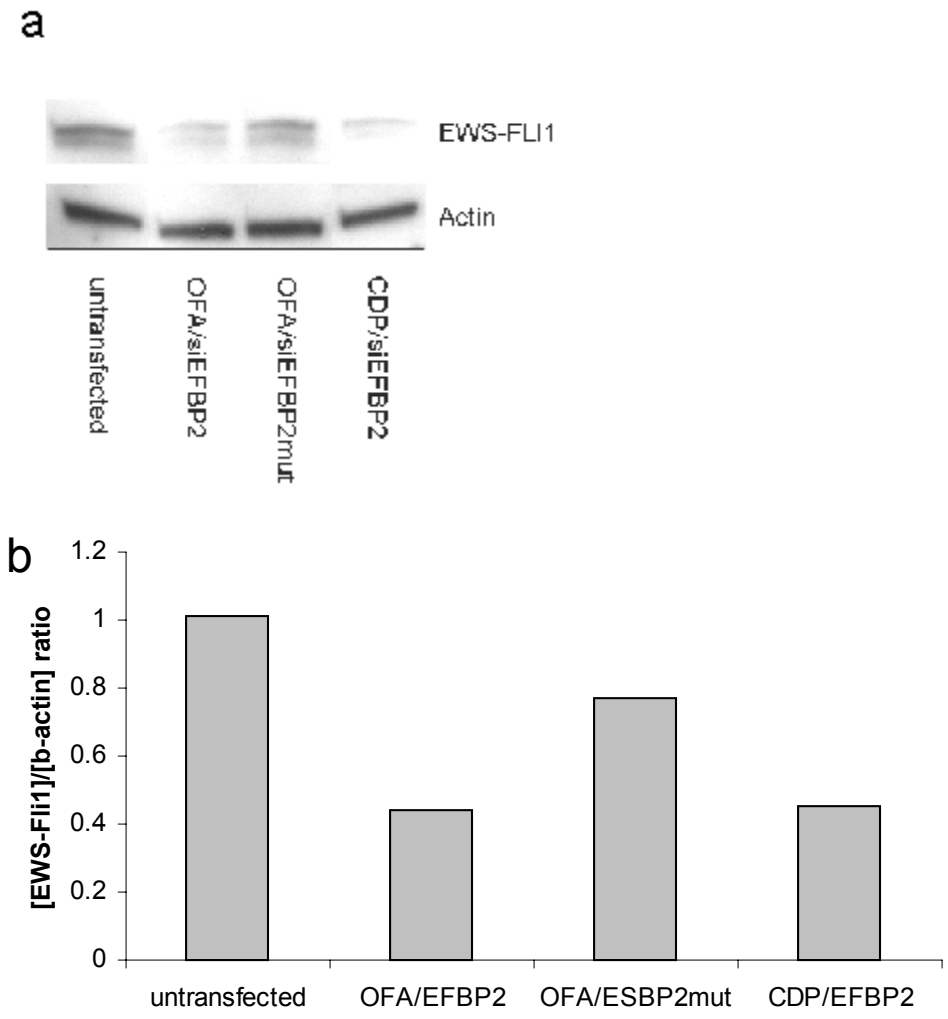

Figure 4.2. CDP/siRNA down-regulates oncogenic EWS/Fli-1 in cultured Ewing's sarcoma cells. Lipoplexes made with Oligofectamine (OFA) or polyplexes made with cyclodextrin-containing polycation (CDP) and siRNA targeting the breakpoint of the EWS-Fli1 fusion gene (siEFBP2) or a mutated, non-functional siRNA (siEFBP2mut) were prepared; cultured TC71 Ewing's sarcoma cells were exposed to these complexes for 4 h and lysed 48 h post-transfection. (**a**) The EWS-Fli1 protein levels were measured by Western blot and compared to those of β-actin. (**b**) Quantification of the Western blot; values presented are the ratio of EWS-Fli1 to β-actin band intensities as determined by densitometry.

Using a previously reported siRNA sequence targeting the EWS-FLI1 breakpoint (siEFBP2)[29], we observed comparable and significant (greater than 50%) reduction in EWS-FLI1 protein levels using both Oligofectamine and CDP. Delivery of a mutated

siRNA sequence (siEFBP2mut) failed to elicit such down-regulation (data not shown for CDP), demonstrating the sequence-specific nature of the RNAi effect.

4.4.3 Galactosylated polyplexes down-regulate hepatic luciferase in transgenic mice

After successful demonstration of down-regulation of both endogenous and exogenous targets in cultured cells, siRNA-containing polyplex formulations were then tested for their ability to achieve similar down-regulation *in vivo*. Transgenic C57BL/6 mice were created that constitutively express luciferase exclusively in hepatocytes within their livers. Hepatocytes express high levels of the cell surface asialoglycoprotein receptor (ASGPr), which is known to recognize galactose as a ligand[36-37]. External material that is galactosylated and sufficiently small (less than ~70 nm in diameter[38]) may be endocytosed by hepatocytes. Thus, CDP/siRNA polyplexes were targeted to hepatocytes by galactosylation via incorporation with an AD-PEG-Lactose modifier (galactose is the terminal moiety of lactose, a disaccharide).

Luciferase-expressing mice received three consecutive daily administrations of galactosylated CDP/siRNA polyplexes containing either siRNA targeting luciferase (siGL3) or a single injection of polyplexes containing non-targeting control sequence (siCON1) followed by two consecutive daily administrations of carrier solution only (D5W). The hepatic luciferase signal in these mice was monitored and quantified by whole-animal *in vivo* bioluminescent imaging and is presented in **Figure 4.3**.

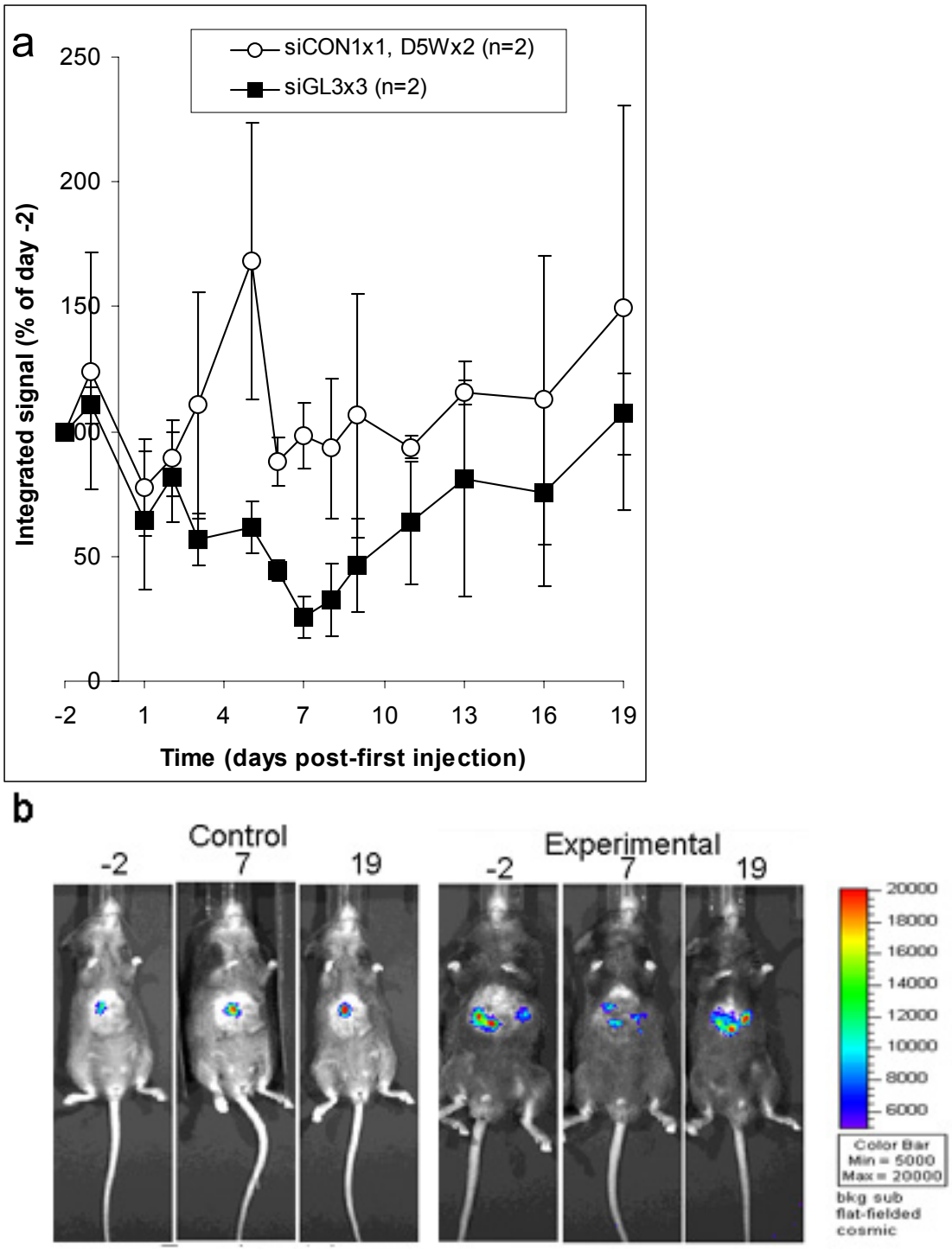

Figure 4.3. Galactosylated CDP/siRNA down-regulates luciferase in livers of transgenic mice. Polyplexes were prepared with CDP, siRNA against luciferase (siGL3) or a non-targeting control sequence (siCON1), and AD-PEG-Lac to target hepatocytes. Transgenic mice bearing hepatocyte-specific luciferase expression received three consecutive daily injections of siGL3-containing formulations by LPTV on Days 0, 1, and 2. Control mice received one injection of the siCON1-containing formulation followed by two consecutive daily injections of carrier solution (D5W). (**a**) The timecourse of

luciferase expression was followed and quantified by whole-animal bioluminescent imaging. Integrated signal is presented as a percentage of the signal on Day –2 (for each mouse). Error bars represent one standard deviation from the mean. (**b**) Images of one mouse from each group are shown from Days –2, 7, and 19 post-injection. Mice receiving the siGL3-containing formulation show significant luciferase down-regulation (up to >50%) that was maximal at Day 7.

Down-regulation of luciferase was observed for mice receiving galactosylated siGL3-containing formulations. Luciferase reduction was most significant between days 4 and 9 after the first injection, with a maximal reduction of 75% seen on day 7. Significant reduction was not seen for mice receiving the control injections at any timepoint examined. These results indicate that CDP/siRNA polyplexes targeted with AD-PEG-Lac are suitable for uptake and down-regulation of a target gene in hepatocytes.

4.4.4 Transferrin-targeted polyplexes inhibit Ewing's sarcoma tumor formation in mice

It was shown previously that CDP/siRNA polyplexes are capable of reducing levels of the EWS-Fli1 fusion oncogene in cultured Ewing's sarcoma cells (see Section 4.4.2). Given this result and the *in vivo* knockdown targeting polyplexes produced in transgenic mice expressing luciferase in hepatocytes (see Section 4.4.3), it was hypothesized that polyplexes targeted to Ewing's sarcoma cells could be employed to inhibit Ewing's sarcoma tumorigenesis in mice.

In order to examine this possibility, a target on the cell surface of Ewing's sarcoma cells needed to be identified. Since the membrane-bound transferrin receptor (TfR) has been shown to be up-regulated in a wide variety of cancers[39], we assessed the level of TfR on cultured TC71 Ewing's sarcoma cells. The uptake of fluorescein-labeled transferrin (Tf-FITC) by TC71 cells was measured by flow cytometry and compared to that of cell lines

known to express very high (HeLa) and low (A2780) levels of TfR; the results are shown in **Figure 4.4**.

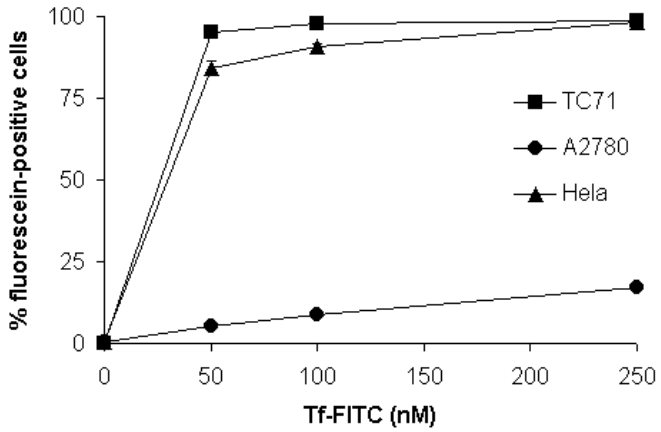

Figure 4.4. TC71 Ewing's sarcoma cells display high levels of transferrin receptor (TfR). Cultured TC71, HeLa, and A2780 cells were each exposed to three different Tf-FITC concentrations (50, 100, and 250 nM) for 1 h at 37 ^{o}C. The fluorescence levels of cells were then measured by flow cytometry. Like HeLa cells, TC71 cells displayed strong fluorescence at all three Tf-FITC concentrations examined. This suggests that TC71 cells express large numbers of TfR molecules on their surface and that TfR may be an appropriate candidate for targeting of polyplexes to TC71 cells *in vivo*.

Because the fluorescence of TC71 cells exposed to all three concentrations of Tf-FITC was very high (>80% compared to untreated control cells), we conclude that TfR levels on TC71 cells are high enough to consider targeting polyplexes to TfR to direct uptake by TC71 cells *in vivo*. Further, analogous to the targeting of ASGPr on hepatocytes with an adamantane-poly(ethylene glycol)-lactose (AD-PEG-Lac) conjugate discussed above (see Section 4.3.3), the synthesis and characterization of an AD-PEG-Tf conjugate, and its use to target TfR-expressing cells, have previously been described[26].

TC71 cells were made to constitutively express luciferase (TC71-LUC cells) via lentiviral infection such that tumor formation could be followed by whole-animal bioluminescence imaging. In order to determine our ability to follow these cells by imaging and the extent of tumorigenesis, NOD/scid mice were injected with TC71-LUC cells by tail vein

injection. The mice were monitored by imaging, and selected tumor-bearing mice were additionally examined by magnetic resonance imaging (MRI). Representative images are shown in **Figure 4.5**.

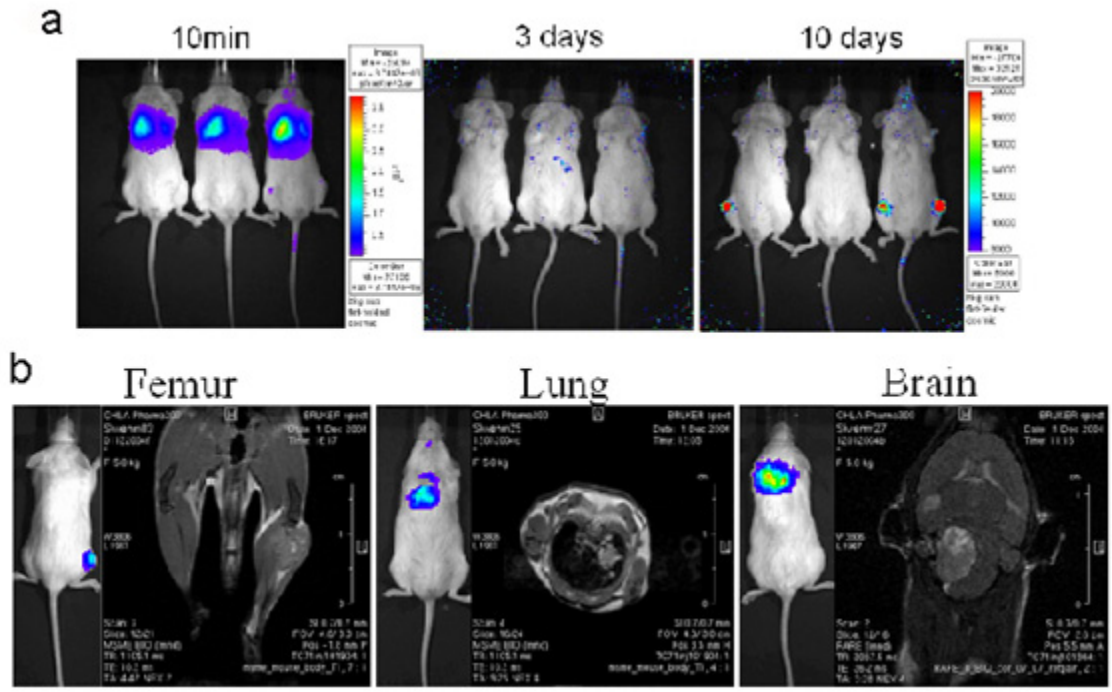

Figure 4.5. Establishment of a disseminated Ewing's sarcoma model in mice.
(**a**) NOD/scid mice injected with TC71-LUC cells developed metastatic tumors. Mice were injected with TC71-LUC cells via the tail vein. At various time points after injection, mice were anesthetized, injected with D-Luciferin, and imaged using a Xenogen IVIS 100 bioluminescence imaging system. (**b**) MRI confirmation of EFT engraftments. Tumor-bearing mice were anesthetized, injected with contrast agent, and imaged. Tumor locations observed by MRI corresponded to bioluminescent signal.

After initially residing in the lung capillary beds, injected TC71-LUC cells disseminated, and tumors were visualized in a variety of locations a couple of weeks after injection. Overall, the tumor engraftment sites observed (lung, vertebral column, pelvis, femur, and soft tissue) were comparable to the most common locations of metastases in EFT patients.

The ability of targeted, siRNA-containing polyplexes to down-regulate EWS-Fli1 in these TC71-LUC-derived tumors was then tested, both indirectly by bioluminescence imaging and directly by qRT-PCR analysis of harvested tumors. Mice that had formed tumors after

injection with TC71-LUC cells were treated with two consecutive daily injections of polyplexes that were targeted with AD-PEG-Lac and contained siRNA targeting the EWS/Fli1 fusion gene (siEFBP2). A summary plot of the imaging results is shown in **Figure 4.6**.

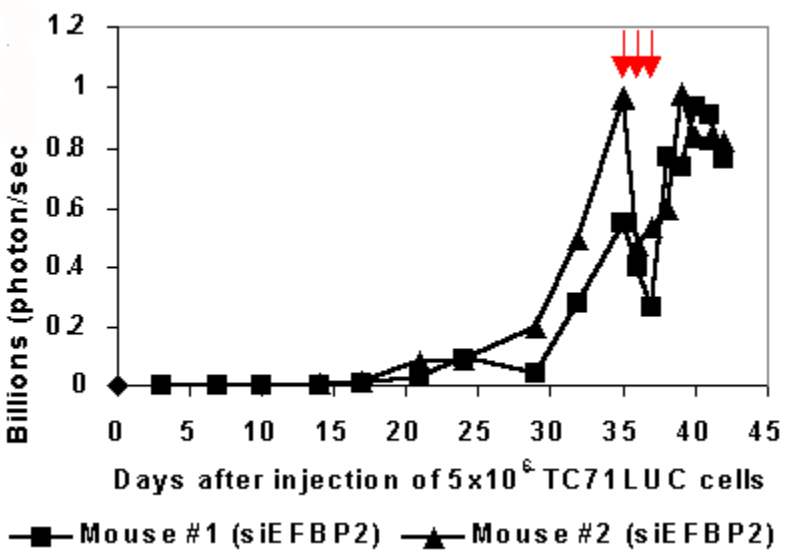

Figure 4.6. Targeted polyplexes containing siRNA against EWS-Fli1 reduced tumor bioluminescence in mice. siRNA against EWS-Fli1 (siEFBP2) was formulated with CDP and targeted with Ad-PEG-Tf. Two tumor-bearing mice received this formulation by low-pressure tail vein (LPTV) injection on three consecutive days (Days 35, 36, and 37; red arrows) after injection of TC71-LUC cells. Tumor size was quantified by integration of bioluminescent flux (photons/sec) at indicated timepoints. Transient reduction in bioluminescence was observed on days 36 and 37.

We hypothesized that targeted siEFBP2-containing polyplexes would reduce the rate of tumor growth in mice receiving them, leading to a transient reduction in the rate of increase, or even a decrease, of tumor bioluminescence. Indeed, a transient reduction in bioluminescence was seen on days 1 and 2 after the first of consecutive daily injections of these formulations. While indirect, this result suggested that the expected knockdown of the EWS/Fli1 gene in TC71-LUC cells *in vivo* was occurring.

To probe this down-regulation more directly, similar (two consecutive daily) injections were made in tumor-bearing mice of targeted polyplexes containing either siEFBP2 or a non-targeting control sequence (siCON1). This time, instead of simply following the bioluminescence, mice were sacrificed the day after the second injection, tumors were harvested, and the levels of EWS/Fli-1 mRNA transcripts were measured by quantitative, real-time PCR (qRT-PCR). The results are shown in **Figure 4.7**.

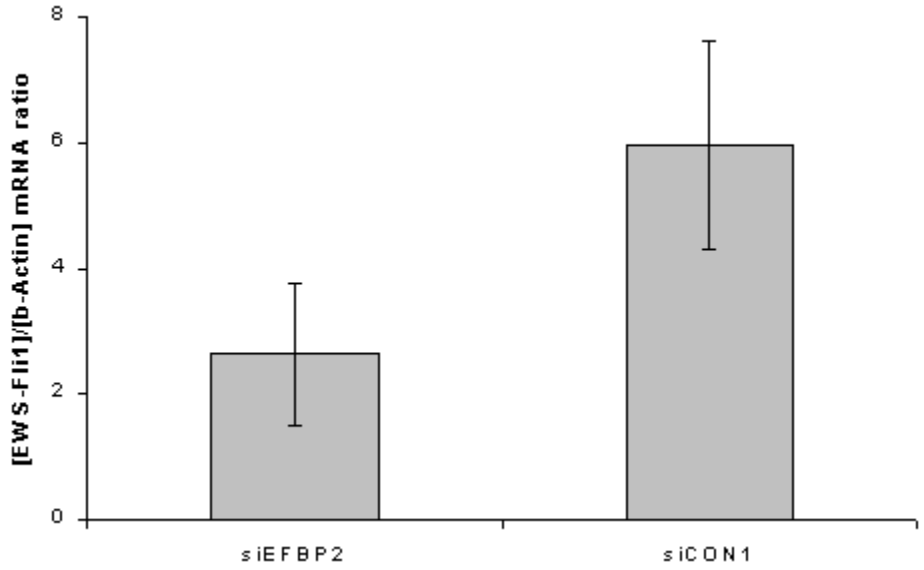

Figure 4.7. Targeted polyplexes containing siEFBP2 reduced EWS-Fli1 mRNA levels in tumors. Formulated siEFBP2 or siCON1 were administered by LPTV injection on two consecutive days in tumor-bearing (TC71-LUC) NOD/scid. Tumors were harvested on the day after the second injection, RNA was extracted from these tumors, and EWS-FLI1 mRNA levels were determined by qRT-PCR (relative to a β-actin control). The mean of three measurements is presented; error bars represent standard deviation.

Two consecutive daily injections of Tf-targeted, siEFBP2-containing formulations reduced EWS-Fli1 transcript levels by greater than 50% compared to formulations made with a control siRNA sequence (siCON1). Taken together with the results of Figure 4.6, this provides both indirect and direct evidence that formulated siRNA can achieve the desired gene knockdown *in vivo*.

The final hypothesis that was examined regarding these formulations was whether or not this target gene knockdown *in vivo* would have a corresponding therapeutic effect, e.g., reduced tumor growth. In order to answer this, a long-term treatment schedule was adopted in which TC71-LUC-treated mice received twice weekly injections of formulations for four weeks, starting immediately after injection of TC71-LUC cells (see **Table 4.1**). Five different treatment groups, containing ten mice each, were established.

Group ID	Mouse IDs	Treatment
A	#1-10	carrier solution (D5W)
B	#11-20	naked siEFBP2
C	#21-30	targeted, formulated siCON1
D	#31-40	targeted, formulated siEFBP2
E	#41-50	non-targeted, formulated siEFBP2

Table 4.1. Treatment groups for long-term tumor inhibition study.

Tumor growth was monitored and quantified by whole-animal bioluminescence imaging; a summary plot of the results is shown in **Figure 4.8** (see **Appendix** for all images).

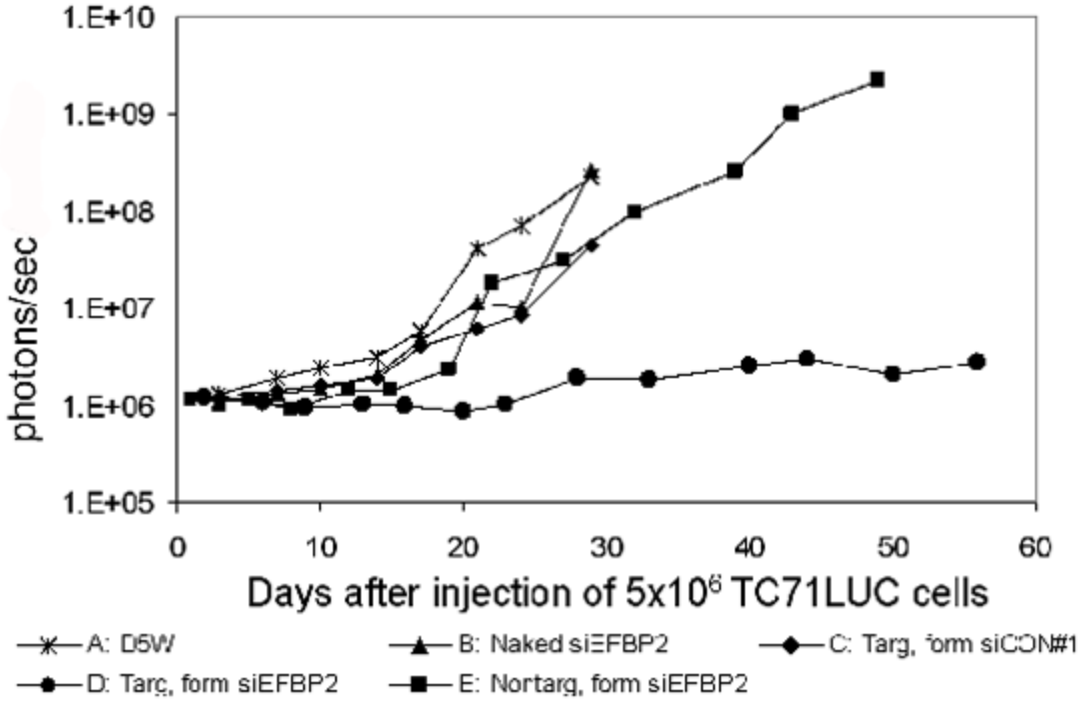

Figure 4.8. Targeted polyplexes containing siEFBP2 reduced tumor growth levels in mice. Starting immediately after injection of TC71-LUC cells, mice were treated with formulations containing siRNA targeting EWS-FLI1 (siEFBP2) or a non-targeting control sequence (siCON1) by LPTV injection twice-weekly for four weeks. The bioluminescence of these mice was monitored twice-weekly. The median integrated tumor bioluminescent signal (photons/sec) for each treatment group [n=8-10] is plotted versus time after cell injection (days). [Treatment groups: A, 5% (w/v) glucose only (D5W); B, naked siEFBP2; C, targeted, formulated siCON1; D, targeted, formulated siEFBP2; E, non-targeted, formulated siEFBP2.]

These long-term (four weeks) injections of siRNA-containing formulations in tumor-bearing NOD/scid mice reveal that only the targeted, formulated siEFBP2 achieves long-term tumor growth inhibition. Neither naked siEFBP2 nor a formulated control siRNA sequence shows any effect on tumor signal compared to the control group receiving only the carrier fluid. These results demonstrate the sequence-specificity of the observed inhibition, the necessity of the targeting agent (AD-PEG-Tf), and the therapeutic potential of this delivery system.

Finally, the safety and immunogenicity of these five formulations were examined. Acute effects were examined after single administrations of each of these formulations in C57BL/6 (non-transgenic) mice. Whole blood and plasma were isolated at both 2 h and 24 h post-injection. Complete blood counts (CBCs) were determined from whole blood samples, while the levels of a number of secreted proteins associated with liver function, as well as two cytokines indicative of an immune response (interleukin-12 (IL-12) and interferon-alpha (IFN-α)), were measured in plasma samples. To investigate chronic toxicity, major organs (liver, lung, heart, kidney, and spleen) were isolated from a mouse in each of three treatment groups, sectioned, subjected to hematoxylin and eosin staining, and examined. All results are shown in **Figure 4.9**.

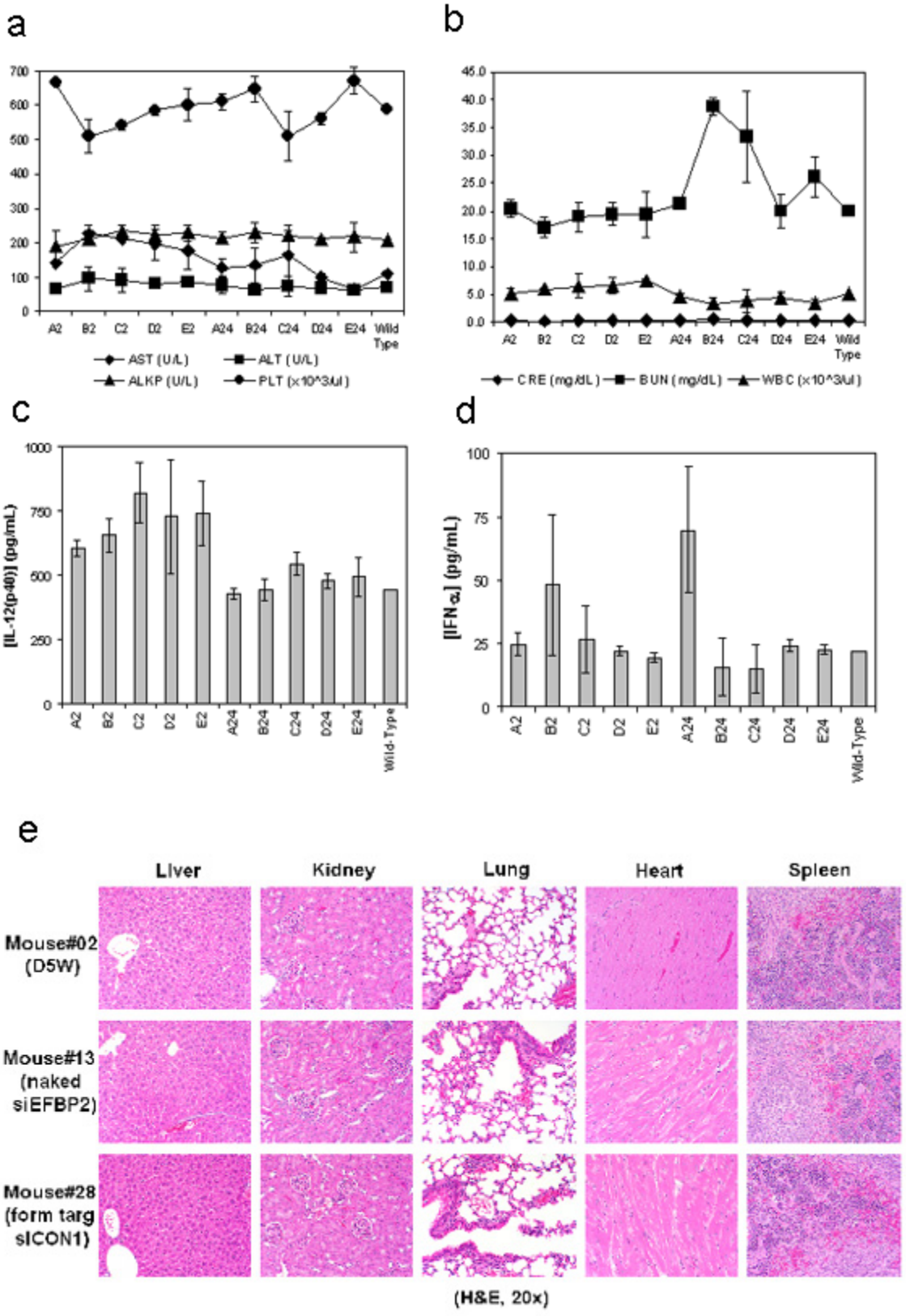

Figure 4.9. Formulated siRNA failed to exhibit toxicity or elicit an immune response in mice. CBC and liver panel results for C57BL/6 mice receiving formulations showed

no toxicity or immune response. Female C57BL/6 mice received a single administration of formulated siRNA. At 2 h or 24 h post-treatment, blood was drawn by cardiac puncture and plasma was isolated. (**a**,**b**) Whole blood was used for determination of platelet (PLT) and white blood cell (WBC) counts. Plasma was used for measurement of aspartate aminotransferase (AST), alanine aminotransferase (ALT), alkaline phosphatase (ALKP), creatinine (CRE), and blood urea nitrogen (BUN). The averages of triplicate mice for each time point are plotted; error bars represent standard deviations. (**c,d**) Cytokine ELISA results for C57BL/6 mice receiving formulations showed no up-regulation of IL-12 or IFN-α. The plasma levels of interleukin-12 (IL-12 (p40)) and interferon-alpha (IFN-α) in mice described above were measured by ELISA. [Treatment groups: A, 5% (w/v) glucose only (D5W); B, naked siEFBP2; C, targeted, formulated siCON1; D, targeted, formulated siEFBP2; E, non-targeted, formulated siEFBP2; Wild-type, uninjected; 2, blood drawn 2 h after injection; 24, blood drawn 24 h after injection.] **(e)** H&E staining of major organs of the NOD/scid mice after long-term treatment. Major organs were collected, formalin-fixed, and processed for routine hematoxylin and eosin staining using standard methods. Images were collected using a Nikon epifluorescent microscope with a DP11 digital camera.

Collectively, none of the formulations show any significant effects on the levels of IL-12, IFN-α, white blood cells, platelets, secreted liver enzymes (ALT and AST), BUN, or CRE in immunocompetent (C57BL/6), and histology of the major organs of mice receiving long-term treatment (twice-weekly injections for four weeks) showed no apparent damage. These results show the safety and low immunogenicity of CDP-containing formulations and demonstrate the attractiveness of this methodology for systemic, targeted delivery of nucleic acids.

4.5 DISCUSSION

Galactosylated CDP/siRNA formulations elicited down-regulaton of luciferase within hepatocytes of transgenic mice. Since galactose is the ligand recognized by asialoglycoprotein receptor (ASGPr) on the surface of hepatocytes, our first investigations with targeting of (DNA-containing) polyplexes to hepatocytes involved synthesis of AD-PEG-galactose (as opposed to AD-PEG-lactose used here). However, our modification at galactose at the C2 moiety had been shown by others to be inferior to modification at the C1 moiety[40] in terms of uptake by hepatoma cells. Because synthesis of an alternative AD-PEG-galactose modified at C1 proved difficult, we instead developed the AD-PEG-lactose conjugate used here[28]. While a 20% AD-PEG-Lac/80% AD-PEG mixture appears here to be adequate to achieve down-regulation of a liver target gene, more work is warranted to determine the amount of AD-PEG-Lac necessary for targeting and to quantify the amount of Ad-PEG-Lac incorporated within the polyplexes (vs. unbound). These subjects will be discussed in more detail in Chapter 5. Also, we attribute the relatively noisy (large error bars) liver luciferase data to the relatively low absolute levels of bioluminescence from these transgenic mice (compared to what we typically observe after HPTV injection of the pApoEHCRLuc plasmid).

We observe that the kinetics of luciferase down-regulation in transgenic mice are significantly slower than those of EWS/Fli1 knockdown in Ewing's sarcoma cells within NOD/scid mice. Indeed, the maximum knockdown in liver-specific luciferase expression was seen seven days after the first of three consecutive injections; in contrast, the biggest reduction in luciferase signal (an indirect measure of EWS/Fli1 knockdown) in TC71-LUC cells was seen just two days after the first of two consecutive treatments. We attribute this

difference to the drastic difference in cell proliferation rates between mainly stationary hepatocytes and actively dividing TC71-LUC cells. It is also worth noting that the timecourse of liver luciferase knockdown seen here (~1-2 weeks) is comparable to that seen after HPTV co-injection of a luciferase-bearing plasmid and siRNA targeting luciferase (see Chapter 2).

While our method of long-term treatment will not translate directly to therapeutic treatment of cancer in humans (administration of formulations was begun the same day as injection of the TC71-LUC cells), we are encouraged at the significant inhibition of tumor growth observed using Tf-targeted, siEFBP2-containing polyplexes. This inhibition persisted even well after the final treatment was administered. This observation speaks well to the potency of these duplexes to prevent tumor engraftment, and future exploration as part of a combination therapy with more traditional chemotherapeutics is warranted. Also, while the effect of Tf-targeting is clear (non-targeted siEFBP2-containing formulations fail to significantly inhibit tumor growth), the extent of targeting, and whether or not this could be improved upon, still remains unmeasured. While we demonstrated that TfR is expressed at high levels (up-regulated) on TC71-LUC cells, it is possible that basal levels of TfR on other cell types are enough to significantly reduce the fraction of polyplexes that reach TC71-LUC cells. If this is true, one should consider using a more cell type-specific target (such as CD99 for Ewing's sarcoma cells) to increase the "effective dose" of polyplexes that are taken up by the desired target cells.

The siCON1 duplex contains a sequence of bases, 5'-UGUGU-3', that has been recognized as a putative immunostimulatory motif [21]. When encapsulated in lipids and administered to immunocompetent mice, multiple siRNA duplexes containing this motif were shown to

significantly increase IFN-a levels and reduce numbers of platelets and white blood cells[21]. In this investigation, targeted CDP/siCON1 polyplexes did not produce any of these effects in immunocompetent C57BL/6 mice. This observation leaves open the possibility that the sequence-specific immunogenicity reported elsewhere may be due, at least in part, to the character of the liposomal delivery system. Given the extreme hydrophilicity of all of the components of the polymeric delivery system examined here, one hypothesis for the difference in results with the two delivery systems lies in the hydrophilicity of all of the components of the polymeric delivery system examined here versus the relatively hydrophobic nature of the liposomes. It seems possible that, within the bloodstream of recipient mice, liposomes may be more likely to partition to peripheral blood mononuclear cells (PBMCs), the cells which have been implicated in the observed responses[21].

Overall, the results of Chapter 4 demonstrate the safety and efficacy of systemically-administered, targeted, siRNA-containing polyplexes *in vivo*. These observations suggest that development of non-viral siRNA delivery systems for human therapeutic applications is indeed possible and, given the tremendous potency of RNAi in general (especially compared to previous-generation molecular therapeutics, such as antisense) and seen here, should be explored in the near future.

4.6 REFERENCES

[1] Lewis DL, Hagstron JE, Loomis AG, Wolff JA & Herweijer H. Efficient delivery of siRNA for inhibition of gene expression in postnatal mice. *Nat. Genet*. **32**, 107-108 (2002).

[2] McCaffrey AP, Meuse L, Pham TT, Conklin DS, Hannon GJ & Kay MA. RNA interference in adult mice. *Nature* **418**, 38-39 (2002).

[3] Song E, Lee SK, Wang J, Ince N, Ouyang N, Min J, Chen J, Shankar P & Lieberman J. RNA interference targeting Fas protects mice from fulminant hepatitis. *Nat. Med*. **9**, 347-351 (2003).

[4] Filleur S, Courtin A, Ait-Si-Ali S, Guglielmi J, Merle C, Harel-Bellan A, Clezardin P & Cabon F. siRNA-mediated inhibition of vascular endothelial growth factor severely limits tumor resistance to antiangiogenic thrombospondin-1 and slows tumor vascularization and growth. *Cancer Res*. **63**, 3919-3922 (2003).

[5] Duxbury MS, Matros E, Ito H, Zinner MJ, Ashley SW & Whang EE. Systemic siRNA-mediated gene silencing: a new approach to targeted therapy of cancer. *Ann. Surg*. **240**, 667-674 (2004).

[6] Soutschek J, Akinc A, Bramlage B, Charisse K, Constien R, Donoghue M, Elbashir S, Geick A, Hadwiger P, Harborth J, John M, Kesavan V, Lavine G, Pandey RK, Racie T, Rajeev KG, Rohl I, Toudjarska I, Wang G, Wuschko S, Bumcrot D, Koteliansky V, Limmer S, Manoharan M & Vornlocher HP. Therapeutic silencing of an endogenous gene by systemic administration of modified siRNAs. *Nature* **432**, 173-178 (2004).

[7] Sioud M & Sorensen DR. Cationic liposome-mediated delivery of siRNAs in adult mice. *Biochem. Biophys. Res. Commun*. **312**, 1220-1225 (2003).

[8] Zhang Y, Boado RJ & Pardridge WM. In vivo knockdown of gene expression in brain cancer with intravenous RNAi in adult rats. *J. Gene Med*. **5**, 1039-1045 (2003).

[9] Zhang Y, Zhang YF, Bryant J, Charles A, Boado RJ & Pardridge WM. Intravenous RNA interference gene therapy targeting the human epidermal growth factor receptor prolongs survival in intracranial brain cancer. *Clin. Cancer Res*. **10**, 3667-3677 (2004).

[10] Schiffelers RM, Ansari A, Xu J, Zhou Q, Tang Q, Storm G, Molema G, Lu PY, Scaria PV & Woodle MC. Cancer siRNA therapy by tumor selective delivery with ligand-targeted sterically stabilized nanoparticle. *Nucl. Acids Res*. **32**, e149 (2004).

[11] Ge Q, Filip L, Bai A, Nguyen U, Eisen HN & Chen J. Inhibition of influenza virus production in virus-infected mice by RNA interference. *Proc. Natl. Acad. Sci. USA* **101**, 8676-8681 (2004).

[12] Urban-Klein B, Werth S, Abuharbeid S, Czubayko F & Aigner A. RNAi-mediated gene-targeting through systemic application of polyethylenimine (PEI)-complexed siRNA in vivo. *Gene Ther*. **12**, 461-466 (2005).

[13] Bertrand JR, Pottier M, Vekris A, Opolon P, Maksimenko A & Malvy C. Comparison of antisense oligonucleotides and siRNAs in cell culture and in vivo. *Biochem. Biophys. Res. Commun*. 296, 1000-1004 (2002).

[14] Minakuchi Y, Takeshita F, Kosaka N, Sasaki H, Yamamoto Y, Kouno M, Honma K, Nagahara S, Hanai K, Sano A, Kato T, Terada M & Ochiya T. Atelocollagen-mediated synthetic small interfering RNA delivery for effective gene silencing in vitro and in vivo. *Nucl. Acids Res*. **32**, e109 (2004).

[15] Takei Y, Kadomatsu K, Yuzawa Y, Matsuo S & Muramatsu TA. A small interfering RNA targeting vascular endothelial growth factor as cancer therapeutics. *Cancer Res*. **64**, 3365-3370 (2004).

[16] Pille JY, Denoyelle C, Varet J, Bertrand JR, Soria J, Opolon P, Lu H, Pritchard LL, Vannier JP, Malvy C, Soria C & Li H. Anti-rhoA and anti-rhoC siRNAs inhibit the proliferation and invasiveness of MDA-MB-231 breast cancer cells in vitro and in vivo. *Mol. Ther*. **11**, 267-274 (2005).

[17] Layzer JM, McCaffrey AP, Tanner AK, Huang Z, Kay MA & Sullenger BA. In vivo activity of nuclease-resistant siRNAs. *RNA* **10**, 766-771 (2004).

[18] Braasch DA, Paroo Z, Constantinescu A, Ren G, Oz OK, Mason RP & Corey DR. Biodistribution of phosphodiester and phosphorothioate siRNA. *Bioorg. Med. Chem. Lett*. **14**, 1139-1143 (2004).

[19] Heidel JD, Hu S, Liu XF, Triche TJ & Davis ME. Lack of interferon response in animals to naked siRNAs. *Nat. Biotechnol*. **22**, 1579-1582 (2004).

[20] Ma Z, Li J, He F, Wilson A, Pitt B & Li S. Cationic lipids enhance siRNA-mediated interferon response in mice. *Biochem. Biophys. Res. Commun*. **330**, 755-759 (2005).

[21] Judge AD, Sood V, Shaw JR, Fang D, McClintock K & MacLachlan I. Sequence-dependent stimulation of the mammalian innate immune response by synthetic siRNA. *Nat. Biotechnol*. **23**, 457-462 (2005).

[22] Hornung V, Guenthner-Biller M, Bourquin C, Ablasser A, Schlee M, Uematsu S, Noronha A, Manoharan M, Akira S, de Fougerolles A, Endres S & Hartmann G. Sequence-specific potent induction of IFN-alpha by short interfering RNA in plasmacytoid dendritic cells through TLR7. *Nat. Med.* **11**, 263-270 (2005).

[23] Gonzalez H, Hwang SJ & Davis ME. New class of polymers for the delivery of macromolecular therapeutics. *Bioconjug. Chem*. **10**, 1068-1074 (1999).

[24] Hwang SJ, Bellocq NC & Davis ME. Effects of structure of beta-cyclodextrin-containing polymers on gene delivery. *Bioconjug. Chem*. **12**, 280-290 (2001).

[25] Pun SH & Davis ME. Development of a nonviral gene delivery vehicle for systemic application. *Bioconjug. Chem*. **13**, 630-639 (2002).

[26] Bellocq NC, Pun SH, Jensen GS & Davis ME. Transferrin-containing, cyclodextrin polymer-based particles for tumor-targeted gene delivery. *Bioconjug Chem*. **14**, 1122-1132 (2003).

[27] Pun SH, Tack F, Bellocq NC, Cheng J, Grubbs BH, Jensen GS, Davis ME, Brewster M, Janicot M, Janssens B, Floren W & Bakker A. Targeted delivery of RNA-cleaving DNA enzyme (DNAzyme) to tumor tissue by transferrin-modified, cyclodextrin-based particles. *Cancer Biol. & Ther*. **3**, 641-650 (2004).

[28] Pun SH, Gonzalez N, Davis ME, Bellocq N & Cheng J. Compositions containing inclusion complexes. **Patent# WO02/49676**. Issued 27 June 2002.

[29] Dohjima T, Lee NS, Li H, Ohno T & Rossi JJ. Small interfering RNAs expressed from a Pol III promoter suppress the EWS/Fli-1 transcript in an Ewing sarcoma cell line. *Mol. Ther*. **7**, 811-816 (2003).

[30] Miao CH, Ohashi K, Patijn GA, Meuse L, Ye X, Thompson AR & Kay MA. Inclusion of the hepatic locus control region, an intron, and untranslated region increases and stabilizes hepatic factor IX gene expression in vivo but not in vitro. *Mol. Ther*. **1**, 522-532 (2000).

[31] Wang X, Rosol M, Ge S, Peterson D, McNamara G, Pollack K, Kohn DB, Nelson MD & Crooks GM. Dynamic tracking of human hematopoetic stem cell engraftment using in vivo bioluminescence imaging. *Blood* **102**, 3478-3482 (2003).

[32] Rehemtulla A, Stegman LD, Cardozo SJ, Gupta S, Hall DE, Contag CH & Ross BD. Rapid and quantitative assessment of cancer treatment response using in vivo bioluminescence imaging. *Neoplasia* **2**, 491-495 (2000).

[33] Vooijs M, Jonkers J, Lyons S & Berns A. Noninvasive imaging of spontaneous retinoblastoma pathway-dependent tumors in mice. *Cancer Res*. **62**, 1862-1867 (2002).

[34] Jackson AL, Bartz SR, Schelter J, Kobayashi SV, Burchard J, Mao M, Li B, Cavet G & Linsley PS. Expression profiling reveals off-target gene regulation by RNAi. *Nat. Biotechnol.* **21**, 635-637 (2003).

[35] Persengiev SP, Zhu X & Green MR. Nonspecific,concentration-dependent stimulation and repression of mammalian gene expression by small interfering RNAs (siRNAs). *RNA* **10**, 12-18 (2004).

[36] Wall DA, Wilson G & Hubbard AL. The galactose-specific recognition system of mammalian liver: the route of ligand internalization in rat hepatocytes. *Cell* **21**, 79-93 (1980).

[37] Schwartz AL, Fridovich SE & Lodish HL. Kinetics of internalization and recycling of the asialoglycoprotein receptor in a hepatoma cell line. *J. Biol. Chem*. **257**, 4230-4237 (1982).

[38] Rensen PCN, Sliedregt L, Ferns A, Kieviet E, van Rossenberg SMW, van Leeuwen SH, van Berkel TKC & Biessen EAL. Determination of the upper size limit for uptake and processing of ligand by the asialoglycoprotein receptor on hepatocytes in vitro and in vivo. *J. Biol. Chem*. **276**, 37577-37584 (2001).

[39] Gatter KC, Brown G, Trowbridge IS, Woolston RE, Mason DY.Transferrin receptors in human tissues: their distribution and possible clinical relevance. *J. Clin. Pathol*. **36**, 539-545 (1983).

[40] David A, Kopeckova P, Rubinstein A & Kopecek J. Enhanced biorecognition and internalization of HPMA copolymers containing multiple or multivalent carbohydrate sidechains by human hepatocarcinoma cells. *Bioconjug. Chem*. **12**, 890-899 (2001).

CHAPTER 5: Recommendations

5.1 ABSTRACT

The results shown in the previous three chapters demonstrate the safety of siRNA duplexes for use as therapeutics, their successful formulation within a polymer-based delivery system, and the efficacy of these small interfering RNA-(siRNA-)containing formulations to achieve targeted gene down-regulation *in vivo*. Despite these successes, the room for further formulation development for even greater potency is large. In this chapter, some ideas and experiments for better understanding of current formulations and modifications for improvement of these formulations are discussed. The importance of and methods for quantification of both the siRNA payload and the amount of targeting ligand incorporated in each polyplex are investigated. I also discuss the prospect of using alternative targeting ligands with greater binding affinity and/or higher relative up-regulation on target cells. Finally, recent literature results suggest that alternative dsRNA duplexes can be more potent RNA interference (RNAi) effector molecules than the 21-nt siRNAs used here; these will be discussed. All of these issues warrant continued development towards production of an optimized formulation for therapeutic RNAi.

5.2 RECOMMENDED FUTURE DIRECTIONS

5.2.1 Quantification of siRNA payload

The characterization of polyplexes made with a cyclodextrin-containing polycation (CDP) and small interfering RNA (siRNA) duplexes detailed in Chapter 3 demonstrates the complete condensation of siRNA within all formulations having a positive (i.e., greater than 1/1 (+/-)) charge ratio. Indeed, it was shown that for all polyplexes prepared at an overall positive charge ratio, the amount of CDP actually within polyplexes was only enough to balance the negative charges on the siRNA; all additional polymer remained unbound. Knowing this information, further determination of the polyplex average molar mass would allow calculation of the average number of CDP and siRNA molecules per polyplex.

The molar mass of a polyplex solution can be determined via multi-angle laser light scattering (MALLS). An extension of the single-angle dynamic light scattering (DLS) used to assess polyplex size in Chapter 3, detectors are employed to measure the light scattered from a polyplex sample at seventeen different angles. From light scattering theory, extrapolation of scattering intensity to zero-angle (0 ^{o}C), along with knowledge of the polyplex solution mass concentration and index of refraction, can be used to determine both the polyplex average hydrodynamic radius and the average molar mass[1].

Armed with polyplex molar mass information, the average number of polymer and nucleic acid molecules per polyplex can be calculated using the system of two equations with two unknowns shown in **Figure 5.1**.

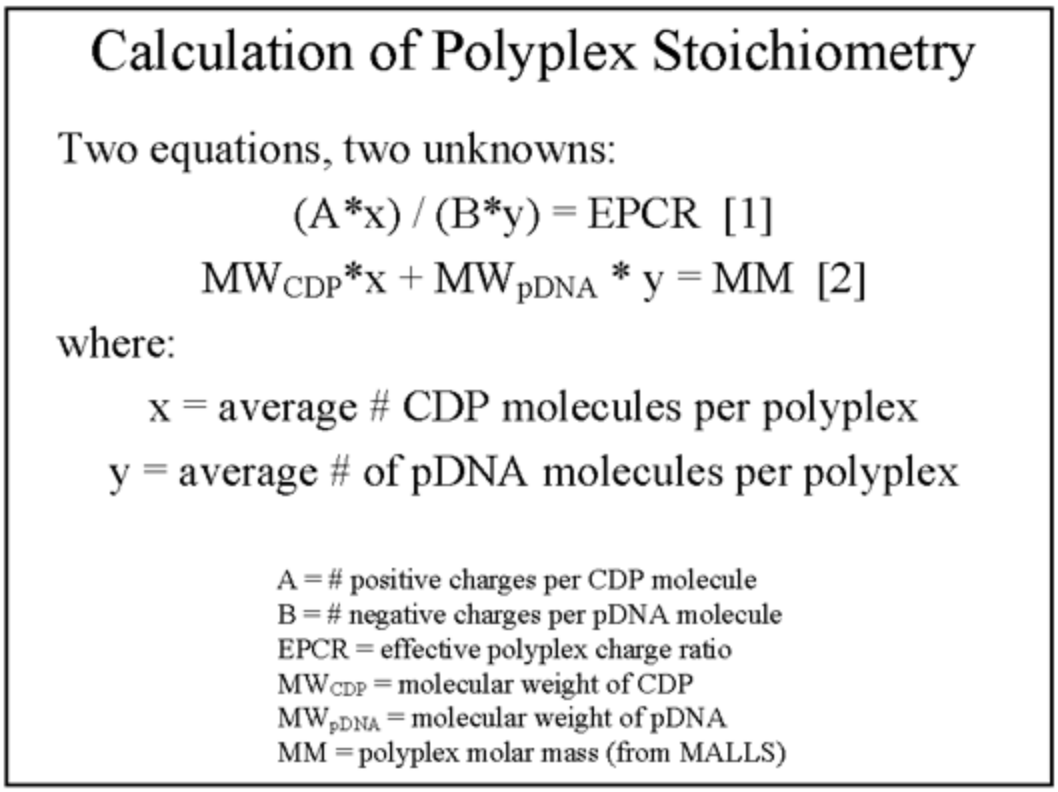

Figure 5.1. Calculation of average polyplex stoichiometry. The average number of polymer and nucleic acid molecules per polyplex can be calculated from the "effective polyplex charge ratio" (EPCR, described in Chapter 3) and the polyplex molar mass. Example values for CDP (two positive charges per repeat unit, repeat unit MW = 1460) and pDNA (5256 bp) are: A = 14, B = 10512, MW_{CDP} = 10,000 (Da), and MW_{pDNA} = 3.5 x 10^6 (Da).

Indeed, MALLS has been employed previously with CDP/pDNA polyplexes in order to determine molar mass and polyplex stoichiometry[2]. The average polyplex molar mass was determined to be ~1 x 10^7 Da, from which the average number of polymer and pDNA molecules per polyplex were calculated to be 1200 and 1.7, respectively. This was an important finding because it indicated that the number of plasmids, and therefore the number of genes, in an individual complex is very small (1 or 2). It also sheds light on the range of target ligand densities that are possible, as will be discussed in further detail below.

I recommend that MALLS be applied to CDP/siRNA polyplexes as well to determine what the number of siRNA molecules per polyplex is and how that number compares to what has been found previously for pDNA. Given the results of Chapter 3 that show nearly identical relationships between polyplex size and concentration for pDNA- and siRNA-containing formulations, under both unPEGylated and PEGylated conditions, it seems reasonable to hypothesize that the total masses of siRNA and pDNA within their respective individual polyplexes are also similar. If that is true, then, owing to the ~100-fold smaller molecular weight of siRNA compared to pDNA, we might expect to find ~170 siRNA molecules per polyplex. Such a result would suggest that CDP-containing polyplexes hold the potential to be much more effective at delivering siRNA for RNAi than at delivering pDNA for gene therapy, if only because the per-polyplex, per-molecule payload is much greater for siRNA-containing complexes. But this remains only a hypothesis until MALS analysis of CDP/siRNA polyplexes and subsequent stoichiometry calculations are performed.

5.2.2 Quantification of ligand density

In Chapter 4, the *in vivo* efficacy of CDP/siRNA polyplexes containing two different targeting ligands is shown. Lactose-containing polyplexes achieved luciferase down-regulation in the livers of recipient mice, while transferrin-containing complexes knocked down levels of the chimeric EWS-Fli1 oncogene in tumors (Ewing's sarcoma). These ligands were selected for targeting of asialoglycoprotein receptor- (ASGPr-)rich hepatocytes and transferrin receptor- (TfR)-rich tumor cells, respectively. While both of these ligands were incorporated into polyplexes in the same way (via tethering to

adamantane-poly(ethylene glycol) (AD-PEG) conjugates), the size and nature of these ligands are very different (lactose is a relatively small disaccharide, while transferrin is a comparatively large protein).

Based on some preliminary *in vitro* work and successful results published elsewhere[3-5], we employed 0.1% (1:1000 w:w) AD-PEG-Tf/AD-PEG and 20% (1:5 w:w) AD-PEG-Lac:AD-PEG loadings, respectively. While these are the total amounts added to the formulation, this is certainly not reflective of the exact amount of these AD-PEG-ligand species within the polyplexes themselves. For example, at 3/1 (+/-) formulation conditions, two-thirds of all CDP molecules remain unbound, and thus AD-PEG-ligand molecules that have formed inclusion complexes with these unbound CDPs will not contribute to polyplex target. If anything, they have the potential to reduce polyplex targeting by competing with ligands on the polyplexes for cell surface receptors.

The recommendation here is that the incorporation of these ligands within polyplexes be further quantified. Essential to such quantification is the ability to separate unbound material from polyplexes, a method for which I have developed using a centrifugal filtration unit (illustrated schematically in **Fig. 5.2**).

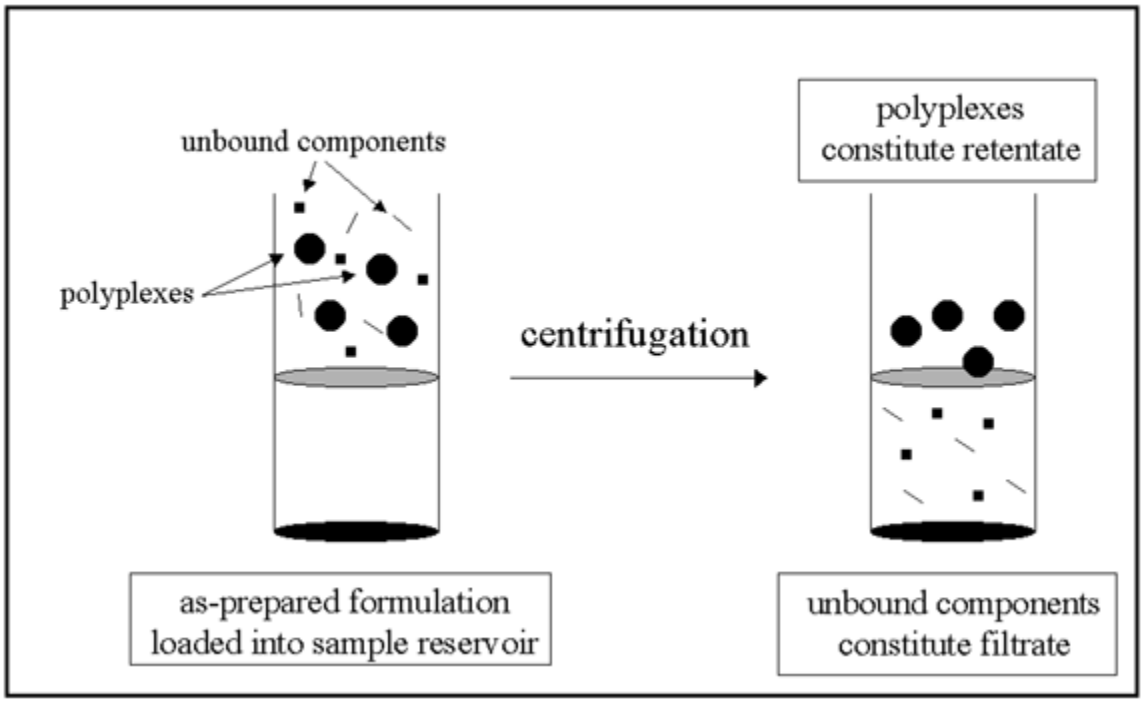

Figure 5.2. Centrifugal filtration to separate unbound material from polyplex formulations. As-prepared polyplex formulations are placed in a centrifugal filtration unit consisting of a reservoir above a membrane having a specified molecular weight cut-off (MWCO, typically 50,000 Da). Centrifugation drives solution containing unbound species (e.g., CDP, AD-PEG, and AD-PEG-Lac) through the filter while retaining polyplexes that are too large to pass through it.

Preliminary work with this separation strategy using CDP/pDNA polyplexes has demonstrated that (1) polyplexes must be PEGylated in order to avoid sticking to the membrane, (2) all polyplexes are retained in the sample reservoir upon centrifugation, and (3) the effective diameter and count rate of polyplexes are unchanged after centrifugal filtration (data not shown).

Centrifugal filtration to remove unbound materials within formulations could be used to quantify polyplex ligand density in multiple ways. For AD-PEG-Lac-containing formulations, separation of free material using a MWCO = 50,000 Da could be followed by direct quantification of galactose using a standard, commercially-available galactose

oxidase assay (described in [6]). Indirect assessment of galactose density could also be performed using an *in vitro* lectin (RCA_{120}) agglutination assay[6]. Membranes having a larger MWCO would be required for AD-PEG-Tf-containing formulations due to the relatively large size (MW ~80,000 Da) of transferrin. The amount of Tf within filtered polyplexes could easily be determined by a standard protein detection assay (e.g., DC Protein Assay, Bio-Rad). Additionally, if fluorophore-containing species of each of these conjugates were prepared (e.g., AD-PEG-FITC-Lac or AD-PEG-FITC-Tf), quantification of ligand density could be performed simply by measurement of fluorescence.

5.2.3 Alternative ligands for improved targeting

While the targeting ligands employed here appeared sufficient to generate target gene knockdown from siRNA-containing polyplexes, it is very possible that improvements in ligand selection and/or design could provide significant improvement of the overall formulation potency.

The monovalent galactose moieities presented here (via AD-PEG-Lactose) are an improvement upon our initial attempts to target hepatocytes but, based on the work of other experimenters, could be greatly improved upon to reach ASGPr-expressing hepatocytes. Initial efforts to target CDP/pDNA polyplexes to hepatocytes were made using AD-PEG-Galactose, as galactose itself is the ligand recognized by ASGPr. However, this conjugation scheme, which involved forming a bond between galactosamine and the adamantane modifier via the C2 position on the sugar[5], was found by others to be inferior for hepatoma cell uptake to modification at the C1 position[7]. This obstacle was overcome by employing a different synthetic scheme that incorporated lactose, instead of galactose,

into the AD-PEG-conjugate[8]. However, there is abundant literature suggesting that multiantennary presentation of galactose, as well as different galactose derivatives (e.g., N-acetylgalactosamine (GalNAc)) having significantly enhanced binding affinity for ASGPr, could lead to improved specificity of targeted polyplexes[9-11]. This issue of binding affinity is particularly important given the relatively few ligand incorporation sites (β-CD moieties within bound CDP molecules) within our polyplexes. The use of stronger binding galactose derivatives should be considered to confer enhanced polyplex targeting to hepatocytes.

Because the transferrin receptor (TfR) has been shown to be up-regulated in actively dividing cells[12], including cancer cells[13] such as Ewing's sarcoma[14], we employed conjugates of AD-PEG containing iron-loaded transferrin (AD-PEG-Tf) to target Ewing's sarcoma (ES) cells. Because all non-cancerous cells have non-zero levels of TfR on their surfaces, however, the possibility of receptor-mediated endocytosis of targeted polyplexes by undesired cell types remains. A ligand/receptor combination that would be more specific to ES cells, if it exists, would be likely to confer even better targeting of formulations to these cells. Literature results indicate that the cell surface molecule CD99, which is over-expressed on Ewing's family of tumors only, may be one such target[15]. In addition to enhanced specificity, engagement of CD99 has been shown to have a functional role in inducing apoptosis[16]. Anti-CD99 antibodies (or antibody fragments) should be considered for incorporation within AD-PEG-conjugates to generate formulations of which an even higher fraction of the administered dose reaches these target ES tumor cells.

5.2.4 Alternative dsRNA duplexes for improved potency

A final point to consider in order to improve potency of these formulations is the nature of the therapeutic agent (siRNA duplex) itself. Very recently, it has been reported that synthetic dsRNA molecules that are somewhat longer than siRNA duplexes (~25-30 nt in length) can be up to two orders of magnitude more potent than corresponding siRNAs[17]. In the discussion of the mechanism of RNAi in Chapter 1, it was mentioned that siRNA duplexes bypass the initial Dicer-mediated cleavage event normally performed on longer dsRNAs to generate the siRNA effector duplexes that are recruited to RISC. These new results support a new hypothesis that these longer dsRNAs, which are Dicer substrates, are more potent because of the coupled nature of the production of siRNA and its incorporation within RISC. Indeed, a separate report indicates that synthetic, 29-bp small hairpins RNAs (shRNAs) are also more potent than corresponding siRNAs and describes the precise nature of Dicer shRNA cleavage products[18]. Both of these studies demonstrate that, if properly designed, longer dsRNAs can be much stronger down-regulators of a given target gene. I recommend that such dsRNAs be explored for subsequent applications of these targeted non-viral formulations.

5.3 REFERENCES

[1] Lai E & van Zanten JH. Real time monitoring of lipoplex molar mass, size and density. *J. Control. Release* **82**, 149-58 (2002).

[2] Heidel JD & Davis ME. The first example of a completely self-assembled non-viral gene delivery system for *in vivo* application. *Annual Meeting, American Institute of Chemical Engineers* (2003).

[3] Bellocq NC, Pun SH, Jensen GS & Davis ME. Transferrin-containing, cyclodextrin polymer-based particles for tumor-targeted gene delivery. *Bioconjug. Chem*. **14**, 1122-1132 (2003).

[4] Pun SH, Tack F, Bellocq NC, Cheng J, Grubbs BH, Jensen GS, Davis ME, Brewster M, Janicot M, Janssens B, Floren W & Bakker A. *Cancer Biol. & Ther*. **3**, 641-650 (2004).

[5] Pun SH & Davis ME. Development of a nonviral gene delivery vehicle for systemic application. *Bioconjug. Chem*. **13**, 630-639 (2002).

[6] Popielarski SR, Pun Sh & Davis ME. A nanoparticle-based model delivery system to guide the rational design of gene delivery to the liver. 1. Synthesis and characterization. *Bioconjug. Chem.,* submitted.

[7] David A, Kopeckova P, Rubinstein A & Kopecek J. Enhanced biorecognition and internalization of HPMA copolymers containing multiple or multivalent carbohydate side-chains by human hepatocarcinoma cells. *Bioconjug. Chem*. **12**, 890-899 (2001).

[8] Pun SH, Gonzalez N, Davis ME, Bellocq N & Cheng J. Compositions containing inclusion complexes. **Patent# WO02/49676**. Issued 27 June 2002.

[9] Connolly DT, Townsend RR, Kawaguchi K, Bell WR & Lee YC. Binding and endocytosis of cluster glycosides by rabbit hepatocytes—evidence for a short-circuit pathway that does not lead to degradation. *J. Biol. Chem*. **257**, 939-945 (1982).

[10] Kolatkar AR, Leung AK, Isecke R, Brossmer R, Drickamer K & Weis WI. Mechanism of N-acetylgalactosamine binding to a C-type animal lectin carbohydrate-recognition domain. *J. Biol. Chem*. **273**, 19502-19508 (1998).

[11] Lee RT & Lee YC. Facile synthesis of a high-affinity ligand for mammalian hepatic lectin containing three terminal N-acetylgalactosamine residues. *Bioconjug. Chem*. **8**, 762-765 (1997).

[12] Thorstensen K & Romslo I. The transferrin receptor: Its diagnostic value and its potential as therapeutic target. *Scand. J. Clin. Lab. Invest.* **53**, 113-120 (1993).

[13] Gatter KC, Brown G, Trowbridge IS, Woolston RE & Mason DY. Transferrin receptors in human tissues: their distribution and possible clinical relevance. *J. Clin. Pathol*. **36**, 539-545 (1983).

[14] Heidel JD, Hu S, Liu XF, Triche TJ & Davis ME. Lack of interferon response in animals to naked siRNAs. *Nat. Biotechnol*. **22**, 1579-1582 (2004).

[15] Scotlandi K, Baldini N, Cerisano V, Manara MC, Benini S, Serra M, Lollini PL, Nanni P, Nicoletti G, Bernard G, Bernard A & Picci P. CD99 engagement: an effective therapeutic strategy for Ewing tumors. *Cancer Res*. **60**, 5134-5142 (2000).

[16] Sohn HW, Choi EY, Kim SH, Lee I, Chung DH, Sung UA, Hwang DH, Cho SS, Jun BH, Jang JJ, Chi JG & Park SH. Engagement of CD99 induces apoptosis through a calcineurin-independent pathway in Ewing's sarcoma cells. *Am. J. Pathol*. **153**, 1937-1945 (1998).

[17] Kim DH, Behlke MA, Rose SD, Chang MS, Choi S & Rossi JJ. Synthetic dsRNA Dicer substrates enhance RNAi potency and efficacy. *Nat. Biotechnol*. **23**, 222-226 (2005).

[18] Siolas D, Lerner C, Burchard J, Ge W, Linsley PS, Paddison PJ, Hannon GJ & Cleary MA. Synthetic shRNAs as potent RNAi triggers. *Nat. Biotechnol*. **23**, 227-231 (2005).

APPENDIX

Images of NOD/scid mice injected with TC71-LUC cells and treated twice-weekly with various formulations.

Images correspond to the following time points:

Immediately after injection of cells (pg. 123)
2 weeks post-injection (pg. 124)
2.5 weeks post-injection (pg. 125)
3 weeks post-injection (pg. 126)
3.5 weeks post-injection (pg. 127)
4 weeks post-injection (pg. 128)

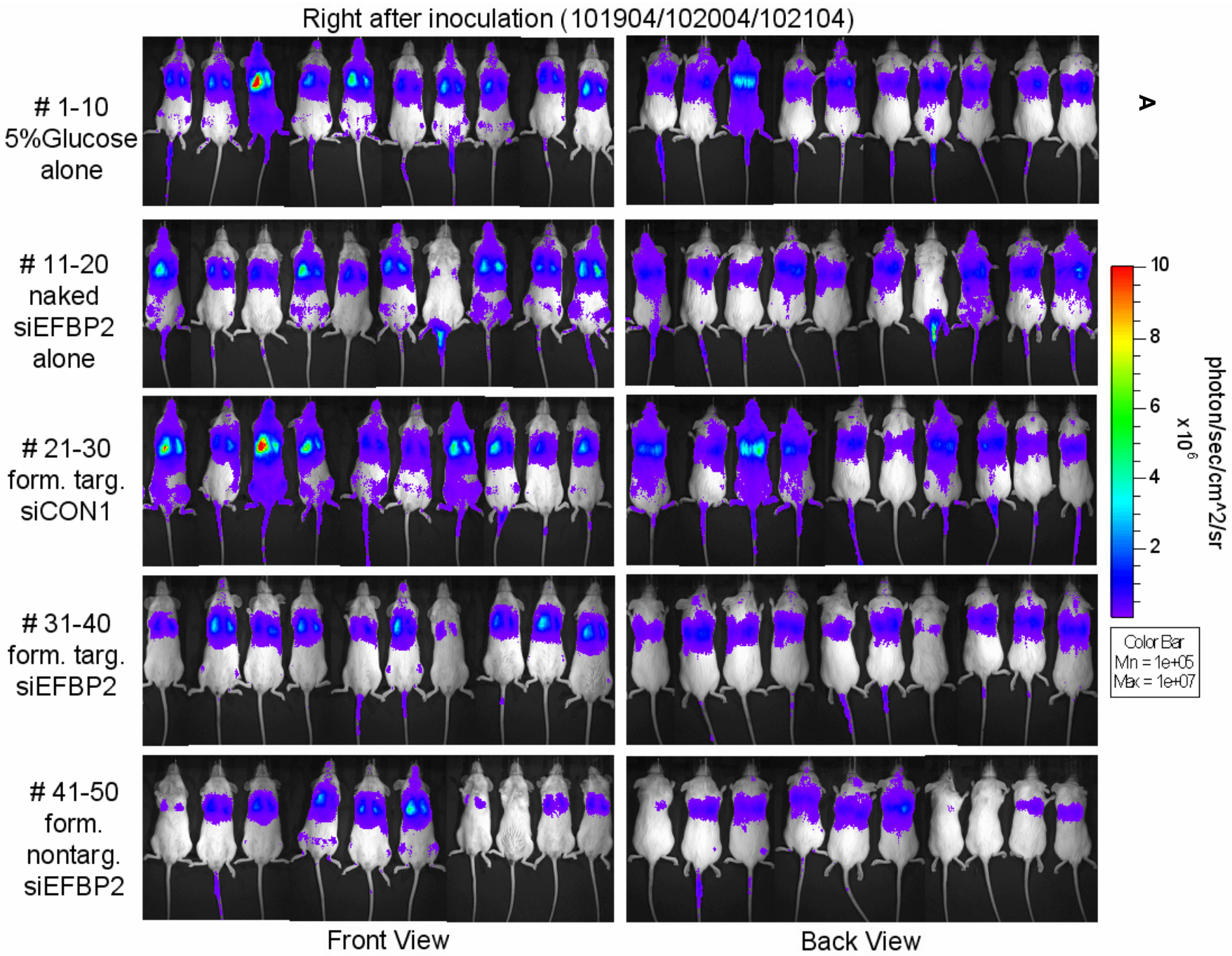
Right after inoculation (101904/102004/102104)
1-10
5%Glucose
alone
11-20
naked
siEFBP2
alone
21-30
form. targ.
siCON1
31-40
form. targ.
siEFBP2
41-50
form.
nontarg.
siEFBP2
Front View
Back View
A
10
8
6
4
2
x 10^6
photon/sec/cm^2/sr
Color Bar
Min = 1e+05
Max = 1e+07

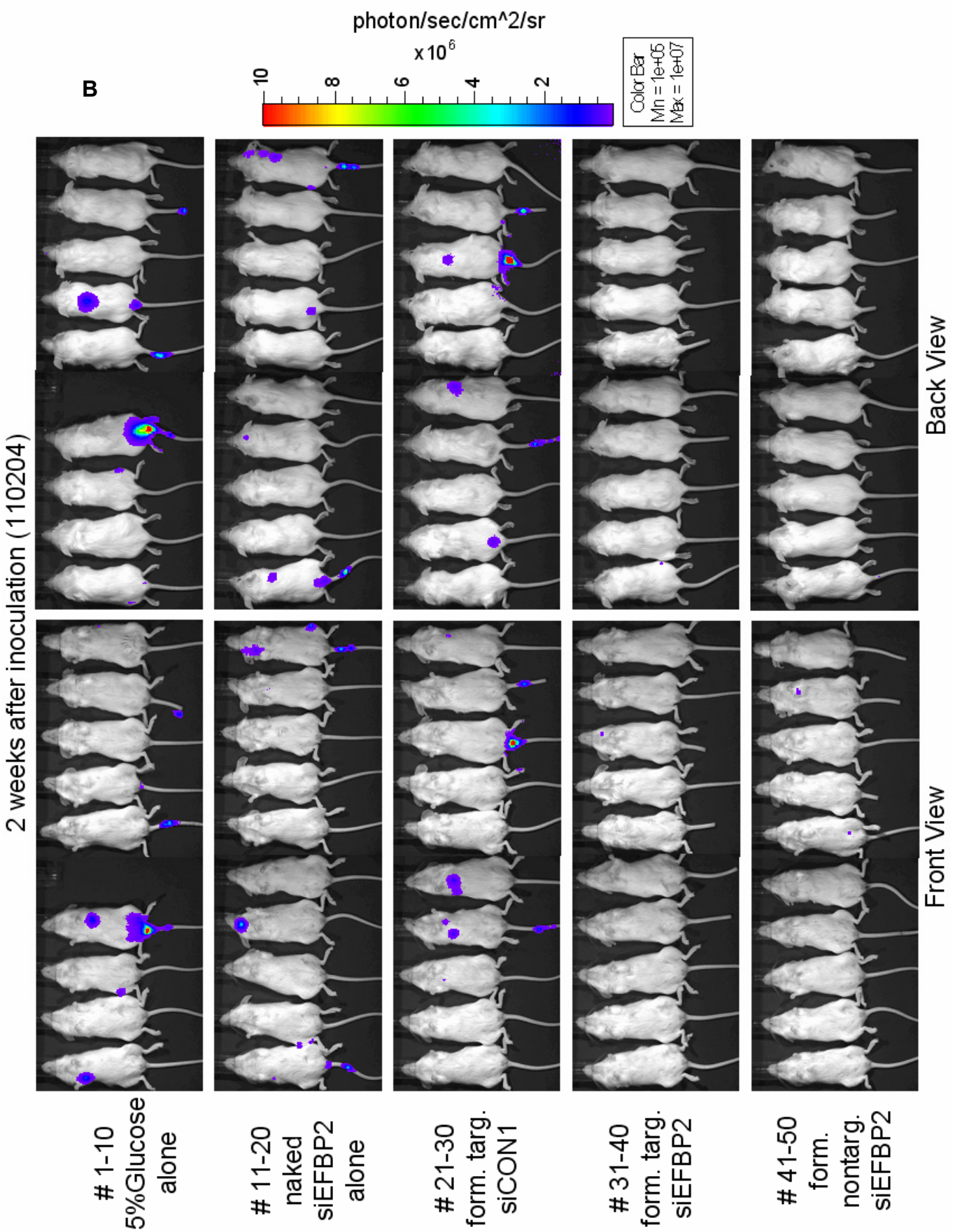
B
photon/sec/cm^2/sr
x 10^6
10
8
6
4
2
Color Bar
Min = 1e+05
Max = 1e+07
2 weeks after inoculation (110204)
1-10 5%Glucose alone
11-20 naked siEFBP2 alone
21-30 form. targ. siCON1
31-40 form. targ. siEFBP2
41-50 form. nontarg. siEFBP2
Front View
Back View

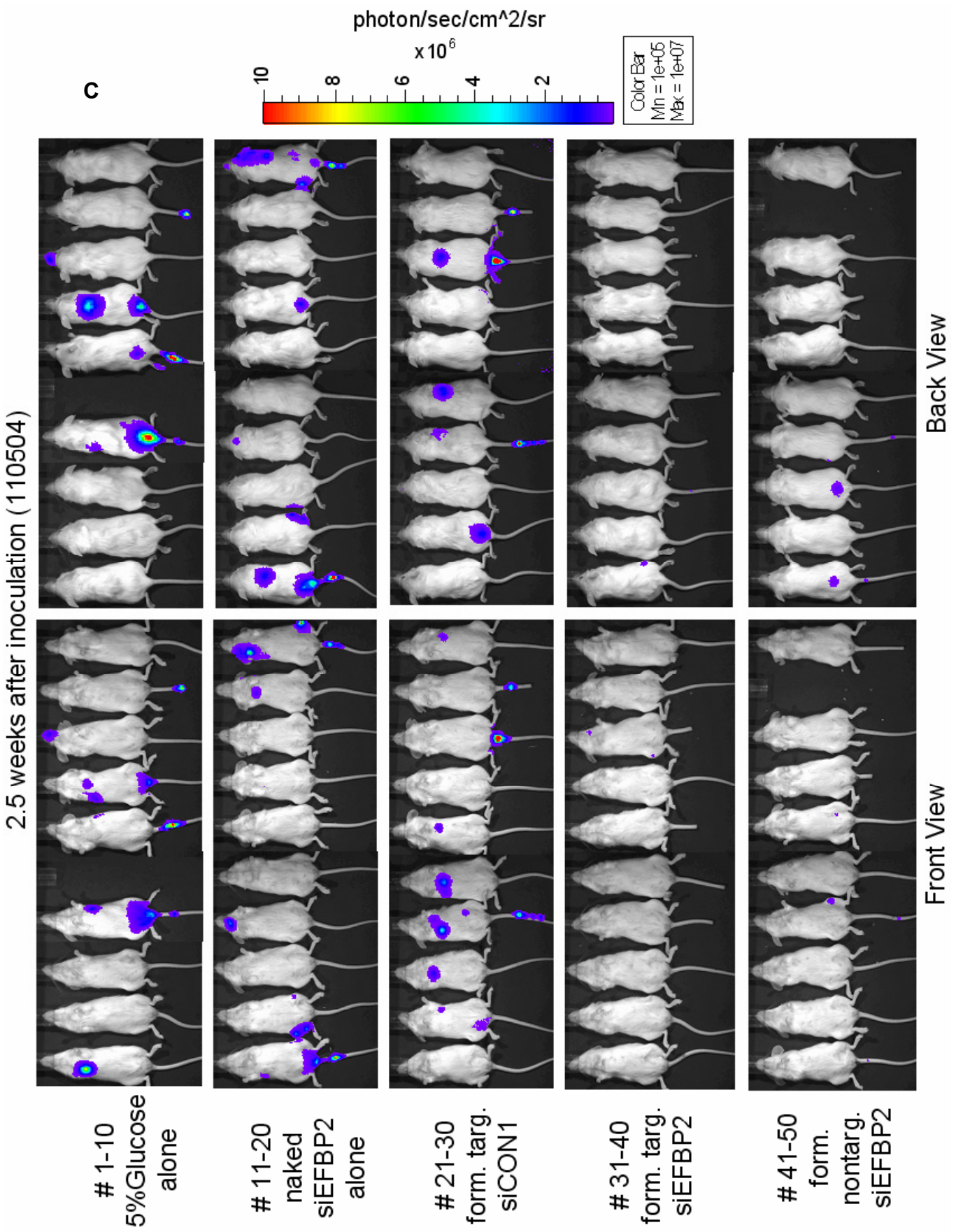
C
photon/sec/cm^2/sr
x 10^6
10
8
6
4
2
Color Bar
Min = 1e+05
Max = 1e+07
2.5 weeks after inoculation (110504)
1-10
5%Glucose
alone
11-20
naked
siEFBP2
alone
21-30
form. targ.
siCON1
31-40
form. targ.
siEFBP2
41-50
form.
nontarg.
siEFBP2
Front View
Back View

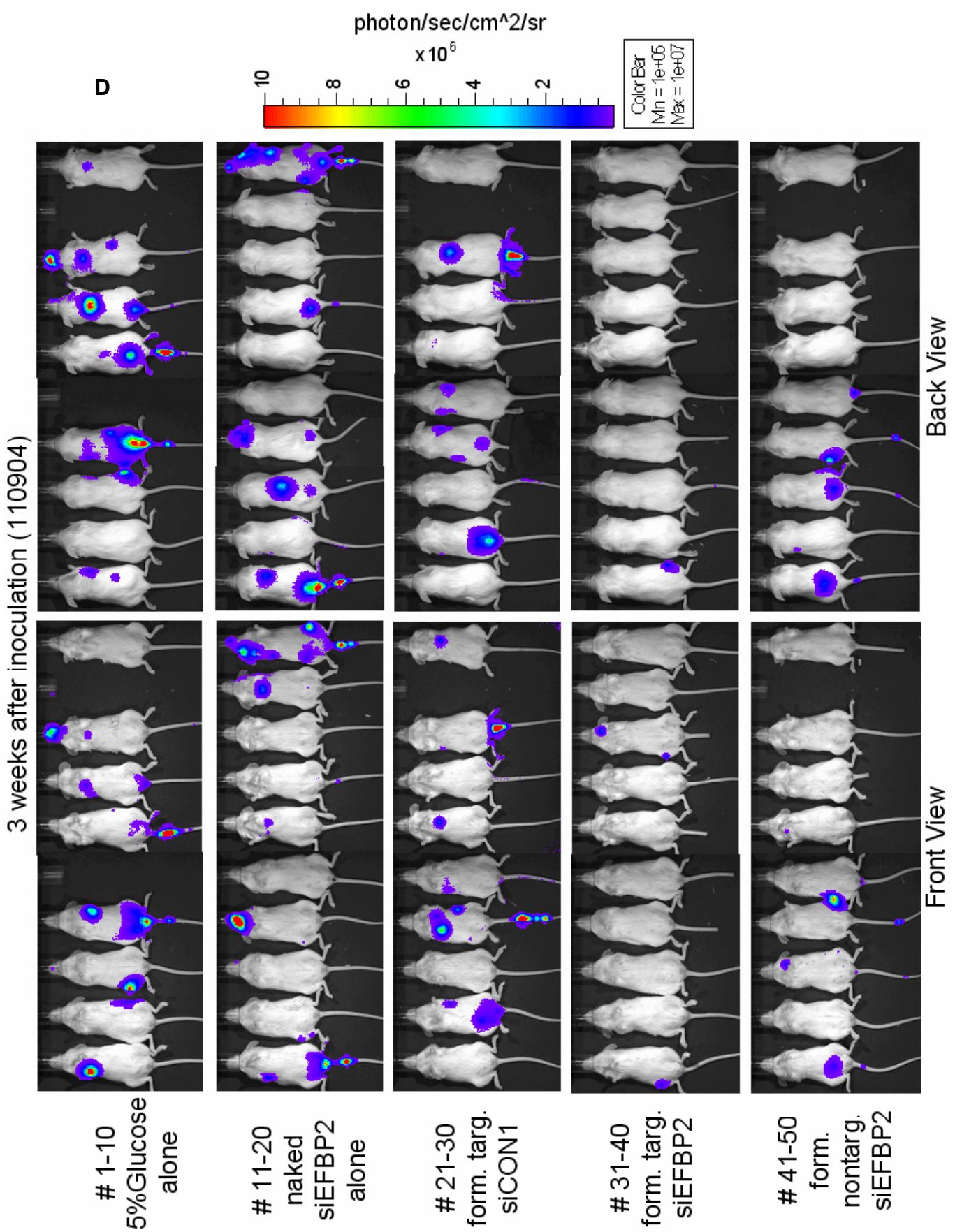
D
photon/sec/cm^2/sr
x 10^6
10
8
6
4
2
Color Bar
Min = 1e+05
Max = 1e+07
3 weeks after inoculation (110904)
1-10 5%Glucose alone
11-20 naked siEFBP2 alone
21-30 form. targ. siCON1
31-40 form. targ. siEFBP2
41-50 form. nontarg. siEFBP2
Front View
Back View

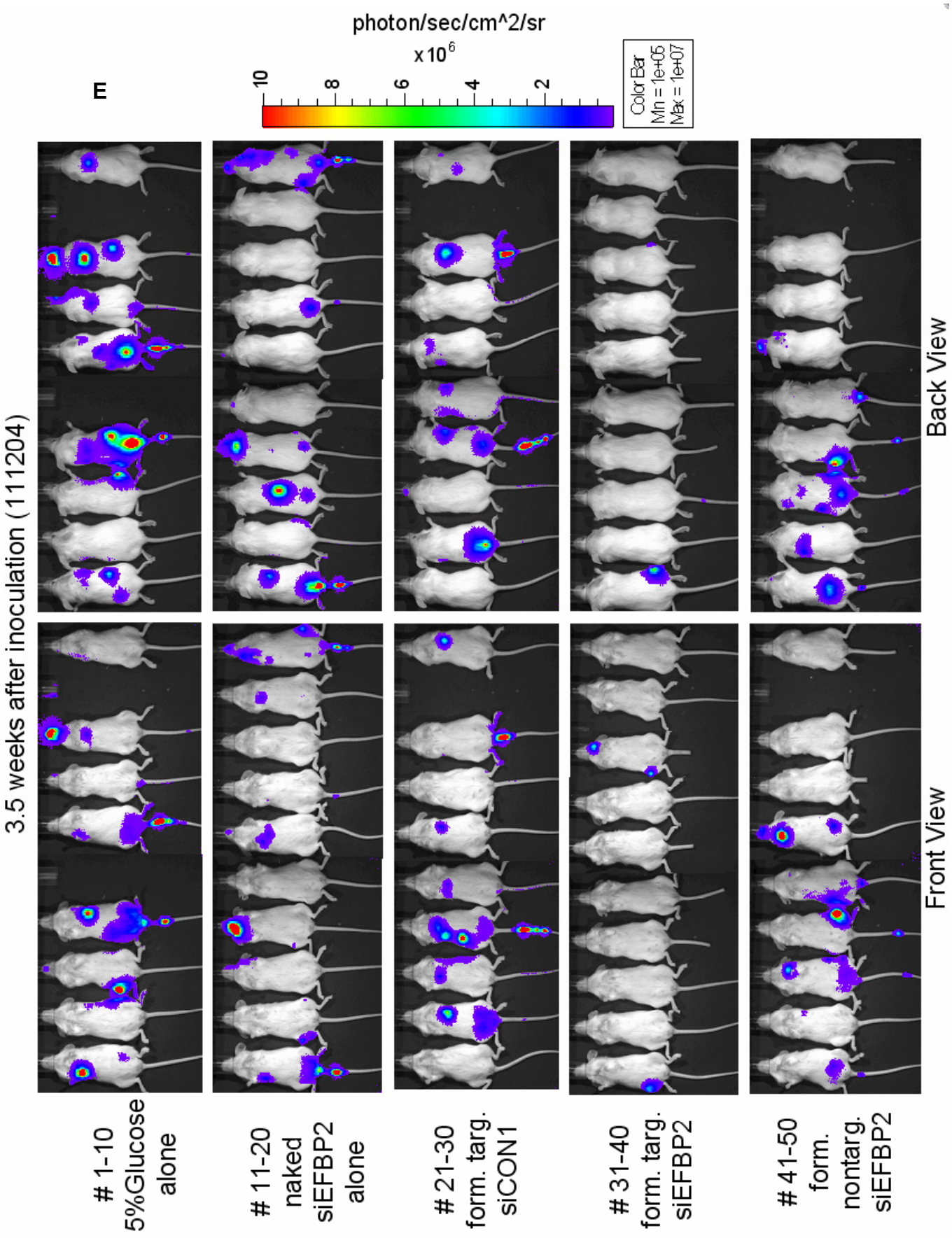
E
photon/sec/cm^2/sr
x 10^6
10
8
6
4
2
Color Bar
Min = 1e+05
Max = 1e+07
3.5 weeks after inoculation (111204)
1-10 5%Glucose alone
11-20 naked siEFBP2 alone
21-30 form. targ. siCON1
31-40 form. targ. siEFBP2
41-50 form. nontarg. siEFBP2
Front View
Back View

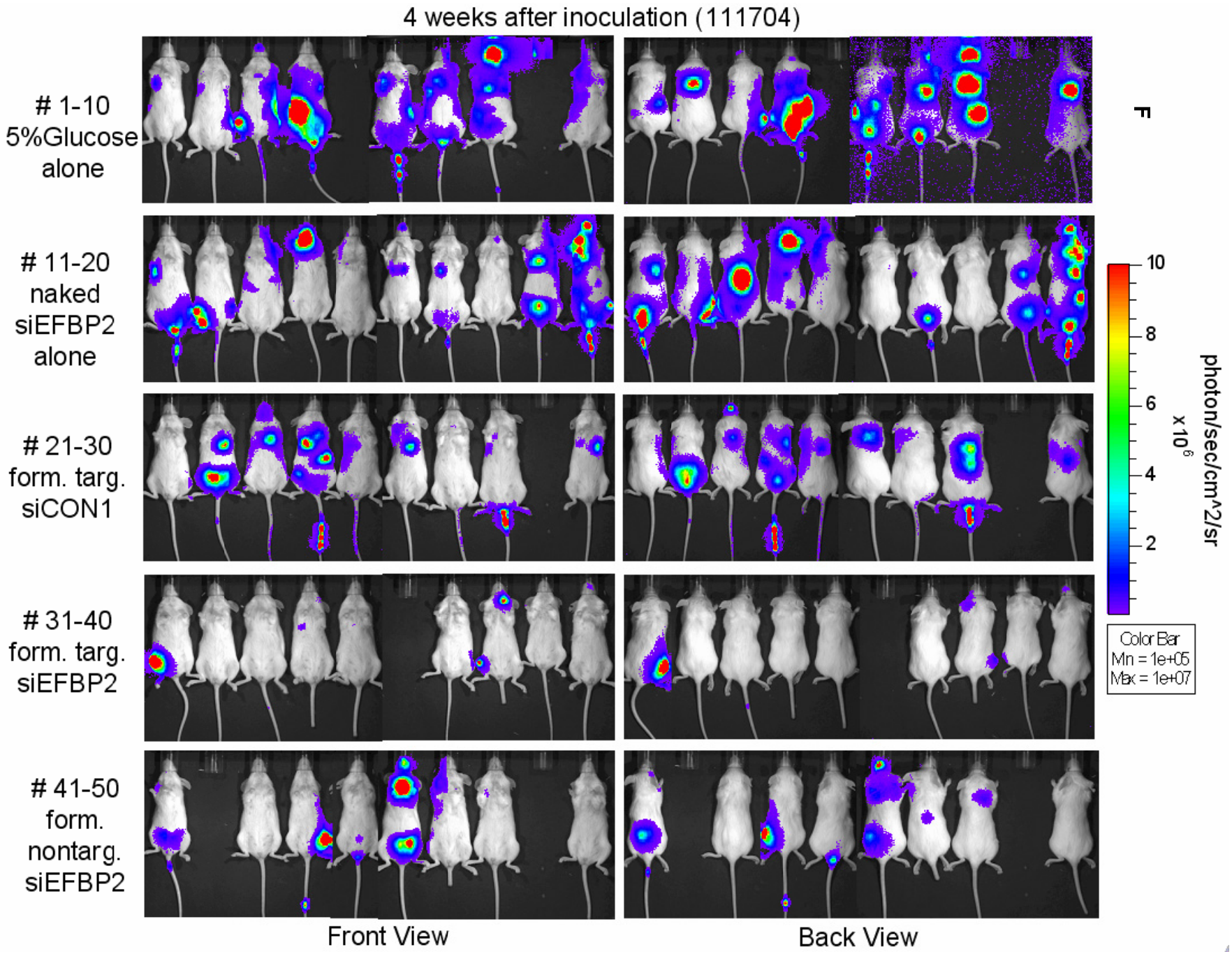
4 weeks after inoculation (111704)
1-10
5%Glucose
alone
11-20
naked
siEFBP2
alone
21-30
form. targ.
siCON1
31-40
form. targ.
siEFBP2
41-50
form.
nontarg.
siEFBP2
Front View
Back View
F
10
8
6
4
2
x 10^6
photon/sec/cm^2/sr
Color Bar
Min = 1e+05
Max = 1e+07